Msc Biomedical Engineering

Assessment of performance in speed skating using IMUs

A. J. Leemreize

December 2024

Supervisors:
dr. J. Reenalda Msc
Ir. B. L. Scheltinga Bsc
dr. A. Marin

Department of Biomedical Engineering
Faculty of Science and Technology
University of Twente

Abstract

Speed skating performance is influenced by biomechanical factors, such as the stroke frequency, knee flexion angle, trunk angle, push-off angle and push-off force. It is not possible to capture these parameters with traditional motion capture systems all over a 400-m ice rink. This thesis evaluates the potential of inertial measurement units (IMUs) in measuring performance-related parameters in speed skating.

Movella DOT sensors were used to measure kinematic data from speed skaters on an indoor ice rink. An algorithm was developed to estimate performance-related parameters, and the results were validated against the MVN Link system.

The DOT sensors successfully detected the number of strokes and provided strong correlations with the MVN system for the push-off and knee flexion angles. However, trunk angle estimation showed significant inaccuracies, likely due to sensor placement.

This study demonstrates the feasibility of using DOT sensors for kinematic analysis in speed skating. Future research is needed to improve the calibration protocol, validate the results of the DOT sensors against video analysis and explore the potential for real-time feedback.

Key words: Speed skating, IMUs, biomechanics, kinematics, stroke frequency, trunk angle, knee angle, push-off angle, push-off force.

Contents

1 Introduction

Speed skating is a technical and endurance-based sport where athletes compete to achieve the fastest time over a set distance on a 400-meter ice rink. Like many sports are driven by 'faster, higher, stronger' [1], records have been set and broken since the beginning of long-track speed skating. For example, the current 10.000 m world record for men (12:30.74) is almost 8 minutes faster than the first world record from 1893 (20:21.4) [2]. Much of the time reduction can be attributed to technological developments: In 1954, the 'Noren' skates were introduced, in 1960 the indoor artificial ice rink, in 1974 the aerodynamic skating suit and in the season 1996-1997, the 'klapskate' made its first entrance on the highest level, causing that many records were broken by several seconds [1, 3, 4]. Yet, there might still be room for improvement, as it is unclear what the optimal skating technique actually is [5]. To keep improving speed skating performance and breaking records, it is important to get a better understanding of the speed skating technique and the parameters related to performance. This knowledge might be relevant for finding the optimal speed skating technique, recognising talent, preventing injuries, and training more efficiently.

1.1 The speed skating technique

The speed skating technique is a cyclic movement in which the skater directs its push-off force perpendicular to the gliding direction of the skate [6]. The centre of pressure moves nearly frictionless over the ice resulting in a sliding push-off point [6, 7].

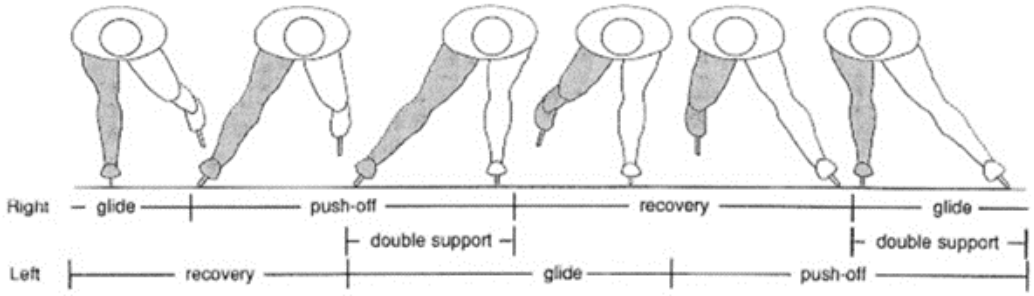

Figure 1: Phases of the speed skating stroke: gliding, push-off and recovery [8]

The speed skating cycle can be divided into different phases (figure 1): the gliding phase, the push-off phase and the recovery phase [5, 8]. During the gliding phase, the body mass is supported with one leg and the distance between ankle and hip remains constant [9, 10]. This means that the knee angle does not change [6]. The push-off phase starts when the push-off leg starts to extend by increasing the angle between the upper and lower leg [6], causing the body mass to move away from the push-off skate [9]. The force that is generated by the skater determines the amount of acceleration of the skater and the orientation of the skate determines in which direction. When the push-off leg is maximally extended, the skate is lifted from the ice and placed under the body on the ice again: the recovery phase. The period where the gliding phase of one leg overlaps with the push-off phase of the other leg, and both skates are in contact with the ice, is called the double stance phase [11].

In long-track speed skating, the skater is always moving counterclockwise over the rink and thus only making turns to the left. The skating technique for the curve is different from the technique for the straight ends, as in the curve the so-called "step-over" technique is applied. In every stroke, the skate is placed to the left of the push-off skate to overcome gravity and centrifugal force [11]. This results in stepping with the right skate over the left skate, causing crossed legs when placing the right skate on the ice.

1.2 Performance related parameters

In the past decades, research has been conducted on factors in the speed skating technique that influence performance, though the number of articles in the field of speed skating is relatively low [12]. The parameters that are frequently mentioned to be related to performance and therefore are assumed to be relevant for this study are discussed in the following paragraphs:

Speed skating performance depends on the power output that is delivered by the skater [13]. The power output of a skater can be described as the work per stroke times the stroke frequency [14]. The stroke frequency can be defined as the number of push-offs per time unit [9]. The work per stroke is dependent on the component of the push-off force, which is directed towards the centre of gravity of the skater [14], in the direction perpendicular to the gliding direction of the skate [9]. The power output is generated by extending the knee during the push-off phase in a very short time span [8, 15, 16]. This results in a sideward and upward increase of velocity of the centre of gravity of the skater [12]. Compared to lower level skaters, elite skaters have a higher angular velocity and thus shorter and more explosive extension of the knee, while showing no different stroke frequency [9, 10, 14, 17]. This is possible when making the push-off phase shorter and the gliding phase longer. This is supported by De Koning et al. [18], who measured push-off force in skaters and found that the push-off time decreased while the peak and mean push-off force did not change for skating at different velocities. There was no significant difference in the magnitude of the push-off force between skaters of different performance levels. Therefore, it can be concluded that the difference in performance between skaters is caused by differences in work per stroke due to push-off mechanics, while differences in power output within a skater are achieved by changing stroke frequency [13, 14]. The first step in estimating the work per stroke is to measure the stroke frequency, the push-off force and its direction.

In literature, three kinematic parameters are reported that are assumed to be related to the delivered power output: the push-off angle, knee angle and trunk angle [12]. The push-off angle (figure 3 B) can be described as the angle between the push-off leg and the ice floor in the frontal plane [13, 19]. Noordhof et al. [20] found a significant association between the push-off angle and velocity in 5000-m races but not in 1500-m races. In a study on junior elite skaters, Stoter [19] found as well that faster skaters have smaller push-off angles during 1500-m races than slower skaters. Based on these findings regarding push-off angle and the findings on push-off power, it can be concluded that a smaller push-off angle leads to a higher work per stroke and thus a better performance.

Elite skaters have a smaller knee angle (figure 3 A) at the beginning of the gliding phase compared to lower-level skaters, caused by a more horizontal upper leg position [14, 15]. During 1500-m races, faster skaters showed smaller knee angles than slower skaters [19]. In the same skaters, both knee and push-off angles increased throughout the race. It was believed that change in the knee and push-off angles are coupled: Larger knee angles will make it harder to have smaller push-off angles since the leg is already more extended during the gliding phase. Therefore, as the push-off angle is related to velocity, an increase in the knee angle is expected to have a negative effect on velocity.

The trunk angle was described as the angle between the longitudinal axis of the trunk (the line between the hip joint and the middle of the neck [21]) and the horizontal plane (figure 3 A) [9, 13, 15, 17, 22]. A major part of the frictional loss that a skater experiences is caused by air resistance [23]. The aerodynamic resistance can be reduced by optimizing the trunk angle: A smaller trunk angle results in a higher speed with an equal power output [24]. In terms of aerodynamics, the optimal trunk position would be horizontal, which in practice corresponds to a trunk angle of 15 degrees [12].

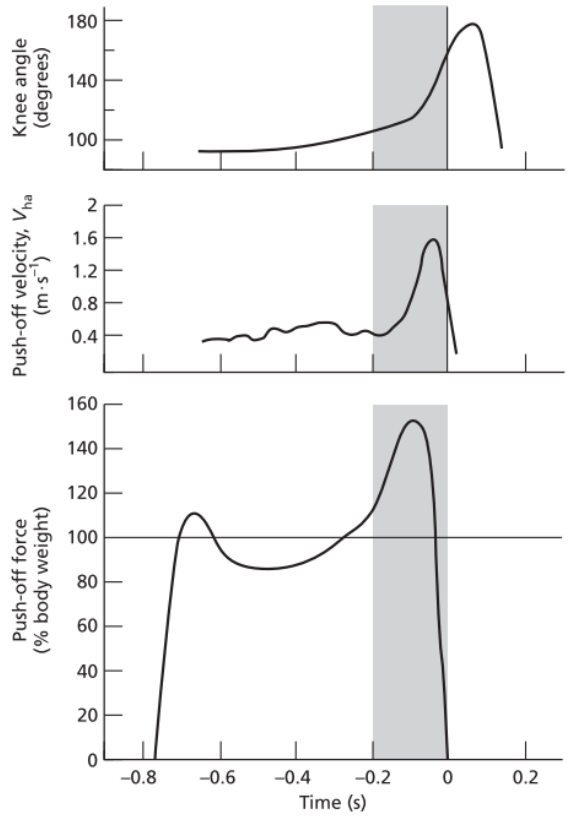

Figure 2: Graphs of the knee angle (top), push-off velocity (middle) and push-off force (bottom) over the stroke time during skating on the straights. The push-off phase is marked as a grey area. [6]

De Koning [6, 25] predicted the finish time of a 1500-m race with a simulation model and showed a decrease in finish time of respectively 2.6% and 3.0% for decreasing the trunk and hip angle by 5°. However, his model deviates from reality, as the skating position is not constant during a race: the knee angle increases and the trunk angle decreases over time [19, 26]. In races on the longer distances, the performance of speed skaters was found to be positively related to a more horizontal trunk position during the push-off [27]. Later, there was no direct relation found between the change in trunk angle and the change in velocity in male speed skaters during a 5000-m World Cup race [13]. This was explained by the fact that the trunk angle decreases in the last section of the race, while the velocity decreases continuously.

A crouched skating position with small knee and hip angles might be biomechanically favourable, as it reduces aerodynamic resistance and extends push-off length [19], but leads to a physiological disadvantage: the small joint angles may decrease the blood flow to the muscles [12]. Increasing the knee angle might be a strategy to deal with muscle fatigue by allowing the blood flow to increase [19].

1.3 Current approaches on measuring speed skating performance

To be able to make such findings as mentioned in section 1.2, one should have a good overview of the kinematics of the speed skater. Speed skating involves high dynamic motions, which are more difficult to capture than slow or static movements seen in gait analysis [28]. As there is no in-laboratory ergo meter to replicate the speed skating motion on [28], the motion capture must take place in the "field" on the ice rink. Up to now, the following technologies and methods have been applied to capture

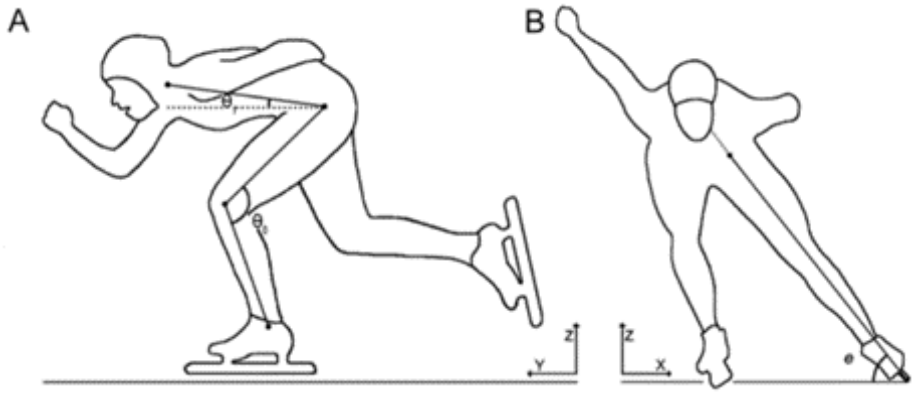

Figure 3: Schematic representation of the A) trunk-, knee- and B) push-off angle [13]

speed skating performance:

Lap times During races, the performance of a speed skate is measured based on only one parameter: the finish time [29]. At Thialf [30], an application has been developed for coaches to monitor their athletes' velocity at 12 specific locations around the ice rink [31, 32]. This is an improvement is an improvement on just the time per lap that can be measured on most ice rinks with the MyLaps system [33]. Hence, this enhancement still fails to explain the factors influencing these lap times or how further improvements might be achieved.

Video analysis In most of the studies regarding the kinematics of speed skating, video analysis is used [12, 34]. Even though video cameras are easy to use, relatively cheap and might be useful for coaches to have access to video images of the skater during training sessions [35], the method has a few drawbacks [34]. First, one camera can only capture a small part of the 400-m ice rink [28, 35]. Most studies using video analysis were only able to capture a few strokes. Capturing the whole ice rink is complex, especially for the curves, and expensive as multiple cameras are needed [35, 36]. Second, video analysis requires a relatively large amount of time for data processing [34, 36]. As a result, video analysis might not be suitable for real-time feedback. Finally, the person of interest must be visible and not be blocked by other persons on the ice rink [34]. This does not have to be a problem during measurements for research, but the problem might occur during training sessions when there are multiple speed skaters on the rink.

Optoelectronic measurement systems Optoelectronic measurement systems are more accurate than other systems, such as electromagnetic systems, image processing systems and inertial measurement units, and are therefore often referred to as the golden standard in motion capture [28]. Van der Kruk captured the movement of a speed skater over 50-m of the straight part with an optical motion capture system (Qualisys [37]) [5, 38, 39]. Twenty cameras were used and subjects were equipped with 22 markers [5]. The experiment had to be performed at night when there were no other skaters on the ice rink [29]. The use of this large number of cameras results in significant practical difficulties regarding cost, portability, calibration, synchronization, labour and set-up [28]. It was not possible to compare their findings with other studies as there were no results on 3D speed skating kinematics in the literature. To date, no other studies using optoelectronic measurement systems on the ice rink have been published.

Inertial Measurement Units The problem of a limited measurement volume can be circumvented by placing sensors on the body of the speed skater. Inertial Measurement Units (IMUs) are relatively small sensors containing an accelerometer, gyroscope and magnetometer [28]. Through sensor fusion, the orientation of the sensor in the global frame can be estimated [28].

Van der Kruk stated that measuring with IMU sensors on an ice rink would be difficult [7]. First, because of the ferromagnetic materials in the surroundings, like the metal blade of the skate and the cooling pipes under the ice floor. Second, because of the linear accelerations that occur when the skate is gliding uninterruptedly over the ice. Nonetheless, she was able to measure the angle between the skate and the ice with a mean RMSE of 5.3 degrees by using IMU sensors placed on both skates and a self-developed complementary filter. In addition, she was able to detect stroke frequency, stroke length, contact time and double stance phase time. Van der Eb [11, 40] placed IMU sensors on both left and right skates as well. He was able to measure among others the stride frequency and double stance phase in long-track speed skaters.

Clement et al. [36] placed a single IMU sensor (T6, 100 Hz) on the lower back of a short-track skater to detect the number and duration of strokes and compared this with video analysis. The stroke detection was based on the acceleration signals in X-, Y- and Z-direction. Errors in detected strokes were corrected manually in a graphical interface. The researchers were able to detect 100% of the strokes identified on the video camera.

Tomita et al. [34] used a sensor set-up consisting of 8 IMUs (myoMOTION, 100Hz) to identify foot contact and foot-off timing in short-track speed skating. The initial contact of the skate and the end of the push-off phase were detected in the high- and low-frequency components of the acceleration signal of the foot sensor. The stance time derived from the inertial measurement system did not differ by more than 3.6% from a pressure insole method. The phase identification method using only IMUs was considered valid.

Kim et al. [41] and Purevsuren et al. [42] both used the Xsens MVN Link suit [43], consisting of 17 IMUs placed on the body, to measure short-track skating athletes. Kim [41] was able to estimate the 3D push-off angle based on the MVN data with a root mean square difference of 6% compared to the angle that was estimated based on pressure insole force data. Purevsuren [42] did not use the IMU sensors as a stand-alone system, but combined the data with pressure insole data to calculate joint kinematics and kinetics. The joint angles derived from the MVN Link system were described but not validated.

Instrumented skate Measuring mechanical power is a useful and objective method to monitor performance in sports [44]. De Koning did this by developing an instrumented conventional skate that measures forces applied by speed skaters on the ice [18]. Almost 30 years later, Van der Kruk used an instrumented klapskate [45]. Here, a force sensor is integrated in the bridge of the klapskate and is able to measure forces in the normal and lateral direction of the skate with an accuracy of respectively 42 and 27 Newton. The measured push-off forces were used to estimate the power per stroke. The orientation of the skate on the ice was estimated using an Inertial Measurement Unit (IMU) placed on the skate. A drawback of the instrumented klapskate is the additional weight compared to a regular klapskate (+0,5 kg) [45]. Van der Eb [46] continued with the development of the instrumented skate. He replaced the force sensors with ultra-light force sensors. The disadvantage of the heavy-weight skates was thereby solved. Regardless of the above-mentioned research projects, to date, no commercially available power meter for speed skating exists [44].

Pressure insoles A more accessible way of measuring push-off forces in skating is by the use of (commercially available) pressure insoles. These insoles are placed inside the (skate)shoe and contain

pressure sensors, making it able to measure GRF and pressure distribution. Kim et al. [41] and Tomita et al. [34] both used pressure insoles to validate respectively the three-dimensional push-off angle and phase detection determined from IMU sensors in short-track speed skating. Purevsuren [42] used IMU sensors and pressure insoles as well, but the measured GRF was used as an input for calculating knee joint forces and moments and not as a validation method. A limitation of these pressure insoles is that they can only quantify the vertical component of the GRF but not the three-dimensional GRF. Furthermore, the skaters have to wear the insoles in their tight-fitting skate shoes which can be experienced as uncomfortable.

1.4 Research gap

As mentioned in section 1.2, parameters such as push-off angle, knee angle and trunk angle are assumed to be related to speed skating performance. At this moment, the most common method to capture these parameters is with video analysis. From the background information described in section 1.3, it can be concluded that motion capture systems involving cameras have a too small measurement volume to capture the whole 400-m ice rink. Instrumented skates and pressure insoles can only measure force, but no body kinematics. IMU sensors are a promising solution for capturing whole body kinematics of a speed skater all over the ice rink, yet the number of studies on this specific topic is low.

In three studies [41, 42, 47] the MVN Link system (Movella, Enschede, the Netherlands [48]) was used. The MVN link system consists of a Lycra suit and 17 wired IMU sensors and comes with a biomechanical model (embedded in the MVN Analyze software) (figure 4). The model combines the data of all 17 IMU sensors resulting in an immunity to the effects of magnetic distortions [43]. This means that the resulting parameters are less negatively influenced by e.g. magnetic materials in the surroundings, which are often present in an indoor ice rink. Next to the sensor readings, the biomechanical model requires at least the body height and shoe length of the subject as input. The system allows offline recordings, which eliminates issues regarding the distance between the skater and a receiver. The collected data is then stored on the system's internal memory and can be opened in the MVN Analyze software and exported to e.g. Matlab or Python.

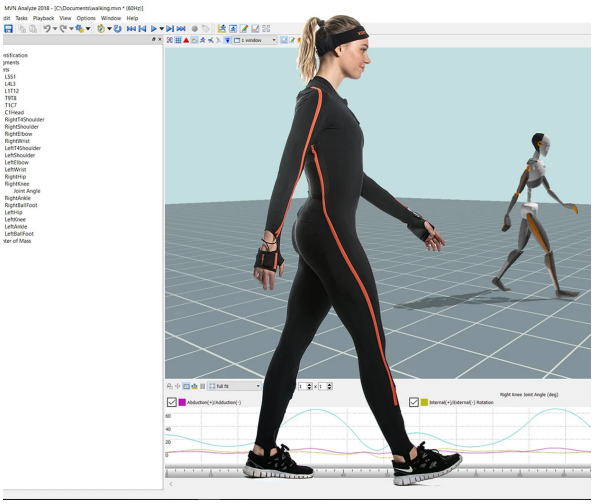

Figure 4: The MVN Link system, consisting of the MVN Link suit and the MVN Analyze software [49]

Movella states that their MVN Link system has an RMSE smaller than 5 degrees for flexion-extension angles of the lower body during walking compared to optical position measurement [43]. Nijmeijer

[50] found a high cross-correlation (>0.92) but also relatively high errors between the MVN Link system and an optical motion capture system (Vicon [51]) for joint angles of the lower body in the sagittal plane during change-of-direction tasks like jumping, landing and side stepping. Debertin [52] showed that the MVN Link system provides good within-day reliability for the estimation of joint angles of the lower extremities during in-field running, especially for the angles in the sagittal plane. Based on these findings, it can be concluded that the MVN Link system estimations of the flexion-extension joint angles of the lower body are accurate during walking but less accurate during change-of-direction tasks. The accuracy of the system during skating is unknown.

The extensiveness of the MVN Link system can be considered as a disadvantage as well. It takes time to set up the system and it might be challenging for a person to put on the suit by oneself. Furthermore, a computer is required to set up the right settings and to process the collected data afterwards, which can be time-consuming. For this processing, a licence for the MVN Analyze software is needed, which can be quite expensive. Last but not least, the biomechanical model does not provide speed skating-related parameters. Therefore, additional calculations are needed to measure speed skating-related parameters with the MVN Link system.

It would be of added value to have a simpler sensor system that is easier to set up, does not need a specific software (or licence) to process the measurement data, is lower in costs but can still give all speed skating performance-related parameters that are discussed in section 1.2. The DOT sensor, developed by Movella as well, might be a suitable system to use for capturing the speed skating kinematics instead of the MVN Link system.

Figure 5: Movella DOT sensor [53]

The DOT sensor (figure 5) is a single IMU sensor containing an accelerometer, gyroscope and magnetometer. The angular velocity and acceleration data are internally sampled at a high frequency and processed into a lower-rate signal by strap-down integration (SDI) [53]. This way, the computational load is suitable for data transmission via Bluetooth signal. Based on the output of the SDI and the magnetometer readings, the sensor orientation estimate is calculated by the Xsens Kalman Filter [54]. The sensors allow offline recording. The collected data is then internally stored and can be exported to e.g. Matlab or Python. Up to seven DOT sensors can be connected to a smartphone via Bluetooth, and be controlled and synchronized via the Movella DOT application. This allows the DOT sensors to be used in a multi-sensor set-up to provide biomechanical analysis. Unlike the MVN Link system, the DOT sensors do not come with a biomechanical model, meaning an algorithm should be developed to calculate relevant parameters. D'Alcala describes a method for biomechanical analysis during walking using five DOT sensors [54]. A static sensor-to-segment calibration was performed based on the subject standing in a neutral body position, and knee and hip flexion angles were extracted as Euler angles. The results were compared to the Awinda system and showed a mean RMSE of 4.53 degrees. Again, the accuracy of these sensors during speed skating is unknown.

1.5 Research objective

This study focuses on measuring relevant parameters of the kinematics of a speed skater with the use of IMU sensors. Push-off force, stroke frequency, trunk angle, knee angle and push-off angle were identified as parameters related to performance (section 1.2). It was chosen to measure these parameters with two different sensor systems: the DOT sensors [54] and the MVN Link system [43]. Seven DOT sensors were used in combination with a self-developed algorithm to calculate the parameters of interest. The MVN system provided joint angles via the MVN Analyze software. Speed skating-specific parameters were calculated based on the provided segment orientation.

The main goal of this thesis is as follows:

This explorative research aims to analyse the potential use of the Movella DOT sensors in capturing performance-related parameters of speed skaters on the indoor ice rink.

The performance-related parameters that will be analyzed in this thesis are the stroke frequency, trunk angle, knee flexion angle, push-off angle and push-off force.

The objectives to reach this aim are:

- To develop an algorithm for calculating parameters related to speed skating performance.
- To validate the feasibility and accuracy of the Movella DOT sensors in capturing these parameters.

The contribution of this research project to the field of biomechanical engineering is to introduce an affordable and low-invasive method for kinematic data collection of speed skating-specific parameters in a natural environment, all over the 400-m ice rink.

1.6 Outline of the thesis

This report is structured as follows: Chapter 2 describes the method that was used for the data collection and the steps that were taken in the data analysis. Chapter 3 presents the results, which are discussed in chapter 4. The conclusion of the thesis is presented in chapter 5.

2 Method

2.1 Data collection

2.1.1 Ethical approval

This study was approved by the Ethics Committee Computer & Information Science of the University of Twente [55] under application number 240070.

2.1.2 Study Population

Nine healthy athletes (sex: 3 female - 6 male, age: 20.1 +- 2.3 years, length: 182.1 +- 6.4 cm) participated in the study after signing an informed consent form (see appendix 5). Five participants were members of a junior elite development speed skating team and competed at national and international level. Four participants were competitive athletes on a university long-track speed skating team and competed in the student league.

2.1.3 Inclusion criteria

To be allowed to participate in this study, subjects had to be:

- aged 16 years or older;
- competing in long track speed skating events at the national level in the junior B, junior A, neo-seniors or seniors category or have a speed skating technique of a similar level;
- skating at least once a week;
- own a pair of klapskates.

2.1.4 Exclusion criteria

Possible participants were excluded when they met one of the following criteria:

- they were injured;
- their coaches/trainers disapproved of participation in this study.

2.1.5 Materials

The participants were equipped with fourteen sensors of the Xsens MVN Link system [43] and seven Movella DOT sensors [54] that were attached to the body segments of interest. The locations of the sensors on the body are shown in figure 6.

The sensors of the MVN Link system were attached to the MVN Link suit on the designated Velcro surfaces. The DOT sensors were taped with Velcro and attached as close to the MVN Link sensors as possible. The sensors were covered with a zip in the Lycra suit to secure them. All participants wore their own klapskates. The MVN Link sensors of the feet were placed on top of the shoelaces of the skate and covered with a zip of the skate shoe. The DOT sensors of the feet were placed on top of or next to the MVN Link sensors and secured with tape.

The following settings were selected for recording the experiment with the MVN Link system: on-body recording, a sample rate of 240 Hz, full body no hands, and single level. To be able to use the 'full body no hands' setting, the sensor for the head was connected to the body pack but tucked away in the back of the suit. For the DOT sensors, a sample frequency of 120 Hz and the dynamic recording profile were selected. The DOT sensors were connected to a smartphone via Bluetooth and the Movella DOT application was used to control them. Magnetic Field Mapping of the DOT sensors was performed before each first measurement of the day.

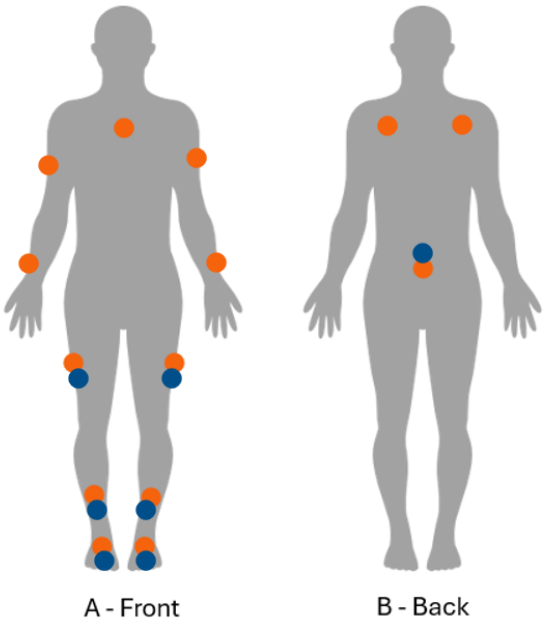

Figure 6: Schematic representation of the locations where the sensors were attached to the front (A) and back (B) of the body. The DOT sensors are shown with the 7 blue dots. The sensors of the MVN system are shown with 14 orange dots.

2.1.6 Study procedure

Data was recorded on the 400-m indoor ice rink in Enschede (IJsbaan Twente [56]), according to the research protocol in appendix 5. Before the skating measurement, the participants performed three times a calibration procedure for the MVN Link system, in which they stood in a neutral pose for 5-10 seconds and walked for approximately 10 meters back and forth over a straight line. Then, they performed a few movements (shown in figure 7) that were necessary for sensor-to-segment calibration (see section 2.2.3) of the DOT sensors. The body height and skate shoe length of all participants were measured.

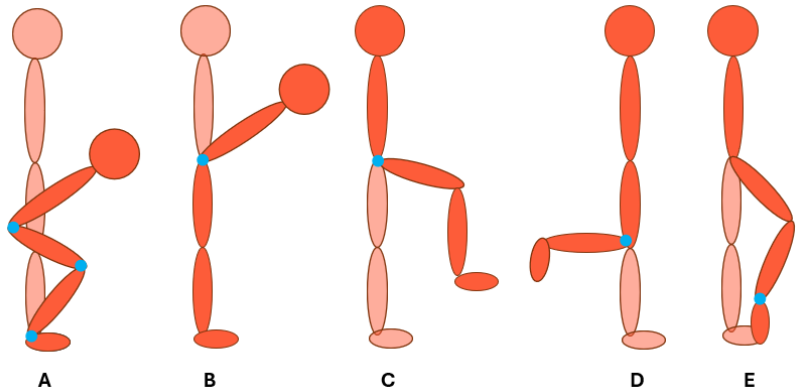

Figure 7: Schematic representation of the movements that were performed during calibration: A) squat; B) bow; C) knee lift; D) heel lift; E) plantar flexion. The blue dots represent the rotation axes of interest.

The participants were allowed to skate a few rounds on the rink as a warming-up before the measure-

ment protocol started. They were instructed to skate two laps at a self-chosen low speed, two laps at a self-chosen comfortable speed and two laps at a self-chosen high speed. All measurements were recorded with both sensor systems.

2.2 Data analysis

2.2.1 Pre-processing

The data of the DOT sensors was saved in .csv files and loaded into Matlab 2024a [57] as a table in which each row represents a sample and each column a parameter. First, the data collected by the DOT sensors was checked for missing samples. If one or more consecutive timestamps were missing, the missing values were added by linear interpolation. Second, extreme values of the accelerometer, gyroscope, magnetometer and estimated orientation were removed and replaced with linear interpolation. Finally, the start and finish times of all DOT sensors were synchronised.

The data of the MVN Link system was downsampled from 240 Hz to 120 Hz in the MVN Analyze software by skipping every 2nd frame [58]. This step was performed to ensure that the datasets from the two systems had the same sample rate. Additionally, it reduced the size of the .mvnx files.

2.2.2 Time synchronization between sensor systems

The timelines of the two sensor systems (DOT and MVN) were aligned using the cross-correlation of the Z-coordinate of the Y-axis from the right upper leg sensors. The Z-coordinate was chosen as it is independent of the heading of the global frame, while the Y-axis shows the largest variance in the Z-coordinate. It was assumed that all sensors within each system were aligned in time.

2.2.3 From sensor orientation to segment orientation

Sensor orientation The orientation of both DOT and MVN Link sensors in their global reference frames were given in quaternions and were converted to 3x3 rotation matrices, of which a schematic representation is shown in figure 8.

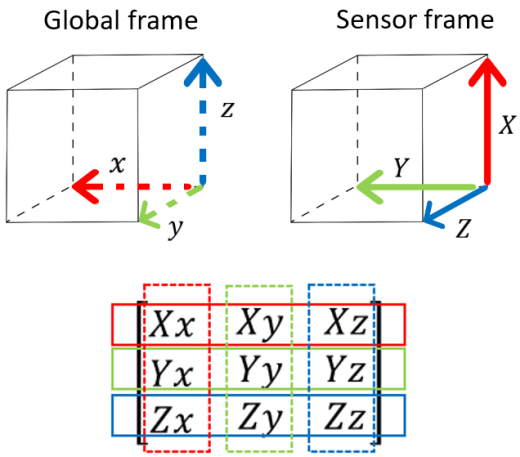

Figure 8: Schematic representation of the sensor orientation expressed in the global reference frame, written in a 3x3 rotation matrix format.

Each row of the matrix represents an axis of the sensor frame. The columns are respectively the X-, Y- and Z-coordinate of each sensor axis in the global reference frame. When the sensor frame (figures 9a and 9b) is aligned with the global reference frame, the rotation matrix is equal to the identity matrix.

(a) DOT sensor coordinate system [53]

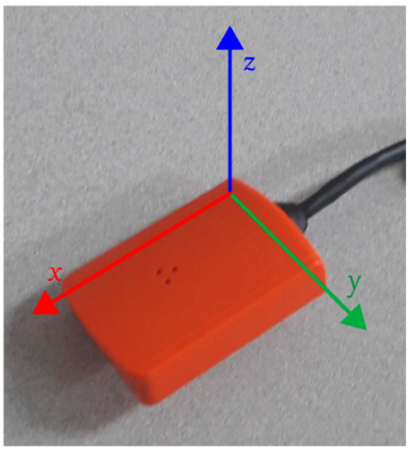

(b) MVN Link sensor coordinate system [59]

Sensor-to-segment calibration Sensor-to-segment calibration describes the relative rotation between the orientation of the sensor and the orientation of the body segment that the sensor is attached to [60] and is constant over time. It was assumed that all body segments are rigid bodies and that the position of the sensor on the segment is fixed e.g. the sensor does not move relative to the segment. In reality, there might be a little movement due to soft tissue.

In this study, an algorithm was written in Matlab 2024a [57] to perform sensor-to-segment calibration for the DOT sensors. First, the vertical axis (Z-axis or gravity-axis) of each segment was derived according to a static calibration method [61]. It was assumed that when a subject is standing in a neutral body pose (N-pose, with their feet parallel to each other and their arms next to their body), the vertical segment Z-axis was aligned with the vertical Z-axis of the global reference frame [61, 62]. The relation between the segment Z-axis and the sensor frame was derived from the estimated sensor orientation. Second, the rotation axis (Y-axis) of each segment was estimated according to a functional calibration method [61]. The participants were instructed to perform rotations around the Y-axis of their body segments (shown in 7). The angular velocity of the rotations was detected by the gyroscope. By taking the principal component of the gyroscope readings, the orientation of the segment Y-axis in the sensor frame was estimated. Third, the segment X-axis was derived from the previously calculated segment Y- and Z-axis by taking their cross-product. The Y-axis was recalculated by taking the cross-product of the X- and Z-axis to make sure that the system was orthogonal. The result was a 3x3 rotation matrix describing the segment orientation in the sensor frame. The orientation of the sensor in the global frame was pre-multiplied with the sensor-to-segment rotation matrix to get the segment orientation in the global frame.

Reference frame correction Each DOT sensor and therefore each segment has its own reference frame which is recalculated at the beginning of each new measurement. To find the relation between the orientation of multiple body segments, the segment orientations must be expressed in the same global reference frame [62]. Therefore, alignment of the segment reference frames was applied (figure 10). It was assumed that all segment reference frames had the same vertical Z-axis defined by the direction of the gravity vector [62]. The difference in the heading of the segment reference frames can be described as a rotation around the vertical Z-axis, determined by the angle between the true segment heading and the measured segment heading.

When standing in N-pose at the beginning of a measurement, it was assumed that each segment was aligned with the global reference frame. First, the mean orientation of each segment in its own reference frame during the N-pose was described in Euler angles. The Z-angle was multiplied with -1

and converted to a rotation matrix that described the rotation that was needed to get from the segment reference frame to the global reference frame. At the beginning of every measurement, the segment reference frames were aligned with the global reference frame by post-multiplying each sample of the segment orientation with the correctional rotation matrix.

In the speed skating measurements, no N-pose was performed. Instead, the true segment heading was retrieved from the MVN segment orientation. The Z-rotation that was applied for reference frame correction was calculated as the MVN Euler Z-angle minus the DOT Euler Z-angle.

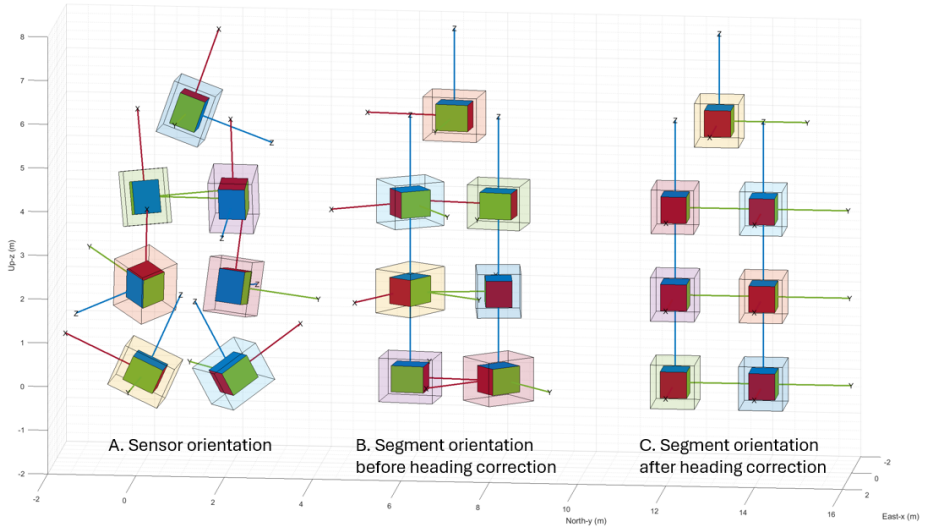

Figure 10: Heading correction. A. shows the orientation of the sensors in the global reference frame during the N-pose; B. shows the segment orientation in the global reference frame calculated from the sensors during the same N-pose; C. shows the segment orientation in the global reference frame with correction of the segment heading.

For the MVN system, sensor-to-segment calibration was performed automatically in the MVN Analyze software.

2.2.4 Stroke detection

Stroke detection was performed on the gyroscope data of the DOT sensors (figure 11). The Y-axis of the gyroscope data in the segment frame of the feet was filtered with a 2.5 Hz low-pass Butterworth filter. The events when the skate was placed on the ice ('foot-on') and the ends of each push-off ('foot-off') were identified with the Matlab function 'findpeaks' [63]. The minimal peak prominence was set at 75 degrees per second and the minimal distance between two peaks was set at 90 samples.

Every 'foot-on' index was matched with the corresponding 'foot-off' index, such that only complete strokes were identified. If one of these two indexes was missing, the other index was deleted. The result is that in chronological order the 'foot-on' peaks were alternated with the 'foot-off' peaks.

Strokes of the right foot were labelled as 'straight', 'curve' or 'other' based on their peak height. A threshold for 'foot-on' was calculated as the mean value of all 'foot-on' peaks of the right foot. The same was done for the 'foot-off' peaks. If both on and off peaks of a stroke lay outside the thresholds, the stroke was identified as a straight stroke (figure 12 A). If both peaks lay within the thresholds, the stroke was identified as a curve stroke (figure 12 C). Otherwise, the stroke was assumed to be a transition between the straight and curve and was labelled as 'other' (figure 12 B and D).

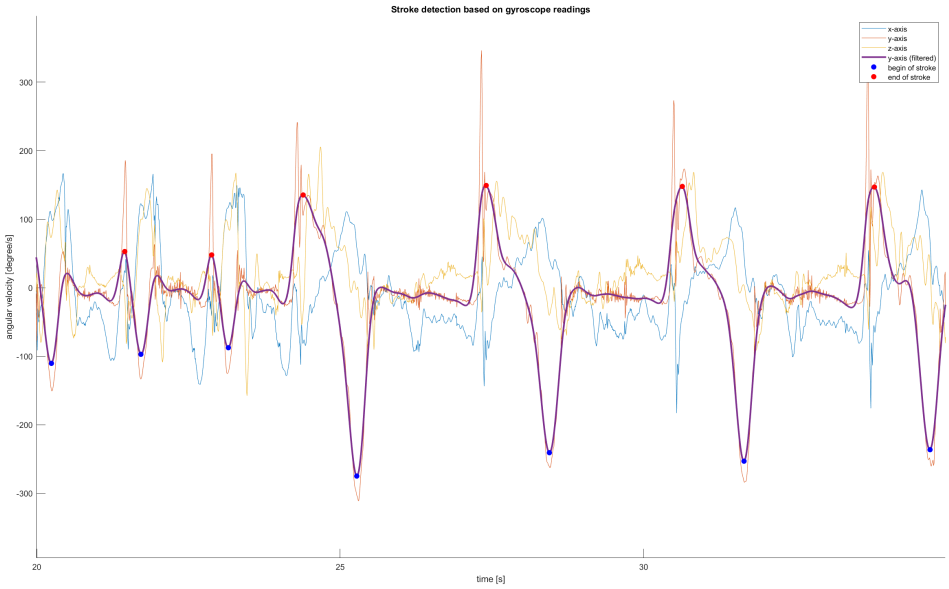

Figure 11: Stroke detection. Low-pass filtered gyroscope readings of the foot y-axis are shown as the purple line. Blue dots represent foot-contact and red dots represent foot-off.

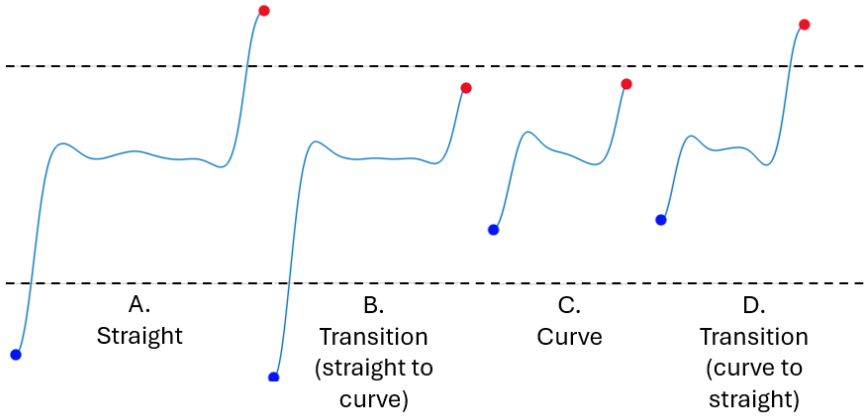

Figure 12: Schematic representation of the low-pass filtered gyroscope signal of the right foot segment y-axis (blue lines) with the foot-on index (blue dots) and foot-off index (red dots) and their peak height relative to the thresholds (black striped lines), given for each label type that could be assigned (A. straight; B. Transition; C. Curve; D; Transition).

The strokes of the left foot were labelled based on the strokes of the right foot because the peaks of the left foot differed less in amplitude between the straights and curves. The boundaries of the sections were defined as the first 'foot-on' of a transition stroke of the right foot. If the 'foot-on' of a left stroke lay within the boundaries of a section, the stroke got the same label as that section (See figure 13).

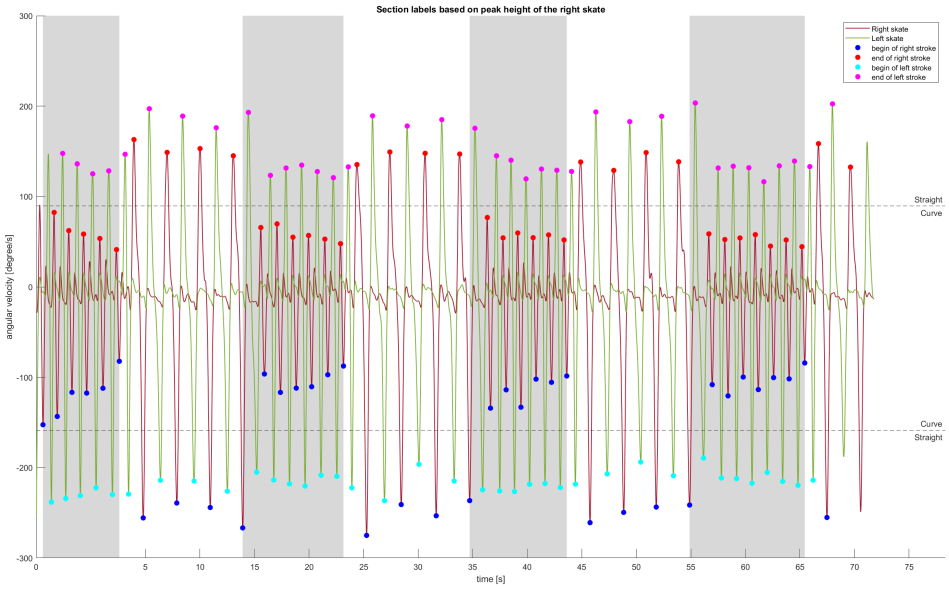

Figure 13: Identification of the straight and curve sections based on the peak height of the gyroscope signal of the right skate. Curves are marked as grey areas. White areas are straights.

2.2.5 Joint angles

The angle between two connected body segments can be calculated if the orientation of these segments is expressed in a shared global reference frame [62]. In this study, 7 DOT sensors were placed on the bodies of the subjects (see section 6), meaning the following 6 joint angles could be estimated: right hip, right knee, right ankle, left hip, left knee, left ankle.

The joint angles were calculated according to the ISB joint coordinate system [58, 64]. First, the DOT segment frames were converted to ISB joint frames by applying a 90-degree counterclockwise rotation around the X-axis of the segment frame, as shown in figure 14.

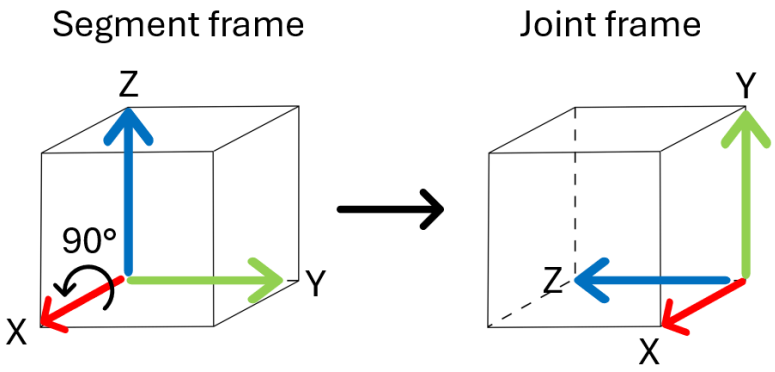

Figure 14: Rotation from segment frame to joint frame by a 90-degree counterclockwise rotation around the X-axis (shown in red).

Second, the orientation of a distal segment with respect to a proximal segment was described in a rotation matrix. This was done by post-multiplying the orientation matrix of the distal segment in the global reference frame with the inverse orientation matrix of the proximal segment in the global

reference frame.

Third, the resulting rotation matrix was converted to Euler angle degrees using the ZXY rotation sequence as proposed by the ISB [64]. This sequence is for most of the joints of the lower body in order of magnitude of range of motion:

- Rotation around the Z-axis: flexion/extension
- Rotation around the X-axis: abduction/adduction
- Rotation around the Y-axis: internal/external rotation

Finally, the Euler angles were converted to anatomical angles. In figure 15, the Euler rotation angle between two segments is shown as a striped pattern. The anatomical joint flexion angle was for the hip and knee calculated as 180 degrees minus the Euler flexion angle. For the ankle, the anatomical flexion angle is equal to the Euler flexion angle, with the plantar flexion angle being positive and the dorsal flexion angle being negative. For all joints, internal rotation and abduction were defined as positive rotations. External rotation and adduction were defined as negative rotations.

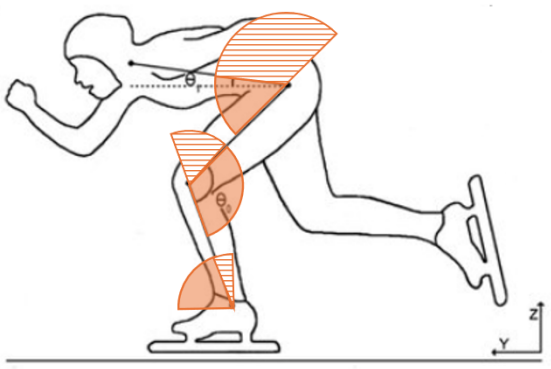

Figure 15: Euler vs anatomical joint angles

The joint angles measured with the MVN system were derived from the MVN Analyze software.

2.2.6 Trunk angle

The trunk angle can be described as the angle between the trunk and the horizontal plane and was calculated as the angle between the vertical Z-axis of the pelvis segment and its projection on the horizontal plane (figure 16). The angle is 90 degrees when standing in the neutral body position and decreases by bending forward.

The trunk angle was calculated for both the DOT sensors and the MVN system. The DOT foot segment orientation was calculated as described in section 2.2.3, and the MVN foot segment orientation was derived from the MVN Analyze software.

2.2.7 Push-off angle

The push-off angle can be described as the angle between the push-off leg and its projection on the horizontal plane [13]. It can be assumed that the push-off force is in line with the vertical axis of the skate [39]. The push-off angle was calculated as the Euler angle of the rotation around the frontal axis of the foot segment. In this way, the push-off angle is described as a rotation around a single axis and not as a combination of rotations. The push-off angle is 90 degrees when standing in a neutral

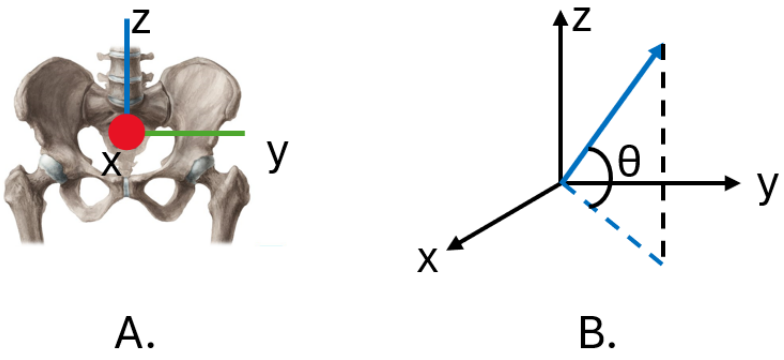

Figure 16: A. Pelvis segment with segment axes; B. Schematic representation of the vertical pelvis axis (blue arrow) and its projection on the horizontal plane (blue striped line) and the angle between these two vectors (theta).

position and decreases towards zero when the skate is leaning towards the medial side (figure 17). The push-off angle was calculated for both the DOT sensors and the MVN system.

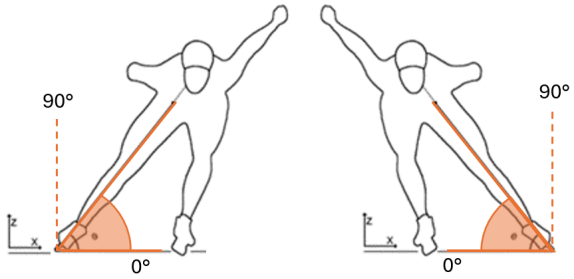

Figure 17: Schematic representation of the push-off angle (orange area) as the angle between the push-off leg and the horizontal. (Adapted from [13])

2.2.8 Push-off force

Force equals mass times acceleration. The body mass of the subjects in this study is unknown. Therefore, to estimate the push-off force, the push-off acceleration was calculated. The linear push-off velocity was calculated as the change in distance between the position of the hip and ankle over time [6]. The ankle position was set to [0,0,0] at all times. The position of the hip with respect to the ankle was calculated based on the length and orientation of the lower leg and upper leg segments. The length of these segments was derived from the MVN biomechanical model and their orientation was calculated as described in section 2.2.3. The angular push-off velocity was calculated as the change in knee flexion angle (see section 2.2.5) over time. Both linear and angular push-off acceleration were calculated as the change in respectively linear and angular velocity over time.

2.2.9 Statistical analysis

The parameters calculated from the DOT sensor data were compared to the parameters derived from the MVN system. All parameters described in the previous subsections (2.2.6,2.2.7 and 2.2.5) were calculated from the data of the DOT sensors. The trunk angle and push-off angle were calculated for

the MVN data as well. The joint Euler angles for the MVN system were automatically calculated in MVN Analyze but were translated to anatomical joint angles.

First, every measurement was split into single strokes, by using the 'foot-on' and 'foot-off' indices (section 2.2.4). For the trunk angle, a stroke was defined as the 'foot-on' of the left skate till the next 'foot-on' of the left skate. For all other parameters, a stroke was defined as a 'foot-on' of one skate till the corresponding 'foot-off' of the same skate, as the focus is on the gliding and push-off phase but not on the repositioning phase. Second, the time length of every stroke was normalized to a length of 100 samples using a cubic spline interpolation function [65]. For every normalized stroke, the Root Mean Squared Error (RMSE) and Pearson Correlation Coefficient between the results of the two sensor systems were calculated. The RMSE is in degrees and represents the absolute difference between the results of the two measurement systems. The Pearson Correlation Coefficient is on a scale from -1 to 1, where 1 means a positive linear correlation and 0 no linear correlation between the results of the two measurement systems.

2.2.10 Exclusion of results

To ensure the accuracy and reliability of the findings, the results of a measurement were excluded from further analysis if they met the following criteria:

- Data from the DOT sensors is missing;
- Data from the MVN system is missing;
- The quality of the MVN calibration is indicated as 'poor' in MVN Analyze;
- The results show a relatively large offset (> 20 degrees) between the results of DOT and MVN that is not seen in other subjects;
- The graphs are shaped differently compared to other subjects and literature, caused by errors in the calibration or stroke detection.

3 Results

In this section, the results of the parameters calculated according to the steps described in chapter 2.2 are presented. The interpretation of these results will be given in section 4.

3.1 Description of the dataset

Carrying out three measurements per subject with nine subjects resulted in a total of 27 measurements. Based on a visual inspection of the results for the presence of the exclusion criteria described in section 2.2.10, the results of the following subjects were excluded for further analysis:

- Subject 3 is excluded from analysis for all parameters because there is no MVN data for this subject due to a technical faillure.
- Subject 7 is excluded from analysis for all parameters. Due to a calibration error, the results are out of range and do not meet the expectations.
- Subject 9 is excluded from analysis for all parameters because the calibration quality of the MVN system was 'poor'.
- Subject 5 is excluded from analysis of the trunk angle because of missing data from the DOT sensor placed at the pelvis.
- The third measurement of subject 2 is excluded from analysis of the left knee angle and left knee angular push-off velocity and acceleration, because of an offset of more than 37 degrees between the DOT and MVN results.

This means that the following measurements were included for analysis of the results:

- Stroke detection: All measurements of subject 1, 2, 4, 5, 6 and 8.
- Knee flexion angle: For the right knee, all measurements of subject 1, 2, 4, 5, 6 and 8. For the left knee all measurements of subject 1, 4, 5, 6 and 8 and measurement 1 and 2 of subject 2.
- Trunk angle: All measurements of subject 2, 4, 6 and 8.
- Push-off angle: All measurements of subject 1, 2, 4, 5, 6 and 8.
- Push-off velocity: For the right leg, all measurements of subject 1, 2, 4, 5, 6 and 8. For the left leg all measurements of subject 1, 4, 5, 6 and 8 and measurement 1 and 2 of subject 2.

A schematic overview of which measurements were included for which analysis is presented in appendix 5.

3.2 Stroke detection

Left and right strokes were identified and labelled based on the gyroscope readings of the DOT sensor placed on top of each skate. A total of eighteen measurements, measured with six subjects (1,2,4,5,6 and 8) were included for analysis of the stroke detection results.

P	1	2	4	5	6	8	mean
Right	129	131	151	115	137	144	134.5
Left	127	132	149	115	136	144	133.8
Total	256	263	300	230	273	288	268.3

Table 1: Number of detected strokes per subject, in total and per skate (left and right).

Table 1 shows for each subject the total number of strokes that were identified and the distribution of the strokes between the right and left skate. The mean number of strokes detected for the right skate was 134.5 and for the left skate 133.8. For all subjects, the number of strokes of the right skate is the same as the number of strokes of the left skate, with a maximum deviation of two. The average number of strokes detected per subject is 268.3. The highest number of 300 strokes is detected for subject 4 and the lowest number of 230 strokes is detected for subject 5.

P	1	2	4	5	6	8	mean
Right straight	39	45	56	34	45	50	44.8
Left straight	49	56	68	44	54	52	53.8
Right curve	67	59	67	60	68	59	63.3
Left curve	78	71	80	71	80	67	74.5
Right other	23	27	28	21	24	35	26.3
Left other	0	5	1	0	2	25	5.5

Table 2: Number of strokes that were assigned a specific label.

Table 2 shows the distribution of the section labels that were assigned to each stroke. Strokes in which the skating technique of the straights was used were labelled as 'straight' and strokes in which the skating technique of the curves was used were labelled as 'curve'. The strokes that involved transitioning from one technique to the other technique were labelled as 'other'.

On average, there were 44.8 right strokes and 53.8 left strokes per subject labelled as 'straight'. For all subjects, more left than right strokes were labelled as 'straight'.

There were 63.3 right strokes and 74.5 left strokes per subject labelled as 'curve' on average. There were more strokes labelled as 'curve' than as 'straight'. For all subjects, more left than right strokes were labelled as 'curve'.

On average, 26.3 right strokes and 5.5 left strokes per subject were labelled as 'other'. The number of right strokes labelled as 'other' was much higher than the number of left strokes labelled as 'other'. Subjects 1 and 5 show zero strokes of the left skate labelled as 'other'. Subject 8 shows the highest number of 25 strokes of the right leg labelled as 'other'.

3.3 Knee flexion angle

The knee flexion angle is calculated as the rotation between the upper leg and lower leg over the frontal axis of the knee joint.

Eighteen measurements of six subjects (1,2,4,5,6 and 8) were included for analysis of the flexion angle of the right knee. Seventeen measurements of six subjects (1,2,4,5,6 and 8) were included for analysis of the flexion angle of the left knee.

Figure 18 shows the flexion angle of the right knee (left graphs) and left knee (right graphs) for strokes on the straights (top graphs) and in the curves (bottom graphs). The shown cycle is averaged over all strokes of the included subjects. The results of the DOT sensors are shown in blue and the results of the MVN system are shown in orange. The normalized stroke time is on the horizontal axis and the knee flexion angle in degrees is on the vertical axis. In appendix 5, the measured knee flexion angle is shown for every subject individually.

The results of the DOT sensors and the results of the MVN system are similar in shape. There is an absolute distance present between the graphs of the two systems which changes over the stroke length.

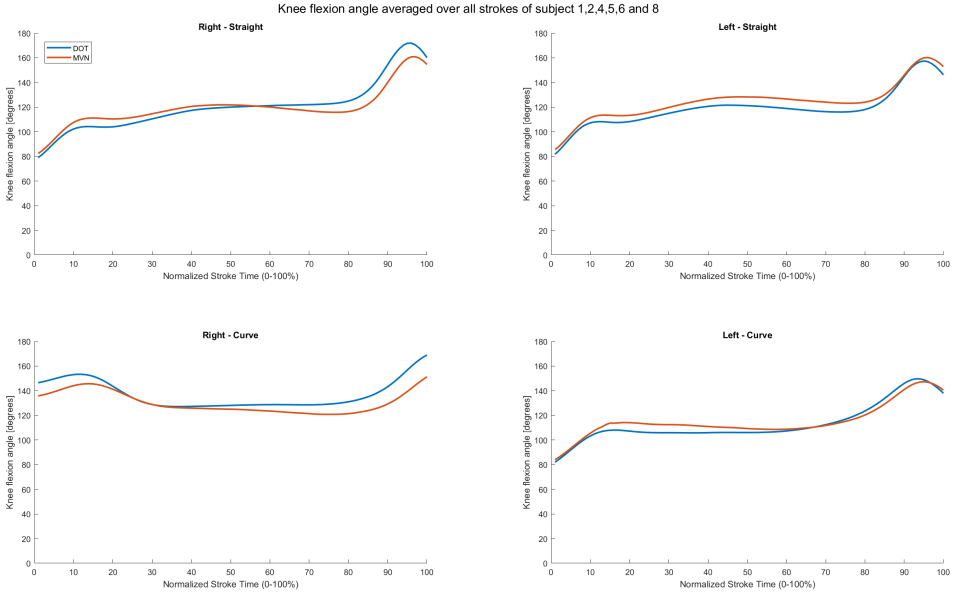

Figure 18: Knee flexion angle over time.

P	1	2	4	5	6	8	mean
RMSE overall	15.0	11.6	15.2	14.0	8.1	14.7	13.9
RMSE Right Straight	15.4	10.5	11.1	12.1	7.1	10.7	11.0
RMSE Left Straight	13.4	14.5	13.1	15.6	6.0	14.4	12.6
RMSE Right Curve	18.3	10.6	13.9	12.4	8.3	12.7	12.9
RMSE Left Curve	13.1	10.7	21.0	15.2	10.1	19.7	15.2

Table 3: Knee flexion angle RMSE in degrees (averaged per subject)

Table 3 shows the RMSE between the knee flexion angle measured with the DOT sensors and the knee flexion angle measured with the MVN system in degrees, averaged over all strokes of each subject. The RMSE ranges from 8.1 to 15.2 degrees with a mean value of 13.9 degrees. The RMSE for the left knee is larger than for the right knee, except for subject 1. The RMSE is on average higher for the strokes in the curves than for the strokes on the straight. The highest RMSE of 21.0 degrees is shown by subject 4 for the left skate in the curves.

P	1	2	4	5	6	8	mean
Pearson overall	0.83	0.93	0.90	0.75	0.93	0.87	0.87
Pearson Right Straight	0.85	0.97	0.91	0.91	0.93	0.94	0.92
Pearson Left Straight	0.73	0.89	0.89	0.79	0.97	0.93	0.87
Pearson Right Curve	0.86	0.89	0.90	0.49	0.90	0.77	0.80
Pearson Left Curve	0.85	0.96	0.90	0.88	0.93	0.87	0.90

Table 4: Knee flexion angle Pearson correlation coefficient (averaged per subject)

Table 4 shows the Pearson Correlation Coefficient between the knee flexion angle measured with the DOT sensors and the knee flexion angle measured with the MVN system on a scale of 0 to 1, averaged per subject. All subjects show a mean correlation > 0.75, which can be considered a strong

correlation. There is no large difference in correlation between the right and left knee and between the straights and the curves. The correlation for the right knee of subject 5 in the curves is low compared to the other subjects.

3.4 Trunk angle

The trunk angle was calculated as the angle between the vertical axis of the pelvis segment and its projection on the horizontal plane, for both the DOT sensors and the MVN system. The orientation of the pelvis segment was derived from a sensor placed on the pelvis.

A total of twelve measurements, measured with four subjects (2,4,6 and 8) were included for analysis of the trunk angle.

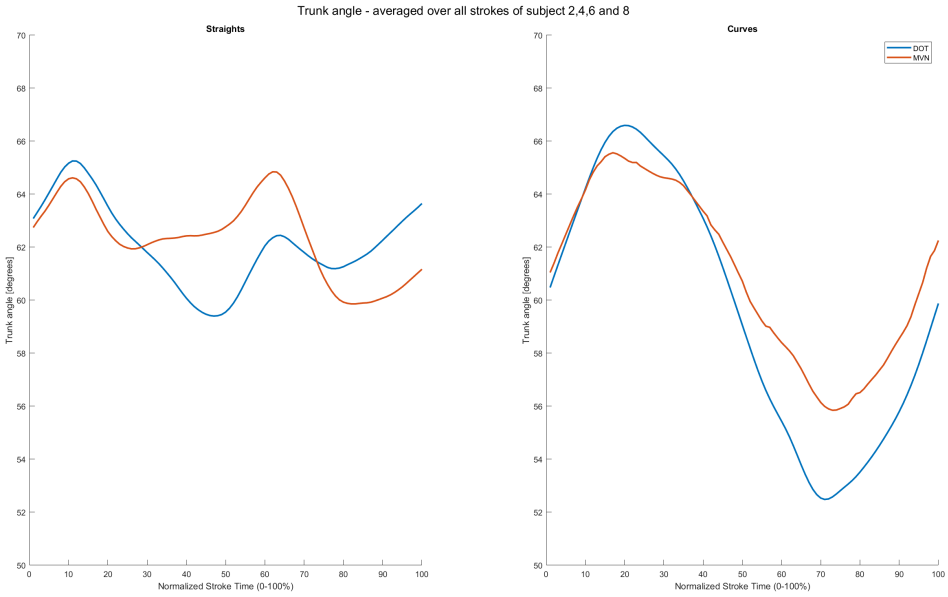

Figure 19: Averaged trunk angle cycle over time. Blue lines are results measured with DOT sensors. Orange lines are results measured with the MVN system.

Figure 19 shows the trunk angle averaged over all strokes of the included measurements. The graph on the left shows the trunk angle for strokes on the straight part of the ice rink and the graph on the right shows the trunk angle for strokes in the curves. The normalized stroke time is on the horizontal axis and the trunk angle in degrees is on the vertical axis. The trunk angle measured with the DOT sensors is shown by the blue lines and the trunk angle measured with the MVN system is shown by the orange line. In appendix 5, the measured trunk angle is shown for every subject individually.

The graphs of the DOT and MVN show a similar sine wave shape for strokes in the curves. The graphs for the strokes on the straights are less similar in shape. They both show positive peaks at the same location in the stroke cycle but are different in peak height. The measured trunk angle is between 50 and 70 degrees for both the DOT sensors and the MVN system.

Table 5 shows the RMSE between the trunk angle measured with the DOT sensors and the trunk angle measured with the MVN system, averaged over all strokes of each subject. For all subjects, the RMSE is between 4.6 and 5.7 degrees, with an average of 5.3 degrees per stroke. On average, the RMSE is larger for strokes in the curves than for strokes on the straights. Only for subject 8, the RMSE is larger for strokes on the straight.

P	2	4	6	8	mean
RMSE overall	4.6	5.7	5.3	5.4	5.3
RMSE straight	4.2	4.6	4.8	5.7	4.8
RMSE curve	4.9	6.6	5.6	5.2	5.6

Table 5: Trunk angle RMSE in degrees averaged over all strokes of a subject, averaged over the straight strokes of a subject and averaged over curve strokes of a subject.

P	2	4	6	8	mean
Pearson overall	0.85	0.78	0.81	0.49	0.74
Pearson straight	0.81	0.71	0.67	-0.06	0.56
Pearson curve	0.88	0.84	0.91	0.91	0.88

Table 6: Trunk angle Pearson Correlation Coefficient in degrees averaged over all strokes of a subject, averaged over the straight strokes of a subject and averaged over curve strokes of a subject.

Table 6 shows the Pearson Correlation Coefficient between the trunk angle measured with the DOT sensors and the trunk angle measured with the MVN system, averaged over all strokes of each subject. The mean correlation was found to be 0.74. For subjects 2, 4 and 6, the correlation between the DOT and MVN results is higher than 0.7 and can be considered as strong. For subject 8, the correlation is less than 0.5 and is considered weak. It is noticeable that subject 8 shows a very strong correlation for the strokes in the curves but no correlation for the strokes on the straight. All subjects show a higher correlation for strokes in the curves compared to strokes on the straights.

3.5 Push-off angle

The push-off angle was calculated as the Euler rotation angle around the X-axis of the foot segment, where there is a rotation of zero degrees when standing upright.

A total of eighteen measurements, measured with six subjects (1,2,4,5,6 and 8) were included for analysis of the push-off angle of both the right and left skate.

Figure 20 shows the push-off angle of the right skate (left graph) and left skate (right graph) for the straights (top graphs) and curves (bottom graphs) over the stroke cycle. The shown cycle is averaged over all strokes of the included subjects. The push-off angle measured with the DOT sensors is shown in blue and the push-off angle measured with the MVN system is shown in orange. The normalized stroke time is on the horizontal axis and the push-off angle in degrees is on the vertical axis. In appendix 5, the measured push-off angle is shown for every subject individually.

In all four graphs, the push-off angle measured with the DOT sensor is similarly shaped as the push-off angle measured with the MVN system. The absolute distance between the two graphs is larger for strokes in the curves than for strokes on the straights. For the right skate, the push-off angle measured with the DOT sensor is smaller than the angle measured with the MVN system. For the left skate is the angle measured with the DOT sensor larger than the angle measured with the MVN system. The range of motion of the averaged push-off angle is in the range of 40-115 degrees on the straights and 40-85 degrees for the right skate in the curves and 100-140 degrees for the left skate in the curves.

Table 7 shows the RMSE between the push-off angle measured with the DOT sensors and the push-off angle measured with the MVN system, averaged over all strokes of each subject. The mean RMSE over all strokes of a subject lies within the range of 8.4 to 12.2 degrees, with an average of 9.4 degrees. For most subjects is the overall RMSE for the left skate slightly larger than the RMSE for the right

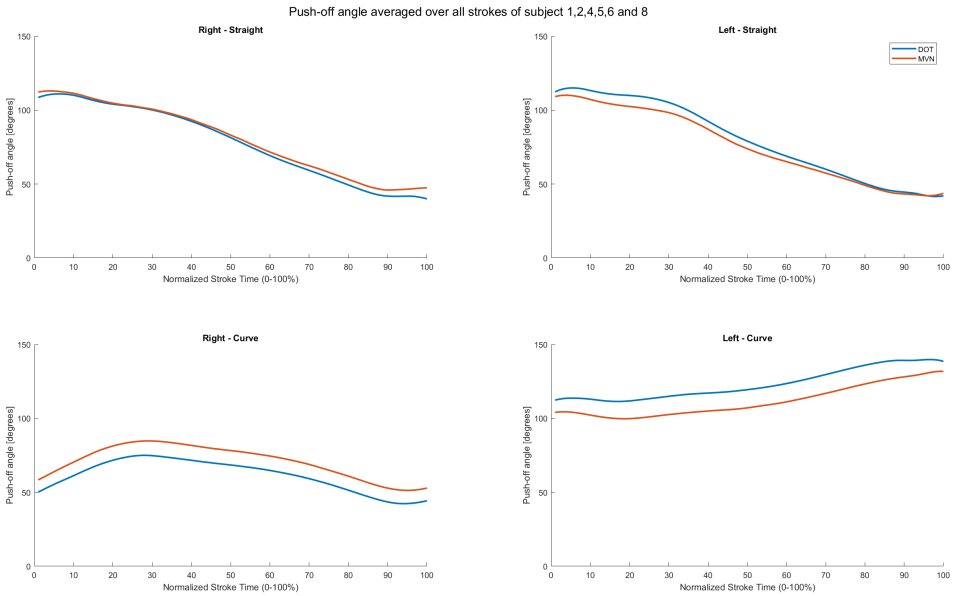

Figure 20: Push-off angle of the right and left skate on the straights and in the curves, averaged over all strokes. The blue line represents the DOT sensor, the orange line represents the MVN system.

P	1	2	4	5	6	8	mean
RMSE overall	8.8	8.4	8.7	12.2	9.7	8.6	9.4
RMSE Right Straight	5.3	6.2	6.2	9.1	5.9	4.8	6.1
RMSE Left Straight	5.4	5.0	6.9	8.4	5.6	4.7	6.0
RMSE Right Curve	9.7	10.4	9.2	12.5	12.1	11.5	10.9
RMSE Left Curve	12.4	10.8	11.4	15.9	12.4	11.8	12.4

Table 7: Push-off angle RMSE in degrees, averaged per subject.

skate. The RMSE for the strokes in the curves is almost two times as high as the RMSE for the strokes on the straights.

P	1	2	4	5	6	8	mean
Pearson overall	0.97	0.96	0.95	0.99	0.98	0.98	0.97
Pearson Right Straight	0.99	0.99	0.98	0.99	1.00	0.99	0.99
Pearson Left Straight	0.99	0.99	0.98	0.99	1.00	1.00	0.99
Pearson Right Curve	0.98	0.99	0.95	0.99	0.99	0.97	0.98
Pearson Left Curve	0.95	0.90	0.90	0.98	0.96	0.98	0.94

Table 8: Push-off angle Pearson Correlation Coefficient, averaged per subject.

Table 8 shows the Pearson Correlation Coefficient between the push-off angle measured with the DOT sensors and the push-off angle measured with the MVN system, averaged over all strokes of each subject. The Pearson Correlation Coefficient between the results of the two systems is for every subject larger than 0.95, which can be considered as a very strong correlation. The correlation for the strokes in the curves is slightly less than for the strokes on the straights, but still very strong. The difference between the right and left skate is increased in the strokes in the curves compared to the

strokes on the straights.

3.6 Push-off force

To estimate the push-off force, the push-off velocity and push-off acceleration were calculated from the DOT data. The results were not compared against the MVN system.

Eighteen measurements of six subjects (1,2,4,5,6 and 8) were included for analysis of the push-off velocity and acceleration of the right skate. Seventeen measurements of six subjects (1,2,4,5,6 and 8) were included for analysis of the push-off velocity and acceleration of the left skate.

Figure 21 shows the push-off velocity (left graph) and acceleration (right graph) over the strokes on the straights, averaged over all left and right strokes on the straights of the included measurements. The linear velocity and acceleration are shown by the blue line and the angular velocity and acceleration are shown by the red line. In appendix 5 and 5, the measured push-off velocity and acceleration are shown for every subject individually.

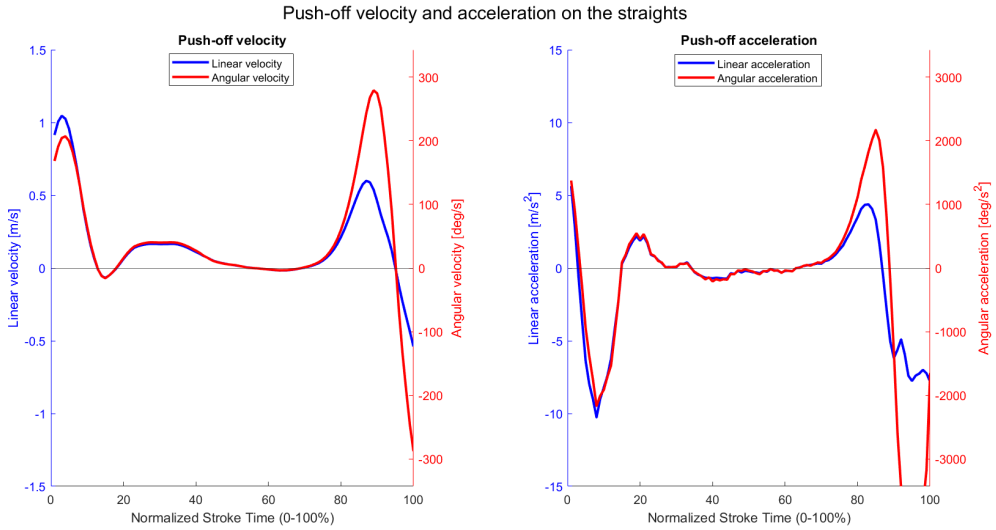

Figure 21: Linear (blue line, left vertical axis) and angular (red line, right vertical axis) push-off velocity (left) and acceleration (right) on the straights. The black horizontal line is the zero line.

A positive velocity means that the distance between the ankle and the hip is increasing or that the knee is extending. A negative velocity means that the hip is moving towards the ankle or that the knee is flexing.

The peak on the very left in the velocity graph is caused by the skate moving away from the hip, towards the floor to place the skate on the ice. The first negative peak around 15% of the stroke time is when the gliding leg starts supporting the body weight, followed by pushing the hip a little upwards. The high peak starting around 80% of the stroke time is the explosive push-off.

In the acceleration graph, the first peak around 20% of the stroke time is the counteracting of the body weight during the transfer from the push-off leg to the new supporting leg [6, 18]. Then, a centrifugal force due to a passive falling movement in which the body and supporting leg act like an inverted pendulum, causes a minimum in the middle of the gliding phase. The last positive peak is caused by a short and explosive push-off, just as in the velocity graph.

Both the linear and angular velocity graphs show the high peak at the end of the stroke cycle like the graphs in literature [6, 14, 18] (figure 2). The average maximum linear push-off velocity is 0.6

m/s, while in literature a maximum of 1.6 m/s is presented [6]. For the angular velocity, the results show a maximum of 280 deg/s on average, while literature [14] shows a maximum of 600 deg/s. The shape of the linear and angular acceleration graphs is the same as the shape of the graphs presented in literature [6, 18], with the two positive peaks and the minimum in between. The maximum linear push-off acceleration is 4.4 m/s^2 on average. For the angular acceleration is this 2170 deg/s^2.

For both the velocity and acceleration, the height difference between the second peak (at 80-100% of the stroke time) and the first peak (at 20-40% of the stroke time) is larger for the angular method compared to the linear method.

4 Discussion

This study was set up with the goal of analysing the potential use of the Movella DOT sensors in capturing performance-related parameters of speed skaters on the indoor ice rink. To achieve this goal, an algorithm for calculating these performance-realted parameters was developed first (described in section 2). Second, the feasibility and accuracy of the Movella DOT sensors in capturing these parameters were validated (presented in section 3). In this section, the findings of this research will be discussed for every parameter separately.

4.1 Stroke detection

The results indicate that an average of 268.3 strokes per subject were detected. For the right and left skates, an average of 44.8 and 53.8 strokes per subject were identified as strokes on the straights, 63.3 and 74.5 strokes per subject as strokes in the curve, and 26.3 and 5.5 strokes per subject as transitional strokes. For all six subjects, the total number of right strokes was equal to the number of left strokes, with a maximum deviation of two strokes.

It was expected that a skater would perform 6-10 strokes per leg on the straight parts and 14-16 strokes per leg in the curves over a complete 400-m lap [40]. For each lap, an estimate of four strokes of the right skate would be labelled as transition strokes. All subjects skated 6 laps in total during the measurements. This corresponds to an expected total of 120–156 strokes per leg, including 36–60 strokes per leg on the straights, 84–96 in the curves, and 24 right-leg strokes labelled as “other”. Five out of six subjects met these expectations, indicating that the stroke detection method performed well overall. However, subject 5 showed fewer strokes than expected, suggesting possible issues with the detection algorithm or a relatively low stroke frequency.

The labelling of the strokes showed more variability in the results. There were fewer right than left strokes labelled as ’straight’ or ’curve’, causing an imbalance in the right and left strokes per stoke type. This could be explained by the possible misclassification of some right strokes as “other,” which reduced the number of strokes labelled as "straight" or "curve." For five subjects, the number of strokes labelled as "straight" matched the expectations for both skates. For subject 5, the lower total number of detected strokes also resulted in fewer strokes labelled as "straight" for the right skate. Subject 4 had more strokes of the left leg labelled as "straight" than expected.

The number of strokes labelled as "curve" was lower than expected for all subjects. This implies that either the expected number of strokes in the curve was overestimated or that the algorithm did not detect or label all strokes in the curves correctly. In contrast, the labelling of "other" strokes showed some alignment with the expectations, as more right than left strokes were labelled as "other". However, only two subjects matched the exact expected number of zero left strokes labelled as "other". Again, subject 5 showed fewer right strokes labelled as "other" than expected. Subject 8 showed significantly more left and right strokes labelled as "other" than expected.

Overall, the stroke detection algorithm successfully identified the start and end points and therefore the number of performed strokes for five out of six subjects. This confirms the feasibility of the method. However, the results of the labelling show limitations in the accuracy of the used method.

While previous studies have already demonstrated reliable methods for stroke and section detection based on IMU sensors placed on the skates [7, 11, 34], this thesis does not provide new insights into this topic other than supporting its feasibility.

A significant limitation of this study is the lack of validation against a second measurement system or manual stroke detection. This means that the true accuracy of the detection and labelling algorithms cannot be assessed. For example, even if the number of detected strokes matches the expectations,

the beginning and end of each stroke may be detected inaccurately. This will influence the shape of the graph of a parameter, but will not result in a larger difference between the DOT and MVN results, as the same interval is selected for both systems. Another limitation is the dependency of the stroke detection algorithm on the quality of the sensor-to-segment calibration of the DOT sensors. Errors in the calibration could lead to inaccuracies in both the stroke detection and labelling.

To improve the accuracy of the stroke detection algorithm, future studies should combine the high- and low-frequency components of the gyroscope signal to detect the start and end of a stroke more precisely, as proposed by Tomita et al. [34]. Furthermore, placing the DOT sensor on the bridge of the skate, which provides a firmer underground than the top of the skate shoe, might result in higher impact peaks in the signal that are easier to detect. Aligning the sensor with the skate frame eliminates the need for sensor-to-segment calibration and the chance of corresponding errors, which simplifies the setup process. Finally, it is recommended to validate the stroke detection and labelling algorithms against a second measurement method, such as video analysis or manual stroke detection. This is needed to establish the accuracy of the proposed method.

4.2 Knee flexion angle

The knee flexion angle was calculated as the Euler angle between the upper and lower leg around the frontal axis, using the orientation of the upper and lower leg, measured with two DOT sensors. The results showed a mean RMSE of 13.9 degrees and a mean Pearson Correlation Coefficient of 0.87 between the knee flexion angles measured with the DOT sensors and those measured with the MVN system. These results suggest a strong correlation but also a relatively large error.

For strokes on the straights, the knee flexion angle is expected to range from 100 to 130 degrees during the gliding phase [6], and to reach 170 degrees at the end of the push-off [16]. These values correspond to the results presented in this thesis, where the shape of the graph also corresponds to the graphs in literature (figure 3) [6]. This indicates that the DOT sensors are capable of capturing the knee flexion angle as the Euler angle between the upper and lower leg.

However, the mean RMSE of 13.9 degrees is a significant error, especially compared to other studies where RMSE values of 5.66-6.66 degrees and a Pearson Correlation Coefficient of 0.98 were reported for knee flexion angles during walking measured with the DOT sensors and the MVN Awinda system [54]. It is important to note that this previous study subtracted the offset of the DOT and MVN results, such that both curves started at zero degrees. Additionally, walking mainly occurs in the sagittal plane, while the speed skating movement happens in the 3D space. These differences in methodology and motion explain the higher RMSE and lower Pearson Correlation coefficient in this thesis.

It is explainable that the errors for joint angles are larger than for the trunk and push-off angles. To calculate a joint angle, the orientation of two segments is used as input. For the trunk and push-off angle, this is only one segment. If each segment has a small error in its estimated orientation, this adds up when calculating the joint angle.

In this thesis, the results for knee flexion angle on the straights were more accurate than those for the curves, with a lower RMSE and a higher Pearson Correlation Coefficient. A possible explanation is that the gravitational forces and the change of direction in the curves make the orientation estimate of the sensor less accurate. These factors make the joint angle measurements in the curves more prone to error than those on the straights.

Furthermore, the reliability of the MVN system as a validation method must be considered. A concurrent validation study compared the MVN system to the Vicon motion capture system and found a mean difference of 11.33 degrees and a cross-correlation of 0.99 for knee flexion angles during change-of-direction tasks. These results suggest that the knee flexion angle provided by the MVN

system has a relatively large error during change-of-direction tasks. The exact accuracy of the DOT sensor can not be determined from the results in this thesis but is expected to be in the same range as the presented results.

While this study demonstrates the feasibility of using the DOT sensors for measuring the knee flexion angle, the relatively large RMSE in combination with a strong correlation indicates that the error is caused by inaccurate calibration. An improvement of the calibration procedure will likely reduce the error.

In this thesis, only the knee flexion angle was analysed. In future work, the hip and ankle flexion angle, as well as the rotation and abduction of these joints, can be estimated using the same method. However, it is expected that movements outside the sagittal plane will be measured less accurately than movements in the sagittal plane [43].

In summary, this thesis demonstrates the potential of the DOT sensors in measuring the knee flexion angle during speed skating with a strong correlation to the MVN system. However, the relatively large RMSE implies the need for improvement of the calibration and validation protocols. The analysis of other joint angles will enhance the potential of the DOT sensors in speed skating.

4.3 Trunk angle

The trunk angle was calculated as the angle between the vertical axis of the pelvis segment and its projection on the horizontal plane. The results showed an average RMSE of 5.3 degrees and an average Pearson Correlation coefficient of 0.74 between the measurements of the DOT sensors and the MVN system. The measured trunk angle ranged between 50 and 70 degrees.

The RMSE for the trunk angle between the two systems is 5.3 degrees on average, which can be considered relatively low. However, it should be taken into account that the trunk angle has a small range of motion of only 20 degrees. The Pearson Correlation Coefficient of 0.74 is only moderate. This mean value is negatively influenced by the absence of correlation in subject 8 for the strokes on the straights.

According to de Koning et al. [6], the trunk angle ranges between 10 and 30 degrees. In contrast, the results in this thesis show a trunk angle of 50-70 degrees. In this thesis, the angle between the pelvis and the horizontal is measured and not the angle between the line from hip to neck and the horizontal (which is more like the trunk angle). This implies that the orientation of the pelvis segment is not a good indicator of the trunk angle, as the trunk angle is smaller than the pelvis angle. These findings should be taken into account when considering measuring the trunk angle with IMU sensors.

To improve the accuracy of estimating the trunk angle, further research should include determining a better location for the IMU sensor(s). Promising locations might be the sternum, C7 or (in between) the scapulae. As the spine is not a rigid body, it might be necessary to use a combination of multiple sensors to estimate the rounding of the back. However, researchers must consider the practical constraint of a maximum of seven DOT sensors in a set-up, which limited the options for sensor placement in this study.

4.4 Push-off angle

The push-off angle was calculated as the Euler abduction angle between the vertical axis of the foot segment and the horizontal plane, with a push-off angle of 90 degrees when standing upright. The results show a mean RMSE of 9.4 degrees and a mean Pearson Correlation Coefficient of 0.97 between the push-off angle measured with the DOT sensors and the MVN system. The measured push-off angle ranged between 40 and 115 degrees over time during strokes on the straights.

According to van der Kruk et al. [7], the range of motion of the push-off angle during speed skating is between 30 and 130 degrees. The results in this thesis correspond to these values. On the straight, the push-off angle is expected to be larger than 90 degrees during the foot contact and to decrease during the gliding- and push-off phase. In the curves, the right skate is placed on the ice on the medial side of the blade, and the left skate is placed on the lateral side of the blade. As a result, the push-off angle of the right skate won't be larger than 90 degrees and the push-off angle of the left skate won't be smaller than 90 degrees, as shown in figure 20.

The average RMSE between the push-off angle measured with the DOT sensors and the MVN system was 9.4 degrees. Similar to the results of the knee flexion angle, the RMSE for the strokes in the curves is almost two times as high as for the strokes on the straights. This may be due to the gravitational forces and the change of direction in the curves, which might influence the estimate of the sensor orientation. Additionally, the used setting of the MVN system (single level) does not allow for a gliding movement of the feet and thus possibly not taking the change of direction of the skate in the curve into account. However, this last argument is only a guess as Movella does not provide full insight into their biomechanical model.

Van der Kruk et al. [7] reported a mean RMSE of 5.3 and 3.6 degrees for the push-off angle of the right and left skate on the straights, measured with IMU sensors placed on the skate and validated against a Qualysis system. In this thesis, a mean RMSE of 6.1 and 6.0 degrees were obtained for the right and left skate on the straights, measured with DOT sensors and validated against the MVN system. As discussed in section 4.2, the results of the MVN system might be inaccurate. The error between the DOT sensor and the MVN system might be different than the error between the DOT sensor and optical motion capture systems like Qualysis or Vicon. Therefore, the exact accuracy of the DOT sensor can not be determined from the results in this thesis, but is expected to fall in the same range as the presented values.

The average Pearson Correlation Coefficient of 0.97 indicates a very strong correlation between the push-off angle measured with the DOT sensors and the MVN system. This very strong correlation in combination with a relatively large RMSE suggests that the error is caused by differences in calibration. A more precise calibration protocol will improve the accuracy of the results.

The findings indicate that the push-off angle can be calculated as the Euler rotation angle around the sagittal axis of the foot. The orientation of the foot can be estimated by placing one DOT sensor on each skate. The results from the DOT sensor are very strongly correlated to the results of the MVN system. However, the accuracy can be improved by performing a better calibration method.

A possible limitation of the presented method for the calculation of the push-off angle is that the eversion of the ankle joint is not taken into account. Whether this is a problem depends on the definition that is used for the push-off angle. This might be an interesting topic to elaborate on in further research.

4.5 Force estimation

The push-off force can be estimated as the push-off acceleration times the mass of the skater. However, since the masses of the skaters were unknown in this study, only the push-off accelerations were calculated. Two methods were used to calculate the push-off velocity and acceleration: the linear velocity at which the hip moves away from the ankle and the angular velocity of the knee extension. Both methods used the orientation of the upper and lower leg, measured by sensors placed on these segments. The linear method used the segment length as input as well.

The similar shapes of the linear- and angular graphs (figure 21) can be explained by the dependence of the hip-ankle distance on the knee flexion angle.

At first sight, the graphs of both the velocity and acceleration do correspond to the graphs presented in the literature (figure 2). They all show two peaks with a minimum in between. However, the values of the measured push-off peaks are lower than those reported in the literature. In addition, the second peak of the linear acceleration was not significantly higher than the first peak, as seen in the literature.

The differences in results might be explained by differences in methodology. For instance, the linear velocity was in this thesis calculated in 3D space. If the literature focuses only on the velocity in the horizontal direction, the passive falling movement of the skater is taken into account. A difference in the definition of the push-off velocity may explain a lower push-off peak than expected.

However, this does not explain the difference in peak height between the linear and angular methods or between the angular method and the literature. The angular method neither includes the passive falling movement. Furthermore, in this thesis and in the literature the angular velocity was calculated as the derivative of the knee flexion angle.

Another explanation for the difference in peak height of the results in this thesis compared to the results in the literature is the fact that the results in the literature were measured on fixed skates and this thesis measured skaters wearing clap skates. By being able to perform plantar flexion with the clap skates, the push-off can be spread over a longer period of time and a larger range of motion, possibly decreasing the peak velocity. The plantar flexion of the ankle is not taken into account in calculating the velocity in this thesis. It is expected that including the ankle plantar flexion would increase the push-off velocity. And last, the measurements in literature were performed during World Cup races. It is possible that these skaters did perform on a higher level than the skaters included in this thesis and thus produced a higher push-off force.

The first step for further research on the push-off acceleration in this dataset would be to analyse the results for the strokes in the curves. Furthermore, the push-off velocity and acceleration should be calculated in the horizontal direction, as only horizontal forces contribute to the push-off power. To do so, the orientation of the skate must be known. The hip position can be expressed in the frontal plane of the skate and the push-off velocity over the frontal axis can be estimated. The angular velocity cannot be converted to horizontal velocity, as this parameter is not expressed in 3D space. In addition, the ankle plantar flexion during the push-off can be taken into account. For the linear method, the orientation and dimensions of the skate should be known. For the angular method, the ankle flexion angle should be used as an input. Last, the relation between the push-off acceleration calculated according to the method proposed in this thesis and the push-off force measured with an instrumented skate should be analysed.

The results of the push-off velocity and acceleration presented in this thesis can give a coach or skater insight into the timing of the push-off. Even though the peak height might not be an accurate representation of the push-off force, the peak width and the location of the peak do give information on respectively the explosiveness and distribution of the push-off.

In conclusion, the push-off acceleration measured with the DOT sensor on the lower and upper leg is a promising parameter for estimating the push-off force. Even though the magnitude of the presented results is different from the results in other studies, the shape of the graph can provide insight into the timing and explosiveness of the push-off. The next step would be to estimate the horizontal component of the push-off force as the acceleration in the horizontal direction.

4.6 Calibration

The results of the push-off angle and the knee flexion angle suggest that the sensor-to-segment calibration method of the DOT sensors should be improved to reduce the RMSE. Several factors influencing the calibration process were identified and discussed below.

The DOT sensors have a function called 'heading reset' which ensures that the orientation estimates of all sensors are expressed within the same global reference frame [53]. Unfortunately, this function was not used during the measurements of this study. Consequently, each sensor had its own global reference frame. The heading of the sensor global reference frames was aligned based on the orientation of the segments provided by the MVN system. As a result, the quality of the sensor-to-segment calibration of the DOT sensors depends on the accuracy of the sensor-to-segment calibration of the MVN system.

Additionally, subjects had to perform certain movements during the functional calibration to determine the segment rotation axis in the sensor frame. It is unlikely that all rotations were pure movements. Especially the ankle flexion was hard to perform for some of the subjects. It is expected that calculating the rotation axes this way might result in errors.

The quality of the sensor-to-segment calibration was not evaluated in this thesis. Each DOT measurement was calibrated individually, and the quality of the calibration procedure has a significant influence on the resulting parameters.

To improve future measurements with the DOT sensor, the following steps are recommended:

For future measurements with the DOT sensors, it is recommended to use the 'heading-reset' function. This way, it is not needed to align the sensor reference frames based on a known body pose.

Second, an alternative movement to find the axes of the foot segment is to rotate the foot over the sagittal axis, from the inside to the outside of the blade and back while standing on both skates, to determine the X-axis instead of the Y-axis. It is expected that this movement is easier to perform and less prone to errors than flexion of the ankle.

A third recommendation is to explore whether combining static and functional calibration, followed by applying a heading reset based on an N-pose, provides comparable results to only a static calibration based on the N-pose. In both cases, it is assumed that the segment frames are aligned with the global reference frame. The static N-pose calibration takes less time and is easier to perform for the subject than the functional calibration, making it a potentially more practical option.

Finally, the settings of the MVN system that were used in this thesis should be evaluated. The MVN data was processed using the 'single level' setting, in which zero velocity updates are applied. In this setting, the software does not recognise foot sliding, resulting in jerky parameter graphs. The 'no level' setting might be more suitable for skating and should be considered in future analyses.

By implementing these recommendations, the accuracy and reliability of the sensor-to-segment calibration, as well as the overall quality of the measurements, can be improved.

4.7 Validation

In this thesis, the results derived from the DOT sensors are validated against those from the MVN system. However, the performance of the MVN system in speed skating is unknown. Prior studies have shown that the MVN system provided similar shaped joint angles with a relatively high amplitude difference during change-of-direction movements compared to the Vicon system [50]. As a consequence, it cannot be assumed that the speed skating parameters derived from the MVN system are correct. In addition, most studies validate their measurements against video analysis, making it hard to compare the present results with existing literature.

It is recommended to validate both the DOT results and MVN against video analysis. This would establish the reliability of the derived parameters. If the MVN system is considered valid in speed

skating, it could be used for validation in future studies. Unfortunately, the video footage collected in this study is unsuitable for such validation due to poor quality.

Once validated, the proposed sensor set-up in combination with the algorithm can be used by coaches to monitor the performance of a skater. The absolute values of the measured parameters but also the changes over time and the difference between individuals might provide a better insight into the speed skating technique and its relation to performance, which is of interest for coaches, athletes and scientists.

The ultimate goal is to provide speed skaters (near) real-time feedback on the measured parameters. In order to achieve this, the developed algorithm must be adjusted to perform real-time calculations. The DOT sensors already allow real-time data streaming via Bluetooth.

5 Conclusion

In this section, the conclusion of the results given in section 3 and discussed in section 4 will be drawn and the research goal will be answered.

This study aimed to analyse the potential use of the Movella DOT sensors in capturing performance-related parameters of speed skaters on the indoor ice rink. To achieve this, an algorithm for calculating these parameters was developed, and the feasibility and accuracy of the DOT sensors in capturing these parameters were validated against the MVN system.

The findings demonstrate that the number of performed strokes can be detected in the gyroscope signal of a DOT sensor placed on each skate. However, the accuracy of the stroke detection and the identification of the stroke type (straight or curve) should be further validated and improved. Since there are already accurate methods for stroke detection presented in the literature, it is recommended to implement these existing methods.

With the currently used set-up of the DOT sensors, which involved a sensor on the back of the pelvis segment, it was not possible to accurately measure the trunk angle. Alternative sensor placements should be explored for estimating the trunk angle with IMU sensors.

The push-off angle and the knee flexion angle were successfully calculated using the DOT sensors. The push-off angle was calculated as the Euler rotation angle around the sagittal axis of the foot, and the knee flexion angle was calculated as the Euler angle between the upper and lower leg. The orientation of the foot can be estimated by placing one DOT sensor on each skate and the orientation of the upper and lower leg by placing one DOT sensor on each segment. For both the push-off angle and knee angle, there was a strong correlation between the results of the DOT sensors and the MVN system. However, the error between the results was relatively large, likely due to calibration issues. Improving the calibration protocol is expected to decrease these errors.

The push-off acceleration measured with DOT sensors on the lower and upper leg is a promising estimate of the push-off force. Although the magnitude of the results did not fully correspond to those in other studies, the shape of the graph provides insight into the timing and explosiveness of the push-off. Future research should focus on estimating the horizontal component of the push-off acceleration, as the horizontal force directly contributes to propulsion.

In summary, the DOT sensors are an affordable and low-invasive method for collecting kinematic data of speed skating-specific parameters, such as the stroke cycle, the push-off angle, the knee flexion angle and the push-off acceleration. Future research should focus on improving the calibration protocol, validating the results of the DOT sensors against video analysis and exploring the potential for real-time feedback.

References

[1] Gerard H. Kuper and Elmer Sterken. Endurance in speed skating: The development of world records. *European Journal of Operational Research*, 148(2):293–301, 7 2003. ISSN 0377-2217. doi: 10.1016/S0377-2217(02)00685-9.

[2] World record progression 10,000 m speed skating men - Wikipedia, . URL https://en.wikipedia.org/wiki/World_record_progression_10,000_m_speed_skating_men.

[3] Klapschaats - Wikipedia, . URL https://nl.wikipedia.org/wiki/Klapschaats.

[4] Jos J. De Koning. World records: How much athlete? How much technology? *International Journal of Sports Physiology and Performance*, 5(2):262–267, 2010. ISSN 15550265. doi: 10.1123/IJSPP.5.2.262.

[5] E. van der Kruk, A. L. Schwab, F. C.T. van der Helm, and H. E.J. Veeger. Getting in shape: Reconstructing three-dimensional long-track speed skating kinematics by comparing several body pose reconstruction techniques. *Journal of Biomechanics*, 69:103–112, 3 2018. doi: 10.1016/J.JBIOMECH.2018.01.002.

[6] J.J. de Koning and G.J. van Ingen Schenau. Performance-Determining Factors in Speed Skating. In *Biomechanics in Sport*, pages 232–246. Wiley, 1 2000. doi: 10.1002/9780470693797.ch11. URL https://onlinelibrary.wiley.com/doi/10.1002/9780470693797.ch11.

[7] E. Van Der Kruk, A. L. Schwab, F. C.T. Van Der Helm, and H. E.J. Veeger. Getting the Angles Straight in Speed Skating: A Validation Study on an IMU Filter Design to Measure the Lean Angle of the Skate on the Straights. *Procedia Engineering*, 147:590–595, 1 2016. ISSN 1877-7058. doi: 10.1016/J.PROENG.2016.06.245.

[8] Todd L. Allinger and Anton J. Van Den Bogert. Skating technique for the straights, based on the optimization of a simulation model. *Medicine and Science in Sports and Exercise*, 29(2), 1997. ISSN 01959131. doi: 10.1097/00005768-199702000-00018.

[9] Ruud W De Boer, Paul Schermerhorn, Jan Gademan, Gert De Groot, and Gerrit Jan Van Lngen Schenau. Characteristic Stroke Mechanics of Elite and Trained Male Speed Skaters. *INTERNATIONAL JOURNAL OF SPORT BIOMECHANICS*, 2:175–185, 1986.

[10] Ruud W De Boer and Kim L Nilsen. The Gliding and Push-off Technique of Male and Female Olympic Speed Skaters. *INTERNATIONAL JOURNAL O F SPORT BtOMECHANICS*, 5:119–134, 1989.

[11] Jeroen van der Eb, Willem Zandee, Timo van den Bogaard, Sjoerd Geraets, DirkJan Veeger, and Peter J. Beek. TOWARDS REAL-TIME FEEDBACK IN HIGH PERFORMANCE SPEED SKATING. In *35th Conference of the International Society of Biomechanics in Sports*, Cologne, Germany, 2017. URL https://www.researchgate.net/publication/330667146_TOWARDS_REAL-TIME_FEEDBACK_IN_HIGH_PERFORMANCE_SPEED_SKATING.

[12] Marco J. Konings, Marije T. Elferink-Gemser, Inge K. Stoter, Dirk van der Meer, Egbert Otten, and Florentina J. Hettinga. Performance Characteristics of Long-Track Speed Skaters: A Literature Review. *Sports Medicine*, 45(4):505–516, 4 2015. ISSN 11792035. doi: 10.1007/s40279-014-0298-z.

[13] Dionne A. Noordhof, Carl Foster, Marco J.M. Hoozemans, and Jos J. De Koning. Changes in Speed Skating Velocity in Relation to Push-Off Effectiveness. *International Journal of Sports Physiology and Performance*, 8(2):188–194, 3 2013. ISSN 1555-0273. doi: 10.1123/IJSPP.8.2.188. URL https://journals.humankinetics.com/view/journals/ijspp/8/2/article-p188.xml.

[14] G. J. van Ingen Schenau, G. de Groot, and R. W. de Boer. The control of speed in elite female speed skaters. *Journal of biomechanics*, 18(2):91–96, 1985. ISSN 0021-9290. doi: 10.1016/0021-9290(85)90002-8. URL https://pubmed.ncbi.nlm.nih.gov/3988788/.

[15] Ruud W De Boer, Gertjan J C Ettema, Hans Van Gorkum, Gert De Groot, and Gerrit Jan Van Lngen Schenau. Biomechanical Aspects of Push-off Techniques in Speed Skating the Curves. *INTERNATIONAL JOURNAL OF SPORT BIOMECHANICS*, 3:69–79, 1987.

[16] Han Houdijk, Jos J. de Koning, Gert de Groot, Maarten F. Bobbert, and Gerrit Jan Van Ingen Schenau. Push-off mechanics in speed skating with conventional skates and klapskates. *Medicine & Science in Sports & Exercise*, 32(3):635–641, 3 2000. ISSN 0195-9131. doi: 10.1097/00005768-200003000-00013. URL http://journals.lww.com/00005768-200003000-00013.

[17] R W De Boer, J Cabri, W Vaes, J P Clarijs, A.P. Hollander, G De Groot, G J Van, and Ingen Schenau. Moments of Force, Power, and Muscle Coordination in Speed-Skating. *mt. J. Sports Mcd*, 8:371–378, 1987.

[18] Jos J De Koning, Ruud W De Boer, Gert De Groot, and Gerrit Jan Van Lngen Schenau. Push-Off Force in Speed Skating. *ORIGINAL INVESTIGATIONS INTERNATIONAL JOURNAL OF SPORT BIOMECHANICS*, 3:103–109, 1987.

[19] Inge K. Stoter, Florentina J. Hettinga, Egbert Otten, Chris Visscher, and Marije T. Elferink-Gemser. Changes in technique throughout a 1500-m speed skating time-trial in junior elite athletes: Differences between sexes, performance levels and competitive seasons. *PLOS ONE*, 15(8):e0237331, 8 2020. ISSN 1932-6203. doi: 10.1371/JOURNAL.PONE.0237331. URL https://journals.plos.org/plosone/article?id=10.1371/journal.pone.0237331.

[20] Dionne A. Noordhof, Carl Foster, Marco J.M. Hoozemans, and Jos J. De Koning. The Association Between Changes in Speed Skating Technique and Changes in Skating Velocity. *International Journal of Sports Physiology and Performance*, 9(1):68–76, 1 2014. ISSN 1555-0273. doi: 10.1123/IJSPP.2012-0131. URL https://journals.humankinetics.com/view/journals/ijspp/9/1/article-p68.xml.

[21] G. J. van Ingen Schenau and G. de Groot. On the origin of differences in performance level between elite male and female speed skaters. *Human Movement Science*, 2(3):151–159, 9 1983. ISSN 0167-9457. doi: 10.1016/0167-9457(83)90013-1.

[22] Zimeng Liu, Meilin Ding, Masen Zhang, Bing Yu, and Hui Liu. Effects of Technique Asymmetry on 500 m Speed Skating Performance. *Bioengineering 2024, Vol. 11, Page 899*, 11(9):899, 9 2024. ISSN 2306-5354. doi: 10.3390/BIOENGINEERING11090899. URL https://www.mdpi.com/2306-5354/11/9/899/htmhttps://www.mdpi.com/2306-5354/11/9/899.

[23] Alexander Spoelstra, Wouter Terra, and Andrea Sciacchitano. On-site aerodynamics investigation of speed skating. *Journal of Wind Engineering and Industrial Aerodynamics*, 239:105457, 8 2023. ISSN 0167-6105. doi: 10.1016/J.JWEIA.2023.105457.

[24] G. J. van Ingen Schenau. The influence of air friction in speed skating. *Journal of Biomechanics*, 15(6):449–458, 1 1982. ISSN 0021-9290. doi: 10.1016/0021-9290(82)90081-1.

[25] Jos J. de Koning, Gert de Groot, and Gerrit Jan van Ingen Schenau. A power equation for the sprint in speed skating. *Journal of Biomechanics*, 25(6):573–580, 6 1992. ISSN 0021-9290. doi: 10.1016/0021-9290(92)90100-F.

[26] Jos J. De Koning, Carl Foster, Joanne Lampen, Floor Hettinga, and Maarten F. Bobbert. Experimental evaluation of the power balance model of speed skating. *Journal of Applied Physiology*, 98(1):227–233, 1 2005. ISSN 87507587. URL https://journals.physiology.org/doi/10.1152/japplphysiol.01095.2003.

[27] Gerrit Jan Van Ingen Schenau, Jos J. De Koning, Frank C. Bakker, and Gert De Groot. Performance-influencing factors in homogeneous groups of top athletes: a cross-sectional study. *Medicine and science in sports and exercise*, 28(10):1305–1310, 10 1996. ISSN 0195-9131. doi: 10.1097/00005768-199610000-00015. URL https://pubmed.ncbi.nlm.nih.gov/8897389/.

[28] Eline van der Kruk and Marco M. Reijne. Accuracy of human motion capture systems for sport applications; state-of-the-art review. *European journal of sport science*, 18(6):806–819, 7 2018. ISSN 1536-7290. doi: 10.1080/17461391.2018.1463397. URL https://pubmed.ncbi.nlm.nih.gov/29741985/.

[29] Eline van der Kruk. Niet over één nacht ijs - Realtime feedback voor betere schaatsprestaties. *Sportgericht nr.3 - jaargang 70*, pages 30–33, 2016. URL https://elinevanderkruk2012.files.wordpress.com/2012/01/niet-over-1-nacht-ijs-real-time-feedback-voor-een-beter-schaatsprestatie.pdf.

[30] Thialf - Schaatshart van de wereld. URL https://thialf.nl/.

[31] Innovatielab Thialf. Sprint Coach | Thialf. URL https://innovatielab.thialf.nl/projecten/sprint-coach.

[32] GoSkate. Alle informatie voor Trainers - GoSkate. URL https://go-skate.nl/trainers/.

[33] Schaatsen & Wintersporten - MYLAPS - Nederland. URL https://www.mylaps.com/nl/active-sports/speed-skating-snow-sports/.

[34] Yosuke Tomita, Tomoki Iizuka, Koichi Irisawa, and Shigeyuki Imura. Detection of Movement Events of Long-Track Speed Skating Using Wearable Inertial Sensors. *Sensors 2021, Vol. 21, Page 3649*, 21(11):3649, 5 2021. ISSN 1424-8220. doi: 10.3390/S21113649. URL https://www.mdpi.com/1424-8220/21/11/3649/htmhttps://www.mdpi.com/1424-8220/21/11/3649.

[35] Jeffrey E. Boyd, Andrew Godbout, and Chris Thornton. In situ motion capture of speed skating: Escaping the treadmill. *Proceedings of the 2012 9th Conference on Computer and Robot Vision, CRV 2012*, pages 460–467, 2012. doi: 10.1109/CRV.2012.68.

[36] J. Clément, F. Croteau, M. Gagnon, and S. Cros. Automatic detection of skate strokes in short-track speed skating using one single IMU: validation of a new method. *Sports Biomechanics*, pages 1–12, 2024. ISSN 17526116. doi: 10.1080/14763141.2024.2331174. URL https://doi.org/10.1080/14763141.2024.2331174.

[37] Motion Capture Technology and Systems | Qualisys | Qualisys. URL https://www.qualisys.com/.

[38] E. van der Kruk, H. E.J. Veeger, F. C.T. van der Helm, and A. L. Schwab. Design and verification of a simple 3D dynamic model of speed skating which mimics observed forces and motions. *Journal of Biomechanics*, 64:93–102, 11 2017. ISSN 18732380. doi: 10.1016/J.JBIOMECH.2017.09.004.

[39] E. van der Kruk, F. C.T. van der Helm, A L Schwabl, and H E J Veegerl. GIVING THE FORCE DIRECTION: ANALYSIS OF SPEED SKATER PUSH OFF FORCES WITH RESPECT TO AN INERTIAL COORDINATE SYSTEM. In *ISBS - Conference Proceedings Archive*, 11 2016. URL https://ojs.ub.uni-konstanz.de/cpa/article/view/6839.

[40] Jeroen Van Der Eb, Hajo Mossink, Esther Kiel, DirkJan Veeger, Peter J. Beek, S Geraets, DirkJan Veeger, and Peter J. Beek. ANALYSIS OF IN COMPETITION SPEED SKATING USING IMU'S. In *36th Conference of the International Society of Biomechanics in Sports*, volume 36, pages 598–601, Auckland, New Zealand, 2018. URL https://commons.nmu.edu/isbs/vol36/iss1/135https://www.researchgate.net/publication/330667152_ANALYSIS_OF_IN_COMPETITION_SPEED_SKATING_USING_IMU'S.

[41] Kyungsoo Kim, Jun Seok Kim, Tserenchimed Purevsuren, Batbayar Khuyagbaatar, Su Kyoung Lee, and Yoon Hyuk Kim. New method to evaluate three-dimensional push-off angle during short-track speed skating using wearable inertial measurement unit sensors. *Proceedings of the Institution of Mechanical Engineers. Part H, Journal of engineering in medicine*, 233(4):476–480, 4 2019. ISSN 2041-3033. doi: 10.1177/0954411919831309. URL https://pubmed.ncbi.nlm.nih.gov/30773989/.

[42] Tserenchimed Purevsuren, Batbayar Khuyagbaatar, Kyungsoo Kim, and Yoon Hyuk Kim. Investigation of Knee Joint Forces and Moments during Short-Track Speed Skating Using Wearable Motion Analysis System. *International Journal of Precision Engineering and Manufacturing*, 19(7):1055–1060, 7 2018. ISSN 20054602. doi: 10.1007/S12541-018-0125-9/METRICS. URL https://link.springer.com/article/10.1007/s12541-018-0125-9.

[43] Martin Schepers, Matteo Giuberti, and Giovanni Bellusci. Xsens MVN: Consistent Tracking of Human Motion Using Inertial Sensing. 2018. doi: 10.13140/RG.2.2.22099.07205. URL https://www.researchgate.net/publication/324007368.

[44] Vera G. de Vette, Dirk Jan Veeger, and Marit P. van Dijk. Using Wearable Sensors to Estimate Mechanical Power Output in Cyclical Sports Other than Cycling—A Review. *Sensors*, 23(1):50, 1 2023. ISSN 14248220. doi: 10.3390/s23010050.

[45] E. van der Kruk, O. den Braver, A. L. Schwab, F. C.T. van der Helm, and H. E.J. Veeger. Wireless instrumented klapskates for long-track speed skating. *Sports Engineering*, 19(4):273–281, 12 2016. ISSN 14602687. URL https://link.springer.com/article/10.1007/s12283-016-0208-8https://www.researchgate.net/publication/303325072_Wireless_instrumented_klapskates_for_long-track_speed_skating.

[46] Jeroen van der Eb, Sjoerd Gereats, and Arno Knobbe. Enhancing the Performance of Elite Speed Skaters Using SkateView: A New Device to Measure Performance in Speed Skating. In *Proceedings of The 13th Conference of the International Sports Engineering Association*, volume 49, page 133. MDPI AG, 8 2020. doi: 10.3390/PROCEEDINGS2020049133. URL https://www.mdpi.com/2504-3900/49/1/133.

[47] Batbayar Khuyagbaatar, Tserenchimed Purevsuren, Won Man Park, Kyungsoo Kim, and Yoon Hyuk Kim. Interjoint coordination of the lower extremities in short-track speed skating. *Proceedings of the Institution of Mechanical Engineers, Part H: Journal of Engineering in Medicine*, 231(10):987–993, 10 2017. ISSN 20413033. doi: 10.1177/0954411917719743.

[48] Movella.com. URL https://www.movella.com/.

[49] MVN Analyze | Movella.com. URL https://www.movella.com/products/motion-capture/mvn-analyze.

[50] Eline M. Nijmeijer, Pieter Heuvelmans, Ruben Bolt, Alli Gokeler, Egbert Otten, and Anne Benjaminse. Concurrent validation of the Xsens IMU system of lower-body kinematics in jump-landing and change-of-direction tasks. *Journal of Biomechanics*, 154:111637, 6 2023. ISSN 0021-9290. doi: 10.1016/J.JBIOMECH.2023.111637.

[51] Award Winning Motion Capture Systems | Vicon. URL https://www.vicon.com/.

[52] Daniel Debertin, Anna Wargel, and Maurice Mohr. Reliability of Xsens IMU-Based Lower Extremity Joint Angles during In-Field Running. *Sensors*, 24(3):871, 2 2024. ISSN 14248220. doi: 10.3390/S24030871/S1. URL https://www.mdpi.com/1424-8220/24/3/871/htmhttps://www.mdpi.com/1424-8220/24/3/871.

[53] Xsens DOT User Manual. 2021. URL www.movella.comwww.movella.com.

[54] E Ribera D'alcala', J A Voerman, J M Konrath, and A Vydhyanathan. Xsens DOT Wearable Sensor Platform White Paper.

[55] Ethics Committee | Faculty of Electrical Engineering, Mathematics and Computer Science (EEMCS). URL https://www.utwente.nl/en/eemcs/research/ethics/.

[56] IJsbaan Twente | Optisport. URL https://www.optisport.nl/schaatsbaan-twente.

[57] MATLAB version 24.1.0.2603908 (R2024a) Update 3, 2024.

[58] MVN User Manual. Technical report, 1 2023.

[59] Jihyeok Jang, Ankit Ankit, Jinhyeok Kim, Young Jae Jang, Hye Young Kim, Jin Hae Kim, and Shuping Xiong. A Unified Deep-Learning Model for Classifying the Cross-Country Skiing Techniques Using Wearable Gyroscope Sensors. *Sensors 2018, Vol. 18, Page 3819*, 18(11):3819, 11 2018. ISSN 1424-8220. doi: 10.3390/S18113819. URL https://www.mdpi.com/1424-8220/18/11/3819/htmhttps://www.mdpi.com/1424-8220/18/11/3819.

[60] Eduardo Palermo, Stefano Rossi, Francesca Marini, Fabrizio Patanè, and Paolo Cappa. Experimental evaluation of accuracy and repeatability of a novel body-to-sensor calibration procedure for inertial sensor-based gait analysis. *Measurement: Journal of the International Measurement Confederation*, 52(1):145–155, 2014. ISSN 02632241. doi: 10.1016/J.MEASUREMENT.2014.03.004.

[61] Léonie Pacher, Christian Chatellier, Rodolphe Vauzelle, and Laetitia Fradet. Sensor-to-Segment Calibration Methodologies for Lower-Body Kinematic Analysis with Inertial Sensors: A Systematic Review. *Sensors 2020, Vol. 20, Page 3322*, 20(11):3322, 6 2020. ISSN 1424-8220. doi: 10.3390/S20113322. URL https://www.mdpi.com/1424-8220/20/11/3322/htmhttps://www.mdpi.com/1424-8220/20/11/3322.

[62] J. Favre, B. M. Jolles, R. Aissaoui, and K. Aminian. Ambulatory measurement of 3D knee joint angle. *Journal of Biomechanics*, 41(5):1029–1035, 2008. ISSN 00219290. doi: 10.1016/J.JBIOMECH.2007.12.003.

[63] findpeaks, . URL https://nl.mathworks.com/help/signal/ref/findpeaks.html.

[64] Thomas Seel, Jörg Raisch, and Thomas Schauer. IMU-Based Joint Angle Measurement for Gait Analysis. *Sensors 2014, Vol. 14, Pages 6891-6909*, 14(4):6891–6909, 4 2014. ISSN 1424-8220. doi: 10.3390/S140406891. URL https://www.mdpi.com/1424-8220/14/4/6891/htmhttps://www.mdpi.com/1424-8220/14/4/6891.

[65] spline - Cubic spline data interpolation - MATLAB - MathWorks Benelux, . URL https://nl.mathworks.com/help/matlab/ref/spline.html?s_tid=doc_ta.

Appendices

Appendix 1: Informed Consent

Proefpersoneninformatie voor deelname aan wetenschappelijk afstudeer onderzoek

Het meten van de schaatsbeweging met draagbare sensoren
Analyseren of er met Inertial Measurement Unit sensoren kan worden gemeten hoe een schaatser over het ijs beweegt.

Inleiding

Geachte heer/mevrouw,

Met deze informatiebrief willen we u vragen of u wilt meedoen aan een afstudeer onderzoek. U leest hier om wat voor onderzoek het gaat, wat het voor u betekent, en wat de voordelen en nadelen zijn. Meedoen is vrijwillig en u kunt uw deelname te allen tijde stopzetten.

Het is veel informatie. Zou u de informatie door willen lezen, en willen beslissen of u mee wilt doen? Als u wilt meedoen, hebben we uw schriftelijke toestemming nodig. Hiervoor kunt u het formulier invullen dat u vindt in bijlage B. Heeft u geen printer? Geen probleem, de onderzoeker neemt dit formulier uitgeprint mee zodat u het bij de start van het onderzoek in kunt vullen.

Stel uw vragen

Mocht u na het lezen van deze informatie nog vragen hebben aarzel dan niet om deze te stellen aan de onderzoeker die u deze informatiebrief heeft gegeven. Alle contactgegevens kunt u vinden bij bijlage A, onderaan deze brief.

1. Algemene informatie

Dit onderzoek zal worden uitgevoerd door de Universiteit Twente (UT). Voor dit onderzoek zijn we op zoek naar 4 tot 8 schaatsers (m/v).

2. Wat is het doel van dit onderzoek?

Door middel van dit onderzoek willen we bekijken of de beweging van een schaatser op het ijs kan worden gemeten met sensoren die op het lichaam worden gedragen.

3. Wat is de achtergrond van dit onderzoek?

De schaatsslag is een complexe beweging die wetenschappers beter proberen te begrijpen. Om beter inzicht in de schaatsbeweging te krijgen wordt deze op dit moment vaak met videocamera's vastgelegd. Een nadeel van een camera is dat je slechts een deel van de 400m ijsbaan in beeld brengen. Daarom richt dit onderzoek zich op een manier om de beweging van de schaatser over de gehele ijsbaan te kunnen volgen. Hiervoor worden *inertial measurement units* (IMU's) gebruikt. Dit zijn kleine sensoren die versnellingen en rotaties kunnen meten. Ze worden al veel gebruikt in onderzoeken naar bewegen in andere sporten, zoals hardlopen, waarbij de sensor op het lichaam wordt gedragen. Het doel van dit onderzoek is om uit te zoeken of deze sensoren ook toegepast kunnen worden in het langebaan schaatsen, om zo inzicht te krijgen in bijvoorbeeld de gewrichtshoeken.

4. Hoe verloopt het onderzoek?

Hoe lang duurt het onderzoek?
Het onderzoek zal in totaal 1 tot 1,5 uur in beslag nemen, inclusief voorbereiding en afronding. Het verloop van de procedure staat hieronder beschreven.

Stap 1 - Bent u geschikt om mee te doen?
Voor dit onderzoek zoeken we gezonde proefpersonen met een leeftijd vanaf 16 jaar. De belangrijkste overige criteria voor deelname zijn:

- U bent 16 jaar of ouder;
- U doet mee aan schaatswedstrijden op nationaal niveau bij de junioren B / junioren A / neo-senioren / senioren of hebt een schaatstechniek van vergelijkbaar niveau;
- U schaatst regelmatig (minimaal een keer per week);
- U heeft op dit moment geen blessure die uw schaatsen negatief beïnvloed;
- U bent in het bezig van eigen klapschaatsen;

Je mag niet deelnemen indien de volgende situaties van toepassing zijn:

- Uw coaches/trainers geven geen toestemming voor uw deelname aan dit onderzoek;

Stap 2 – Voorbereiding van de meting
De voorbereiding van het experiment bestaat uit het aantrekken van de eigen schaatsen en eventueel een transponder en een lycra pak (vergelijkbaar met een schaatspak zonder capuchon) waar in totaal 21 sensoren op zullen worden bevestigd op de volgende locaties:

voet links*, voet rechts*, onderbeen links*, onderbeen rechts*, bovenbeen links*, bovenbeen rechts*, onderrug*, borstbeen, schouder links, schouder rechts, bovenarm links, bovenarm rechts, onderarm links, onderarm rechts.

Op lichaamsdelen met een * worden twee verschillende IMU sensoren geplaatst.

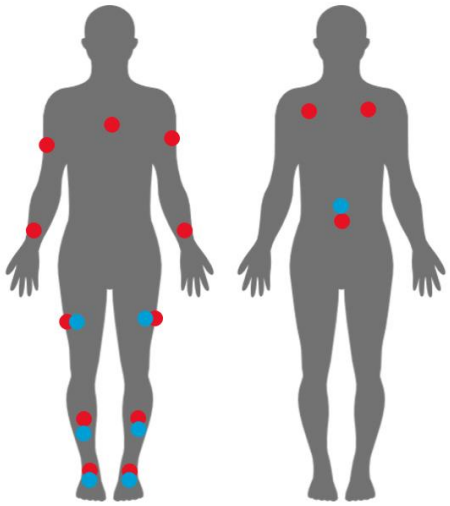

Figuur 1: Links is een schematische weergave van de voorkant van het lichaam, rechts van de achterkant van het lichaam. De gekleurde bolletjes weergeven de locaties waar de sensoren bevestigd zullen worden.

De lichaamsverhoudingen van de proefpersoon worden opgemeten en er wordt een foto van de voorkant en van de zijkant van de proefpersoon gemaakt.

De sensoren zullen worden gekalibreerd door de proefpersoon over een afstand van vijf meter heen en weer te laten lopen. Vervolgens is er indien de proefpersoon dit wenst de mogelijkheid om een aantal ronden op het ijs te schaatsen ter warming-up.

Stap 3 – Uitvoeren van de meting
De meting begint door de sensoren aan te zetten en een video opname te starten. De video opname zal worden gebruikt ter ondersteuning om de gemeten data te interpreteren.

Voor de meting zal de proefpersoon worden gevraagd om de volgende taken in volgorde uit te voeren:

- 3 ronden van 400m op langzame snelheid schaatsen
- 3 ronden van 400m op een zelf gekozen comfortabele snelheid schaatsen
- 3 ronden van 400m op snelle snelheid schaatsen

Het is van belang dat de proefpersoon deze rondes zelfstandig rijdt en niet dicht achter een andere schaatser rijdt. Tussen de blokken mag de proefpersoon rust houden als daar behoefte voor is.

Na het uitvoeren van de hierboven weergeven taken kan de proefpersoon het pak met sensoren uittrekken en is het experiment afgelopen.

5. Van welke bijwerkingen, nadelige effecten of ongemakken kunt u last krijgen?

Tijdens het bewegen kan het zijn dat u de sensoren voelt zitten. Daarnaast is het mogelijk dat het pak licht op de huid schuurt tijdens het dragen.

6. Wat zijn de voordelen en de nadelen als u meedoet aan het onderzoek?

U ervaart geen voordelen aan deelname aan het onderzoek. Indien gewenst kunt u toegang krijgen tot de video opnames en delen van de meetresultaten van de sensoren van uw eigen meting voor eigen gebruik.

Meedoen aan het onderzoek kan de volgende nadelen hebben:

- Meedoen aan het onderzoek kost u tijd.
- Tijdens de meting kunnen de sensoren onprettig aanvoelen.
- Het dragen van het lycra pak zou voor lichte huidirritatie kunnen zorgen.

Wilt u niet meedoen?
U beslist zelf of u meedoet aan het onderzoek.

7. Wanneer stopt het onderzoek?

In deze situaties stopt voor u het onderzoek:

- Als u het protocol heeft afgerond.
- U wilt zelf stoppen met het onderzoek. Dit mag op ieder moment. Meld dit dan bij de onderzoeker. U hoeft er niet bij te vertellen waarom u stopt.
- Uw coach vindt het beter voor u om te stoppen (als uw coach aanwezig is bij het onderzoek).

- De onderzoeker vindt het beter voor u om te stoppen. Voorbeelden van zo'n situatie zijn wanneer het niet lukt om de opdrachten uit het protocol uit te voeren of wanneer u tijdens de meting op het ijs bent gevallen.

Wat gebeurt er als u stopt met het onderzoek?
De onderzoekers gebruiken de gegevens die tot het moment van stoppen zijn verzameld.

8. Wat gebeurt er na het onderzoek?

Wat doen we met uw gegevens?
Bij deelname aan het onderzoek geeft u toestemming om uw gegevens te verzamelen, gebruiken en bewaren.

We bewaren de volgende gegevens:

- uw naam
- uw geslacht
- (optioneel) uw emailadres
- Data die we tijdens het onderzoek verzamelen (hier wordt mee bedoeld: sensor data, videobeelden, rondetijden, lichaamsafmetingen)

Waarom verzamelen, gebruiken en bewaren we uw gegevens?
We verzamelen, gebruiken en bewaren uw gegevens om de vragen van dit onderzoek te kunnen beantwoorden en om de resultaten te verwerken in een verslag.

Hoe beschermen we uw privacy?
Om uw privacy te beschermen geven wij uw gegevens een code. De sleutel van de code wordt op een beveiligde plek op de Universiteit Twente bewaard. Als we uw gegevens verwerken gebruiken we steeds alleen die code, en geen persoonsgegevens zoals uw naam. Afbeeldingen zullen worden geanonimiseerd door het gezicht af te dekken.

In mogelijke rapporten en publicaties zal geen persoonlijke informatie worden gedeeld en de gegevens zullen zo worden gepresenteerd dat deze niet te herleiden zijn naar de proefpersoon.

Hoe lang bewaren we uw gegevens?
We bewaren de code en uw met code beschermde data totdat dit onderzoek is afgerond. Dit is in het jaar 2024. Na deze periode zullen uw gegevens worden verwijderd, of zal de data compleet geanonimiseerd worden. Dit betekent dat we de code die uw persoonlijke gegevens aan de data koppelt vernietigen en uw persoonlijke informatie verwijderen. Videobeelden zullen na het afronden van het onderzoek worden verwijderd. Niemand kan dan nog achterhalen van welke persoon de data afkomstig is.

Mogen we uw gegevens gebruiken voor vervolgonderzoek?
Uw gegevens kunnen na afloop van dit onderzoek ook nog van belang zijn voor ander wetenschappelijk onderzoek op het gebied van bewegingsanalyse van de schaatsbeweging met draagbare sensoren. Daarvoor zullen uw geanonimiseerde gegevens 15 jaar worden bewaard. In het toestemmingsformulier geeft u aan of u dit goed vindt. Geeft u geen toestemming? Dan kunt u nog steeds meedoen met dit onderzoek. U volgt dan hetzelfde protocol.

Kunt u uw toestemming voor het gebruiken van uw gegevens weer intrekken?
U kunt uw toestemming voor het gebruiken van uw gegevens op ieder moment intrekken. Geef

dat dan aan bij het onderzoeksteam. Maar let op: trekt u uw toestemming in, en hebben de onderzoekers dan al gegevens verzameld voor een onderzoek? Dan mogen zij deze gegevens nog wel gebruiken.

Wilt u meer weten over uw privacy?
- Wilt u meer weten over uw rechten bij de verwerking van persoonsgegevens? Kijk dan op www.autoriteitpersoonsgegevens.nl.
- Heeft u vragen over uw rechten? Of heeft u een klacht over de verwerking van uw persoonsgegevens? U kunt dan contact opnemen met het secretariaat van de Ethics Committee Information & Computer Science: ethicscommittee-CIS@utwente.nl.
- Als u klachten heeft over de verwerking van uw persoonsgegevens, raden we u aan om deze eerst te bespreken met de onderzoekers. U kunt ook naar de Ethics Committee Information & Computer Science van de UT gaan. Of u dient een klacht in bij Autoriteit Persoonsgegevens.

9. Krijgt u een vergoeding als u meedoet aan dit onderzoek?

Deelnemen aan dit onderzoek kost u niets. U krijgt ook geen vergoeding als u meedoet. Ook (extra) reiskosten worden niet vergoed.

10. Heeft u vragen?

Vragen over het onderzoek kunt u stellen aan het onderzoeksteam (zie bijlage A voor contactgegevens).

Heeft u een klacht? Bespreek dit dan met de onderzoeker. Wilt u dit liever niet? Neem dan contact op met de Ethics Committee Information & Computer Science van de UT via ethicscommittee-CIS@utwente.nl.

11. Hoe geeft u toestemming om mee te doen aan dit onderzoek?

U kunt eerst rustig nadenken over dit onderzoek. Daarna vertelt u de onderzoeker of u de informatie begrijpt en of u wel of niet wilt meedoen. Wilt u meedoen? Dan vult u het toestemmingsformulier in dat u bij deze informatiebrief vindt (Bijlage B). U en de onderzoeker krijgen allebei een getekende versie van deze toestemmingsverklaring.

Bijlage A – Contact gegevens

Onderzoeksteam
Anne Leemreize
Master student Biomedical Engineering, Universiteit Twente, Enschede
Email: a.j.leemreize@student.utwente.nl

Dr. Jasper Reenalda
Associate Professor Universiteit Twente, Enschede, Nederland
Email: j.reenalda@utwente.nl

Ethics Committee Information & Computer Science
Email: ethicscommittee-CIS@utwente.nl

Bijlage B – Toestemmingsformulier

Ik heb de studie-informatie gelezen en begrepen. Ik heb vragen kunnen stellen over het onderzoek en mijn vragen zijn naar tevredenheid beantwoord.	○ Ja ○ Nee
Ik geef vrijwillig toestemming om deel te nemen aan dit onderzoek en begrijp dat ik kan weigeren vragen te beantwoorden of taken uit te voeren en dat ik me op elk moment, zonder reden te geven, uit het onderzoek kan terugtrekken.	○ Ja ○ Nee
Ik geeft toestemming voor het verzamelen, bewaren en gebruiken van mijn gegevens voor de beantwoording van de onderzoeksvraag van dit onderzoek.	○ Ja ○ Nee
Ik begrijp dat over mij verzamelde persoonlijke informatie die mij kan identificeren, zoals mijn naam, niet buiten het onderzoeksteam zal worden gedeeld.	○ Ja ○ Nee
Ik geef toestemming om mijn geanonimiseerde studiegegevens langer te bewaren en te gebruiken voor toekomstig onderzoek op het gebied van het meten en analyseren van de schaatsbeweging.	○ Ja ○ Nee
Ik geef toestemming voor het verzamelen van beeldmateriaal (foto's en video's) tijdens het onderzoek. Beeldmateriaal zal altijd geanonimiseerd worden als het wordt gebruikt in presentaties, verslagen, publicaties of andere uitingen.	○ Ja ○ Nee
Ik wil per mail de resultaten van de meting waar ik aan deel heb genomen ontvangen. (Indien ja, noteer dan uw e-mail adres.)	○ Ja ○ Nee
Ik wil per mail op de hoogte worden gebracht over de uitkomst van dit onderzoek. (Indien ja, noteer dan uw e-mail adres.)	○ Ja ○ Nee

Naam van deelnemer:

E-mail adres:

Handtekening: Datum:

Ik verklaar dat ik deze proefpersoon volledig heb geïnformeerd over het genoemde onderzoek. Als er tijdens het onderzoek informatie bekend wordt die de toestemming van de proefpersoon zou kunnen beïnvloeden, dan breng ik hem/haar daarvan tijdig op de hoogte.

Naam onderzoeker:

Handtekening: Datum:

Als je vragen hebt over je rechten als proefpersoon of als je informatie wilt verkrijgen, vragen wilt stellen of zorgen over dit onderzoek wilt bespreken met iemand anders dan de onderzoeker(s), neem dan contact op met de secretaris van de Ethische Commissie Informatie & Informatica: ethicscommittee-CIS@utwente.nl

Appendix 2: Research Protocol

Meetprotocol data verzamelen @ ijsbaan

Doel: Het doel van dit experiment is het verzamelen van data van een schaatser die over het ijs beweegt met MVN Link en DOT sensoren om later te analyseren. De invloed van de snelheid van de schaatser op het meetresultaat wordt meegenomen door de proefpersoon op verschillende snelheden te laten schaatsen.

Samenvatting: De meting vindt plaats op een 400m ijsbaan. De proefpersoon zal worden uitgerust met een lycra pak waarop IMU's worden bevestigd. Er wordt gevraagd om 3 rondes te rijden op langzame snelheid, 3 rondes op een zelfgekozen comfortabele snelheid en 3 rondes op een snellere snelheid. De proefpersoon zal 1 tot 1,5 uur bezig zijn.

Informatie voor en van deelnemer, een paar dagen voor de meting:

1. Stuur de proefpersoneninformatie en informed consent.
2. Vraag de proefpersoon om het volgende mee te nemen naar de meting:
    a. Ondertekend informed consent formulier;
    b. korte strakke sportbroek of boxershort;
    c. klapschaatsen;
    d. schaatshoezen;
    e. handschoenen;
    f. muts;
    g. transponder (wanneer de proefpersoon deze bezit).
3. Stuur de proefpersoon, indien nodig, de dag voor de meting een reminder over de datum, tijd, locatie en mee te nemen materialen.

Logistieke voorbereiding, afstemmen met derden:

1. Zorg dat de IJsbaan Twente op de hoogte is van je komst.
2. Zorg dat je de licentie dongel kunt gebruiken tijdens de meting.
3. Zorg dat je de DOT sensoren en LINK sensoren kunt gebruiken tijdens de meting.

Voorbereiding door de onderzoeker, dag voor de meting:

4. Laad de UT telefoon volledig op.
5. Laad de DOT sensoren volledig op en wis het geheugen.
6. Plak op 10 DOT sensoren plakband op de achterzijde.
7. Laad beide powerpacks volledig op. Wis geheugen van het bodypack.
8. Laad accu's van camera's volledig op. Zorg dat er voldoende geheugen vrij is om minimaal 30 minuten te kunnen filmen.
9. Controleer of alle materialen op de materiaallijst aanwezig zijn en leg deze klaar (in een tas of opbergbak).

Voorbereiding door de onderzoeker, 60 minuten voor de meting, op de ijsbaan:

1. Laat aan de persoon achter de balie van de ijsbaan weten dat je er bent en wat je gaat doen.
2. Haal de Link sensoren uit de koffer en haal ze uit de knoop.
3. Sluit de Link sensoren en battery pack aan op het bodypack. Plug de USB-dongel in de laptop. Open MVN Analyze 2021. Sluit de bodypack met de USB-kabel of ethernet kabel aan op de laptop. Klik op het knopje op de bodypack om het Link systeem te activeren.
4. Zet de configuratie voor On Body Recording (OBR) op:
    a. Suit configuration: full body (no hands)

    b. Scenario: single level
    c. Accept system: Link
    d. Max update rate: 240 Hz
5. Koppel het bodypack los van de laptop.

   Note: bovenstaande stap 1 t/m 5 hoeven niet op de meetlocatie worden uitgevoerd

6. Plaats de Link sensoren voor de pelvis en het sternum in het pak.

7. Zet de DOT sensoren aan door de houder en laptop te verbinden met de USB-kabel.
8. Verbindt 5 DOT sensoren met de Movella DOT applicatie op de smartphone.
9. Zet de samplefrequentie van de sensoren op 60 Hz en voer Magnetic Field Mapping uit.
10. Zet de samplefrequentie van de sensoren terug op 120 Hz. Verbreek de verbinding met de applicatie.
11. Herhaal stap 6 t/m 8 voor de andere 5 DOT sensoren.
12. Verbindt 7 DOT sensoren met de applicatie en synchroniseer.
13. Plak Velcro tape aan de achterzijde van 5 DOT sensoren.
14. Plak dubbelzijdig tape aan de achterzijde van 2 DOT sensoren. (Deze worden straks op de schaatsschoen geplaatst.)

Voorbereiding met proefpersoon, op de ijsbaan (duur: 45 minuten)

1. Geef een korte samenvatting over hoe de deelname aan het onderzoek er uit zal zien.
2. Vraag aan de proefpersoon of hij/zij nog vragen heeft over het onderzoek.
3. Teken samen met de proefpersoon het informed consent formulier in tweevoud (2x).
4. Vraag of de proefpersoon nog naar het toilet moet. Dit kan niet meer wanneer het pak met sensoren aan is getrokken.

5. Laat de proefpersoon het Xsens pak, schaatsen met hoezen en transponder aantrekken.
6. Plaats de link sensoren op de juiste locaties:
    a. Linker voet
    b. Rechter voet
    c. Linker onderbeen
    d. Rechter onderbeen
    e. Linker bovenbeen
    f. Rechter bovenbeen
    g. Pelvis
    h. Sternum
    i. Linker schouder
    j. Rechter schouder
    k. Linker bovenarm
    l. Rechter bovenarm
    m. Linker onderarm
    n. Rechter onderarm

7. Verbindt de sensor voor het hoofd wel, maar verberg deze onder de rits op de rug van het pak.
8. Plaats de batterij links op de onderrug en het body pack rechts op de onderrug. Verbindt de sensoren en de batterij met het bodypack.

9. Plaats 7 DOT sensoren precies op of direct naast de LINK sensoren, op de volgende locaties:
    a. Linker voet
    b. Rechter voet
    c. Linker onderbeen
    d. Rechter onderbeen
    e. Linker bovenbeen
    f. Rechter bovenbeen
    g. Pelvis

10. Noteer op het formulier welke DOT sensor op welke locatie op het lichaam is bevestigd.
11. Maak een close-up foto van elke sensorlocatie. (Zodat je sensor nummers en oriëntatie weet)
12. Meet het lichaam van de proefpersoon op en noteer de afmetingen op het formulier. Maak foto's van de proefpersoon in T-pose van de voorkant en N-pose van de zijkant. (Zo kun je op een later moment afmetingen opnieuw opmeten. Belangrijk dat ritsen van het pak open staan zodat sensoren zichtbaar zijn.)
13. Sluit de ritsen van het pak.

Kalibratie met proefpersoon: (10 minuten)

1. Controleer of de DOT sensoren nog gesynchroniseerd zijn. Zo niet, synchroniseer opnieuw.
2. Start een video opname met de camera. Zorg dat de proefpersoon volledig in beeld is.
3. Start de meting met de DOT sensoren in de applicatie.
4. Start de kalibratiemeting van het Link systeem door eenmaal op de knop op het bodypack te drukken. Het lampje gaat snel knipperen wanneer de meting is gestart.
5. Laat de proefpersoon 10 seconden in N-pose staan, gevolgd door 5m heen en weer lopen (met schaatsen aan). Eindig de kalibratie met 10 seconden in N-pose staan op dezelfde positie als de eerste N-pose. Druk op de knop om de kalibratie meting te stoppen.
6. Voer de kalibratie in totaal 3x uit.
7. Stop de meting met de DOT sensoren.

8. Start een nieuwe meting met de DOT sensoren.
9. Start een nieuwe meting met de LINK sensoren.
10. Laat de proefpersoon de volgende bewegingen uitvoeren: (de proefpersoon mag zich vasthouden. De bewegingen zullen worden gebruikt voor sensor-to-segment kalibratie van de DOT sensoren)
    a. 3x stampen met linker voet
    b. 3x stampen met rechter voet
    c. 3x squat beweging
    d. 3x naar voren buigen (rug)
    e. 3x linker knie (bovenbeen) optillen
    f. 3x rechter knie (bovenbeen) optillen
    g. 3x linker knie (onderbeen) buigen
    h. 3x rechter knie (onderbeen) buigen
    i. 3x linker enkel flexie
    j. 3x rechter enkel flexie
    k. 3x stampen met linker voet
    l. 3x stampen met rechter voet
11. Stop de meting met de LINK sensoren.
12. Stop de meting met de DOT sensoren.

13. Stop de video opname met de camera.

Instructie aan proefpersoon: (5 minuten)

1. Ga met de proefpersoon naast het ijs staan.
2. Geef de proefpersoon een instructie over wat hij/zij moet doen tijdens de meting. Benoem hierbij de verschillende rondes die hij/zij zal rijden. Benoem dat het belangrijk is om zelfstandig te rijden en niet dicht achter iemand te gaan rijden omdat dit het schaatspatroon kan beïnvloeden. Vraag de proefpersoon om zo veel mogelijk in de binnenste snelrijdersbaan te rijden.
3. Vraag of de proefpersoon de uitleg heeft begrepen en of hij/zij nog vragen heeft.
4. Benoem dat de proefpersoon op elk moment mag stoppen.

De proefpersoon mag nu de hoezen van de ijzers verwijderen en naar de start van de 1000m schaatsen. De onderzoeker loopt om het ijs heen en plaatst ondertussen de camera's op de juiste posities.

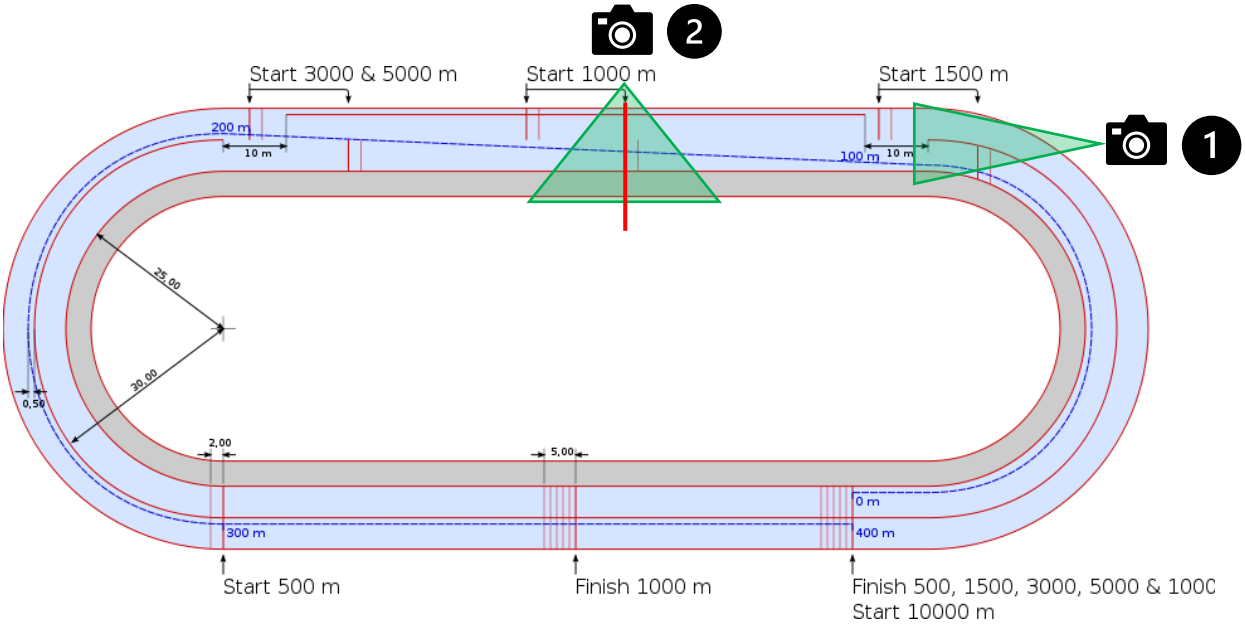

Camera's in positie zetten: (5 minuten)

1. Zet een camera op een statief in het verlengde van het rechte eind, zodat de camera de schaatsers van de rugzijde filmt. (camera 1 in afbeelding)
2. Start de opname met camera 1 en loop naar het startpunt van de meting (rode streep).

Meting op het ijs: (15 minuten)

1. Laat de proefpersoon halverwege het rechte eind staan (rode streep). (Vanaf nu heet deze plek: startpunt meting.) Ga zelf op hetzelfde punt langs de boarding aan de buitenkant van de baan staan.
2. Zet de camera op een statief neer bij het startpunt van de meting (camera 2 in afbeelding). Deze moet binnen handbereik van de onderzoeker zijn, zodat zij met de camera de proefpersoon kan volgen.
3. Start de opname met camera 2.

4. Start de meting met het LINK systeem door op de knop op de bodypack te drukken. Het lampje gaat snel knipperen.
5. Start de meting met de DOT sensoren via de applicatie op de smartphone.
6. Vraag de proefpersoon om 3x met de linker schaats op het ijs te stampen en daarna 3x met de rechter schaats op het ijs te stampen. Zorg dat het stampen zichtbaar is voor de camera. (Voor het synchroniseren van de verschillende systemen.)
7. De proefpersoon schaatst rustig vanuit stilstand weg. Geen start.
8. **Onderzoeker start de stopwatch. Meet elke keer de rondetijd wanneer de proefpersoon langsrijdt.**
9. **Onderzoeker volgt de schaatser met de camera.**
10. De proefpersoon rijdt 3 rondes op langzame snelheid met lage slagfrequentie (rondetijd van +- 60 seconden?)
11. Wanneer proefpersoon dit wil: 400m rechtop rijden
12. De proefpersoon rijdt 3 rondes op een zelf gekozen comfortabele snelheid (rondetijd van +- 50 seconden?)
13. Wanneer proefpersoon dit wil: 400m rechtop rijden
14. De proefpersoon rijdt 3 rondes op hogere snelheid met hoge slagfrequentie (rondetijd van +- 40 seconden?)
15. Wanneer proefpersoon dit wil: 400m rechtop uitrijden
16. De proefpersoon gaat bij het startpunt van de meting stilstaan. Vraag de proefpersoon 3x te stampen met links en daarna 3x stampen met rechts.

Meting beëindigen:

1. Stop de meting met het Link systeem door op de knipperende knop op het bodypack te drukken. Wanneer de meting is gestopt knippert deze niet meer.
2. Stop de meting met de DOT sensoren in de applicatie.
3. Stop de video opname van de camera's.

Afronding met proefpersoon: (5 minuten)

1. Benoem dat de meting is afgerond en instrueer de proefpersoon om van het ijs af te stappen.
2. Benoem dat de proefpersoon de videobeelden en .mp4 bestand van het Link systeem kan ontvangen indien gewenst. Vraag of de proefpersoon dit wil.
3. Benoem dat de contactgegevens van de onderzoeker en de ethische commissie op de informatiebrief staan voor vragen over het onderzoek.
4. Verwijder de sensoren uit het pak.
5. De proefpersoon mag het Xsens pak uittrekken en zich omkleden.
6. De onderzoeker ruimt alle materialen op.

Data opslaan na de meting:

1. Maak een scan van het informed consent formulier en sla deze op in de beveiligde drive.
2. Vul de naam van de proefpersoon in in het sleutelbestand en geef de proefpersoon een nummer.
3. Sluit de DOT sensoren één voor één aan op de computer. Exporteer de bestanden van de DOT sensoren. Sla deze op in een beveiligde one-drive. Vermeldt in de naam van het bestand de locatie van de sensor en het proefpersoon nummer.
4. Sluit de bodypack van het Link systeem aan op de computer. Kopieer de bestanden op de bodypack naar de beveiligde drive. Open de bestanden in MVN Analyze. Selecteer de eerste drie bestanden als kalibratie metingen. Voer de lichaamsafmetingen van de proefpersoon in

en sla deze op onder het bijbehorende proefpersoon nummer. Exporteer de overige bestanden naar .mvnx format.

5. Zet de foto’s en videobestanden van de camera op de beveiligde drive. Zorg dat het gezicht van de proefpersoon niet zichtbaar is (wanneer dit wel het geval is, bewerk de beelden zodat dit niet meer het geval is). Zet het proefpersoon nummer in de bestandsnaam.

Checklist materialen

Materiaal	Check
Informatiebrief geprint	
Informed consent formulier geprint (2x)	
Pen (2x)	
2x Camera (+ accu + geheugenkaart)	
2x Statief	
Laptop	
Laptop oplader	
MVN Link sensoren voor boven- en onderlichaam	
MVN powerpack (2x)	
MVN bodypack	
Ethernet kabel	
USB-kabel	
2x Xsens suit (maat M en L)	
Dongel met MVN Analyze Pro licentie	
UT Smartphone met Movella DOT applicatie	
Set van 5 DOT sensoren (2x)	
Velcro tape	
Plakband	
Dubbelzijdig tape	
Ducttape	
Schilderstape	
Fysiotape	
Schaar	
Meetlint	
Rolmaat	
Stopwatch	
Korte sportbroek (reserve)	
Schaatshoezen (reserve)	
Formulier body dimensions geprint	
Tijdschrift/boekje/voorwerp om op hoofd te leggen bij lengte meten	

Invulformulier: Sensor locaties & lichaamsafmetingen

Datum	
Proefpersoon #	
Omschrijving	

DOT #	**Locatie**
	Linker voet
	Rechter voet
	Linker onderbeen
	Rechter onderbeen
	Linker bovenbeen
	Rechter bovenbeen
	Pelvis

Afmeting	**cm**	**Beschrijving**
Body height		Grond tot kruin
Shoe length		Hak tot teen
Shoulder height		Grond tot C7
Shoulder width		Acromion tot acromion
Elbow span		Olecranon tot olecranon
Wrist span		Ulnar styloid tot ulnar styloid
Arm span		Vingertop tot vingertop
Hip height		Grond tot caput femur
Hip width		SIAS tot SIAS
Knee height		Grond tot laterale epichondyl
Ankle height		Grond tot laterale malleolus
Sole thickness		Hoogte met schaatsen – hoogte zonder schaatsen

Notities:

	Subject	1			2			3			4			5			6			7			8			9		
	Measurement	1	2	3	1	2	3	1	2	3	1	2	3	1	2	3	1	2	3	1	2	3	1	2	3	1	2	3
Number of detected strokes	Total	75	79	102	88	86	89	120	125	92	109	89	102	73	77	80	79	90	104	89	86	103	90	97	101	51	87	108
	Right	38	40	51	43	44	44	60	63	47	54	45	52	37	38	40	40	45	52	44	43	52	45	48	51	26	43	54
	Left	37	39	51	45	42	45	60	62	45	55	44	50	36	39	40	39	45	52	45	43	51	45	49	50	25	44	54
	Right straight	10	10	19	17	13	15	13	13	14	19	16	21	11	11	12	15	13	17	15	12	8	16	15	19	8	12	23
	Left straight	13	13	23	22	15	19	19	19	18	25	19	24	14	15	15	18	16	20	20	2	1	16	17	19	10	14	26
	Right curve	21	22	24	17	20	22	29	38	25	23	21	23	19	20	21	17	24	27	12	11	7	19	17	23	12	23	23
	Left curve	24	26	28	23	23	25	35	42	26	29	25	26	22	24	25	21	28	31	18	35	24	22	19	26	13	27	27
	Right other	7	8	8	9	11	7	18	12	8	12	8	8	7	7	7	8	8	8	17	20	37	10	16	9	6	8	8
	Left other	0	0	0	0	4	1	6	1	1	1	0	0	0	0	0	0	1	1	7	6	26	7	13	5	2	3	1
Knee Flexion Angle	RMSE total	12,1	19,4	13,9	10,3	13	47,2				13,9	16	15,9	11,1	16,6	14	6,9	8,2	9	11,8	12,2	14,7	15,6	13	15,3	52,6	53,9	69
	RMSE right straight	11,1	28	11	9,2	12,3	9,2				9,2	13,7	10,8	11,4	10,2	14,4	8,7	5,4	6,9	7,9	8,7	12,3	11	7,5	13	76,3	76,9	79,7
	RMSE left straight	13	10,5	15,2	16	12,3	78,6				11,4	14,8	13,6	11,4	21,6	13,7	5,1	6,5	6,3	14,6	12,9	19,4	14,2	13,2	15,5	37,5	42,9	56,9
	RMSE right curve	10,4	32,4	12,3	8,7	12,1	9,3				14	16,4	11,6	10,7	14,8	11,6	6,2	8	9,8	8,4	10,1	9,8	19,7	8,2	10,1	65,7	63,9	80,5
	RMSE left curve	13,6	9,5	16,1	6,9	14,5	79,6				19,1	18,1	26,1	11,2	17,9	16	7,8	10,6	11,2	14,1	14	16,8	16,5	21,3	21,3	37,6	41	61,6
	Pearson total	0,79	0,86	0,83	0,94	0,92	0,43				0,94	0,92	0,84	0,71	0,71	0,84	0,93	0,92	0,93	0,95	0,92	0,95	0,88	0,87	0,86	0,03	-0,06	0,07
	Pearson right straight	0,91	0,7	0,9	0,99	0,95	0,97				0,93	0,89	0,91	0,93	0,96	0,85	0,86	0,98	0,95	0,96	0,96	0,92	0,93	0,98	0,92	0,03	-0,13	0,06
	Pearson left straight	0,44	0,83	0,84	0,84	0,97	-0,65				0,95	0,95	0,78	0,92	0,53	0,93	0,98	0,95	0,98	0,96	0,96	0,9	0,96	0,95	0,88	0,02	-0,11	0,03
	Pearson right curve	0,84	0,93	0,82	0,97	0,82	0,85				0,87	0,95	0,87	0,21	0,57	0,66	0,96	0,88	0,88	0,92	0,84	0,94	0,69	0,77	0,82	0,09	-0,03	0,25
	Pearson left curve	0,88	0,88	0,8	0,96	0,96	0,55				0,97	0,9	0,83	0,88	0,83	0,93	0,93	0,92	0,93	0,95	0,93	0,97	0,94	0,81	0,85	-0,01	-0,02	-0,03
Trunk Angle	RMSE total	39,3	38,8	37,8	3,9	4,3	5,6				4,8	5,3	7,2				4,9	5,1	5,7	27,3	27,1	26,8	4,5	4,7	6,7	14	19,8	23,1
	RMSE straight	38,9	38,5	37,8	3,5	3,5	5,5				4,4	4,6	4,9				5,1	4,7	4,7	26	25	20,5	5	5,7	6,2	12,4	19	22,6
	RMSE curve	39,5	38,9	37,7	4,2	4,9	5,7				5,1	5,8	9,2				4,8	5,4	6,3	28,7	27,2	27,1	4,1	3,7	7,1	15,4	20,2	23,6
	Pearson total	0,84	0,87	0,81	0,88	0,85	0,82				0,9	0,84	0,6				0,8	0,8	0,83	0,58	0,57	0,57	0,75	0,31	0,41	0,05	-0,07	-0,04
	Pearson straight	0,75	0,84	0,79	0,83	0,8	0,79				0,84	0,76	0,52				0,65	0,58	0,76	0,65	0,24	0,86	0,44	-0,4	-0,15	-0,22	0	0,03
	Pearson curve	0,89	0,89	0,83	0,93	0,88	0,84				0,96	0,9	0,67				0,93	0,92	0,88	0,51	0,59	0,56	0,97	0,94	0,83	0,28	-0,11	-0,11
Push-off Angle	RMSE total	9,1	9,9	8,2	8,3	9,2	7,8				9,4	8,1	8,3	12	13,7	11,1	9,3	10,4	9,2	33,1	30,7	36	7,3	8,4	9,8	28,4	33,4	33,9
	RMSE right straight	4,6	5,1	5,9	6,5	6,5	5,7				5,2	5,5	7,5	6	15,1	6,5	5,6	5,1	6,8	34,6	33,1	35,6	2,9	4,4	6,8	25,5	29,8	30,4
	RMSE left straight	5,8	6,5	4,6	5,2	5,8	4,3				5,8	6,6	8,3	7,4	11,4	6,2	5,5	6,4	5,1	34,7	31,8	23,6	4,6	3,5	5,8	24,6	29,6	28,7
	RMSE right curve	10	10	9	12,2	11,9	7,5				12	8,3	7,2	14,2	8,9	14,4	12,6	12,1	11,8	28,4	28,6	34,3	9,2	12,1	13	23,3	30,6	34,7
	RMSE left curve	11,9	13,3	12	9,8	10,7	12				13,3	10,7	9,9	16,1	18,5	13,3	12,7	13,7	11	33,1	30,5	37,1	10,8	12,5	12,1	37,7	39,4	41,3
	Pearson total	0,99	0,99	0,95	0,98	0,94	0,96				0,99	0,97	0,89	0,99	0,97	0,99	0,98	0,98	0,98	-0,01	0,05	0,29	0,99	0,99	0,97	-0,04	-0,03	0,09
	Pearson right straight	0,99	0,99	1	0,99	0,99	0,99				0,99	0,99	0,97	0,99	0,99	0,99	0,99	1	1	0,36	0,36	0,37	0,99	0,99	0,99	0,01	-0,06	0,15
	Pearson left straight	0,99	0,99	1	0,99	0,99	0,99				0,99	0,98	0,96	1	0,98	0,99	0,99	1	1	0,18	0,44	-0,58	1	1	1	0,14	-0,08	0,18
	Pearson right curve	1	0,99	0,96	0,99	0,99	0,99				0,99	0,97	0,89	0,99	0,98	0,99	0,99	0,99	0,99	-0,42	-0,11	0,22	0,99	0,99	0,95	-0,01	0,17	0,05
	Pearson left curve	0,99	0,98	0,89	0,96	0,85	0,89				0,98	0,96	0,75	0,99	0,95	0,99	0,96	0,96	0,96	-0,24	-0,03	0,32	0,99	0,99	0,96	-0,23	-0,17	-0,01

Figure 22: Columns are measurements, rows are parameters. Green cells were included for analysis of the results, red cells were not. For the empty cells, either the DOT or MVN data was missing. RMSE numbers are red if > 20 degrees, Pearson Correlation Coefficient numbers are red if < 0.5. Numbers of detected strokes are red if they do not correspond to the expected value.

Appendix 4: Knee flexion angle

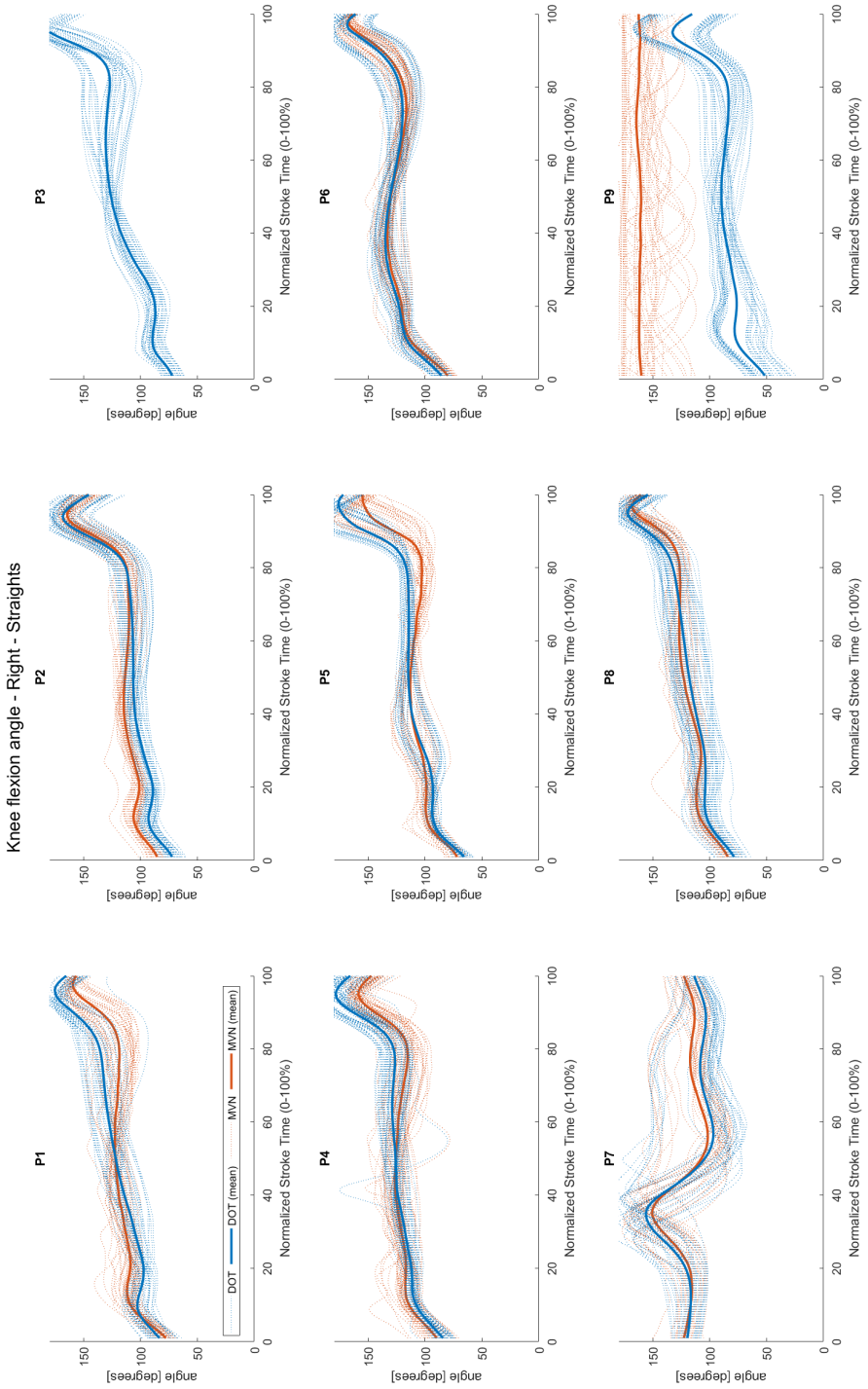

Figure 23: Flexion angle of the right knee on the straights. Blue = DOT, orange = MVN.

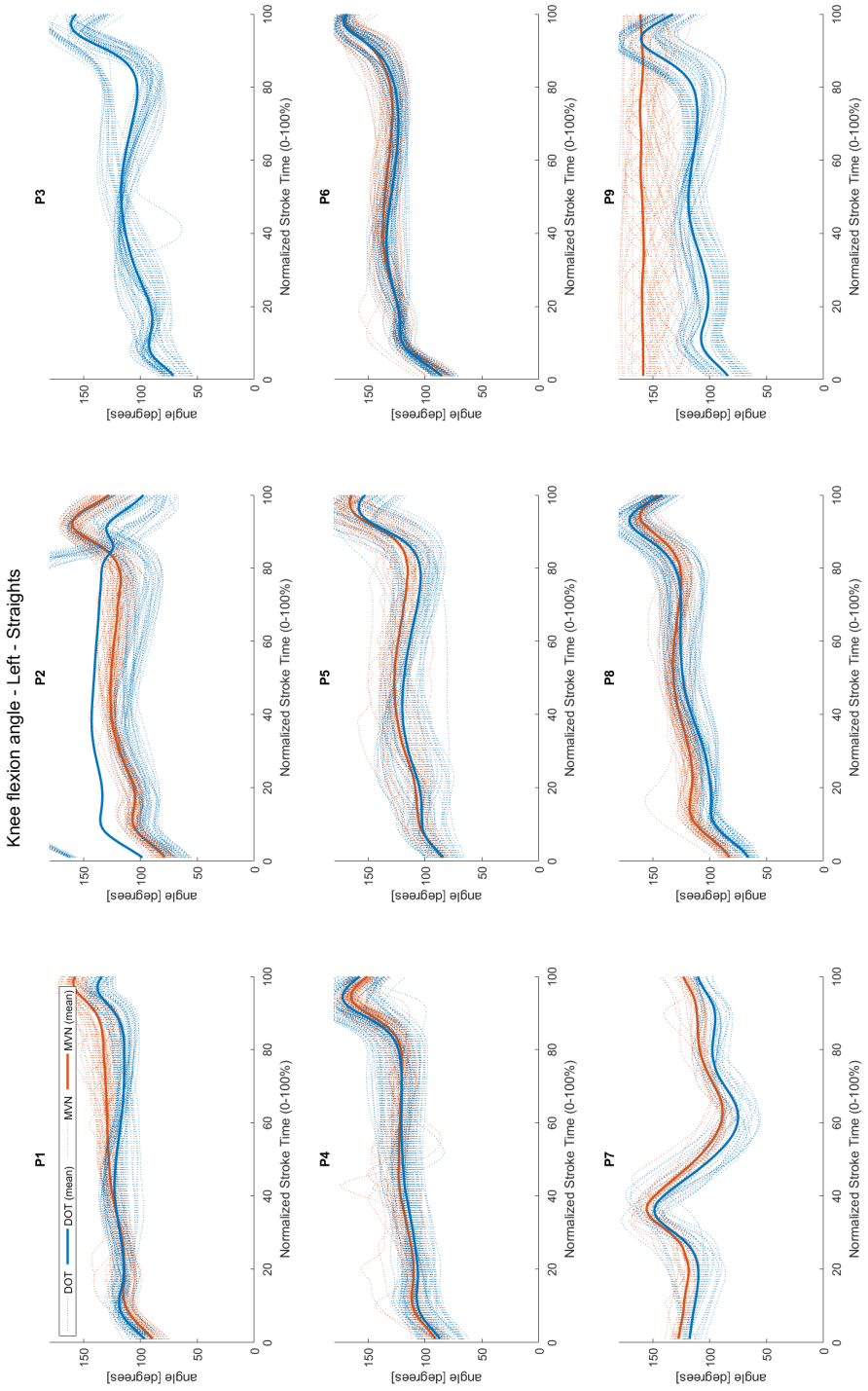

Figure 24: Flexion angle of the left knee on the straights. Blue = DOT, orange = MVN.

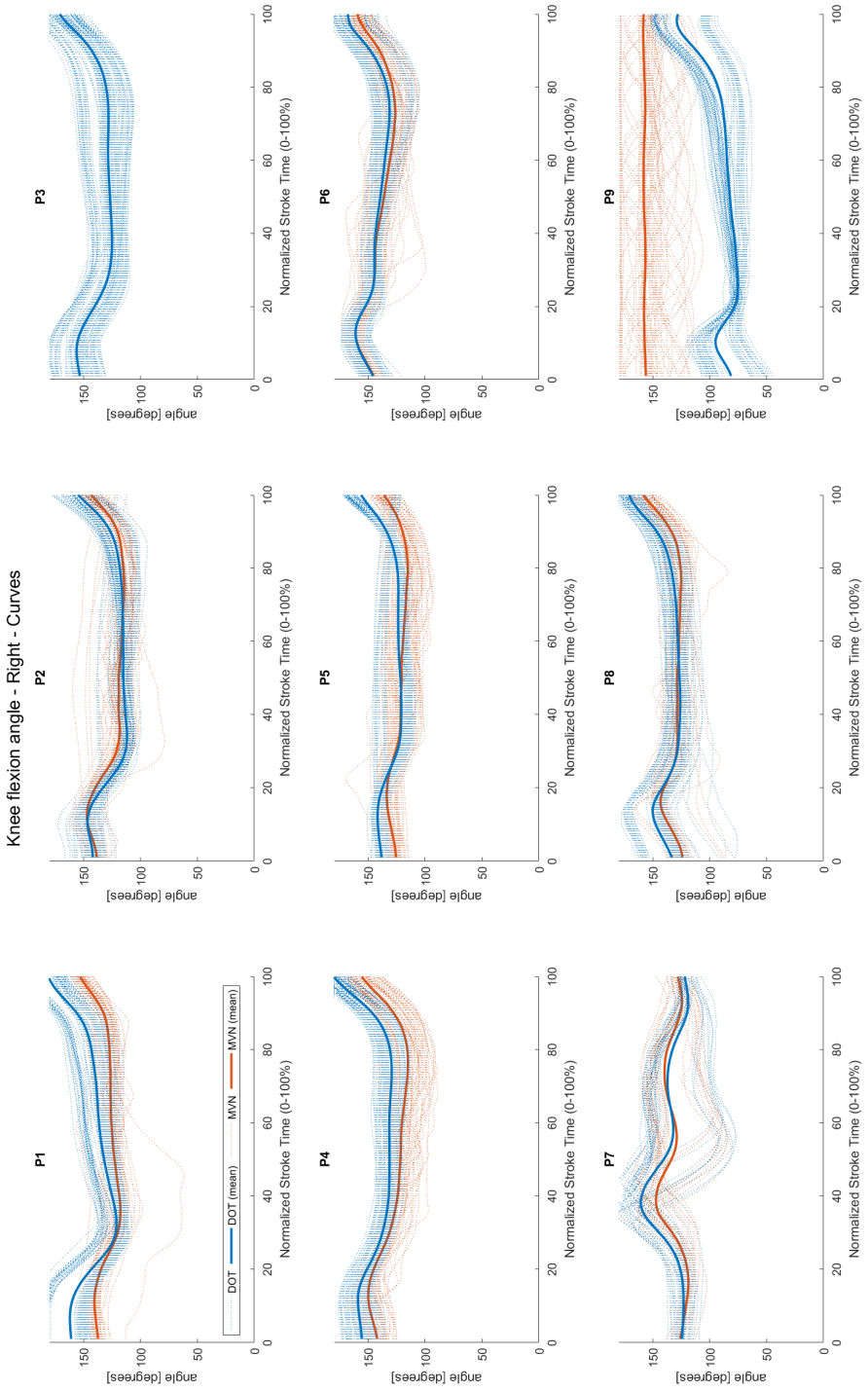

Figure 25: Flexion angle of the right knee in the curves. Blue = DOT, orange = MVN.

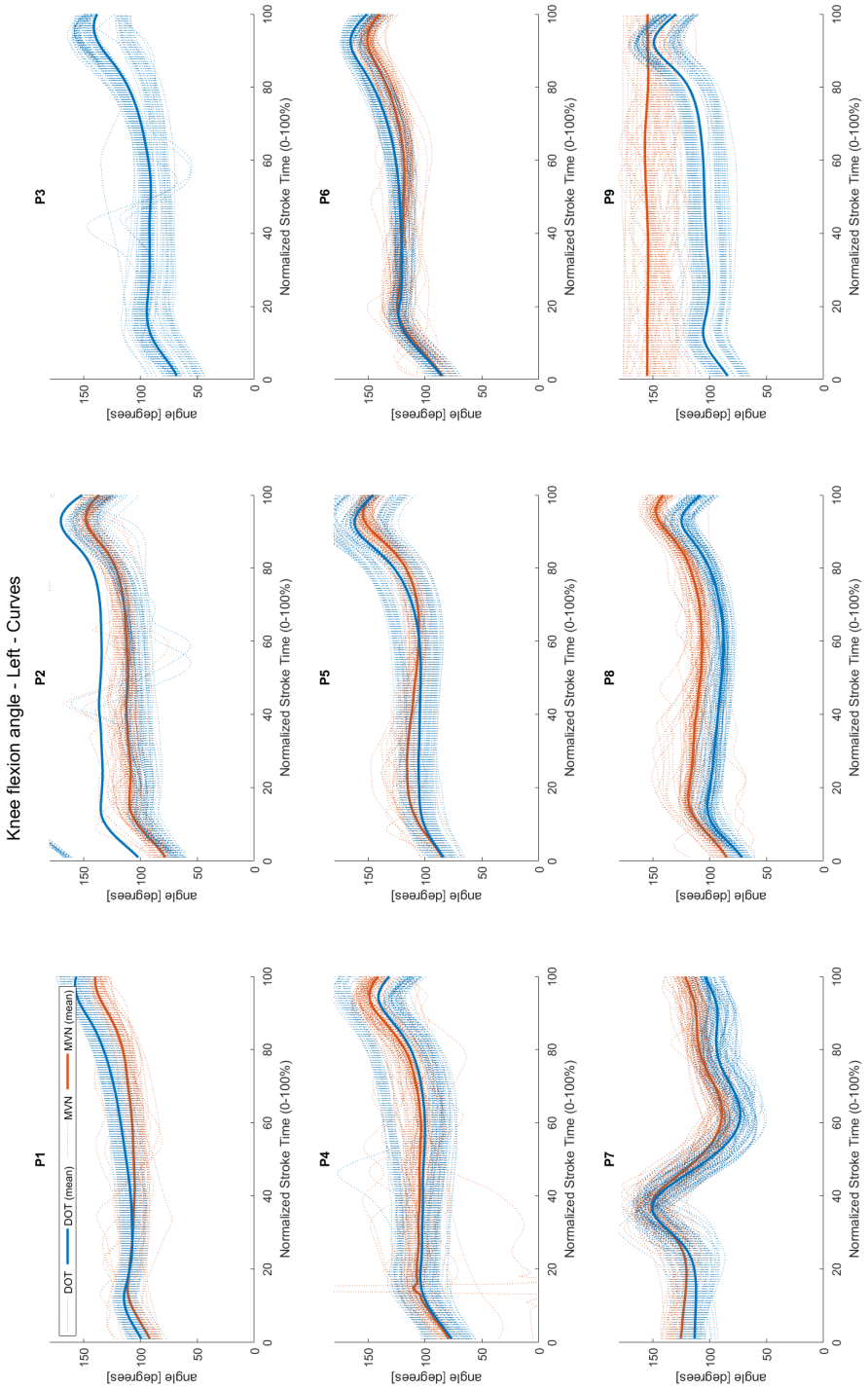

Figure 26: Flexion angle of the left knee in the curves. Blue = DOT, orange = MVN.

Appendix 5: Trunk angle

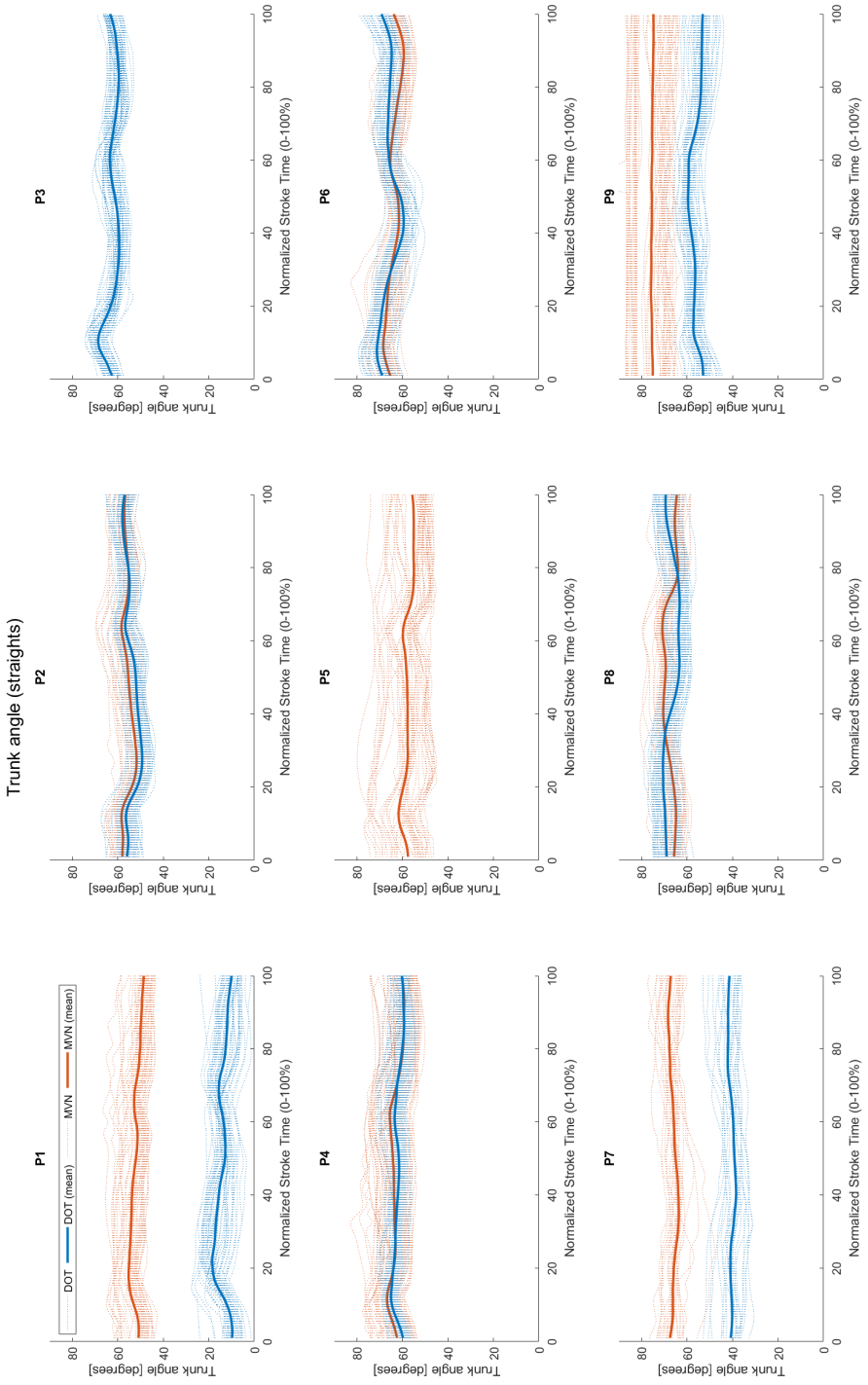

Figure 27: Trunk angle on the straights. Blue = DOT, orange = MVN.

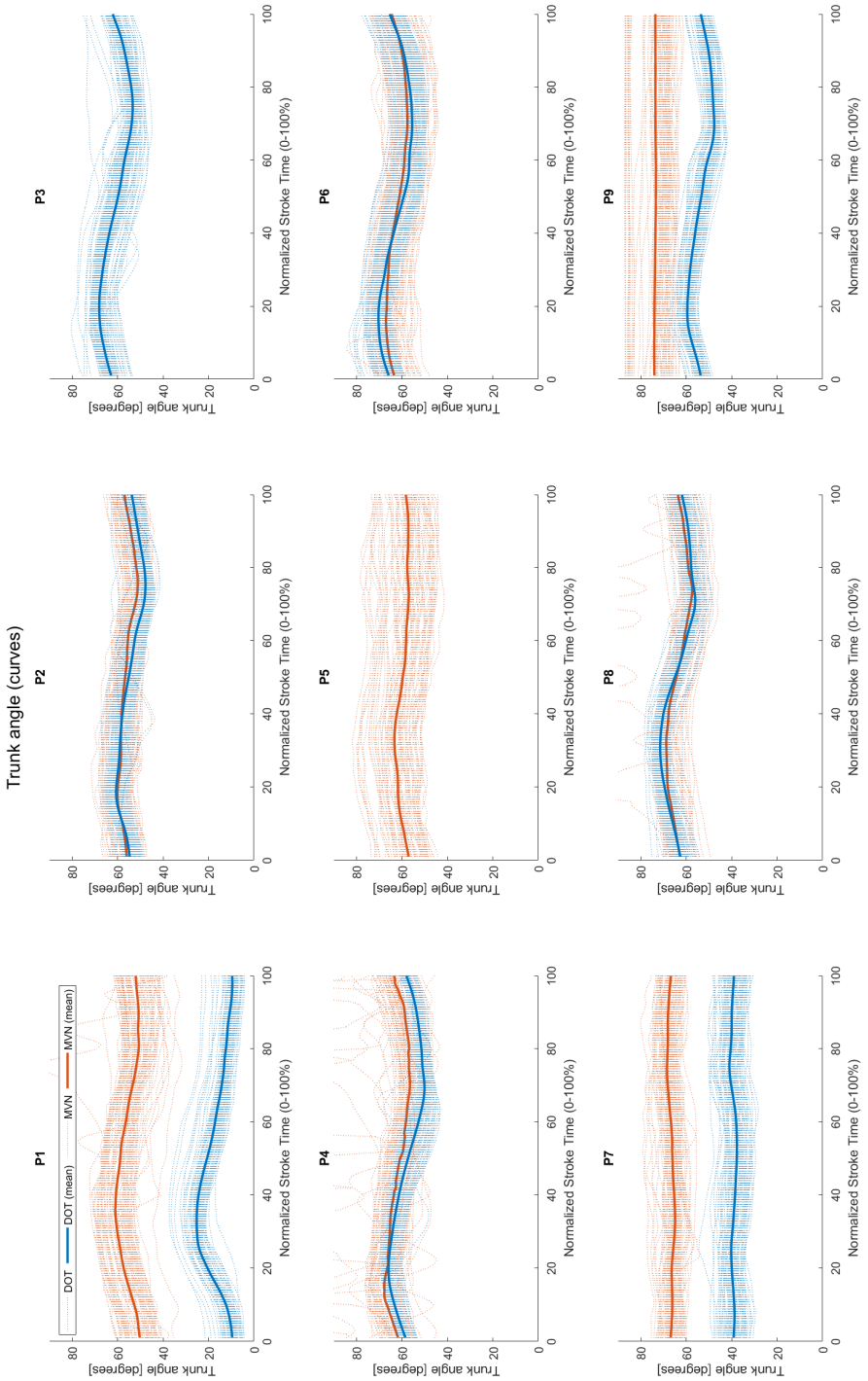

Figure 28: Trunk angle in the curves. Blue = DOT, orange = MVN.

Appendix 6: Push-off angle

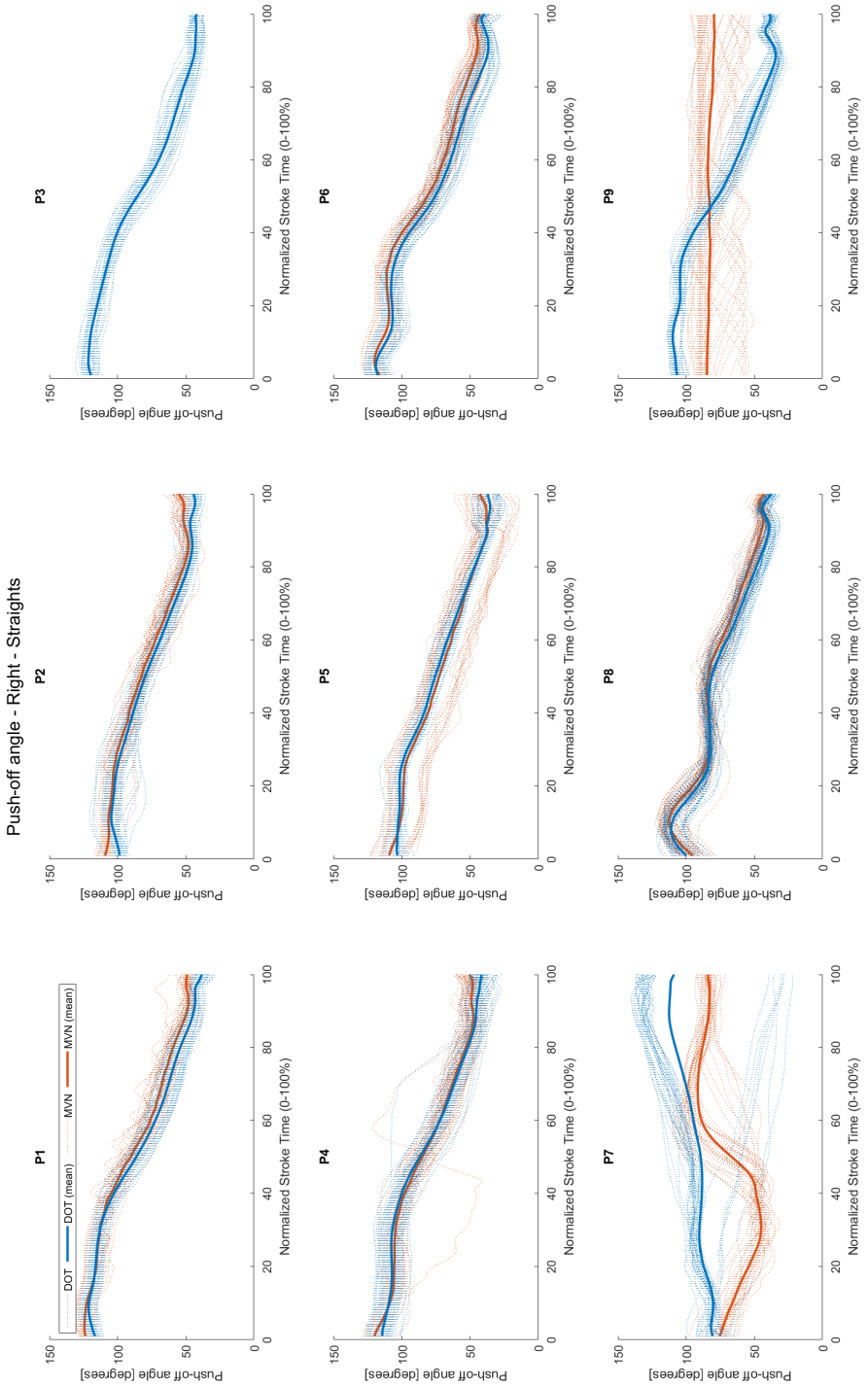

Figure 29: Push-off angle of the right skate on the straights. Blue = DOT, orange = MVN.

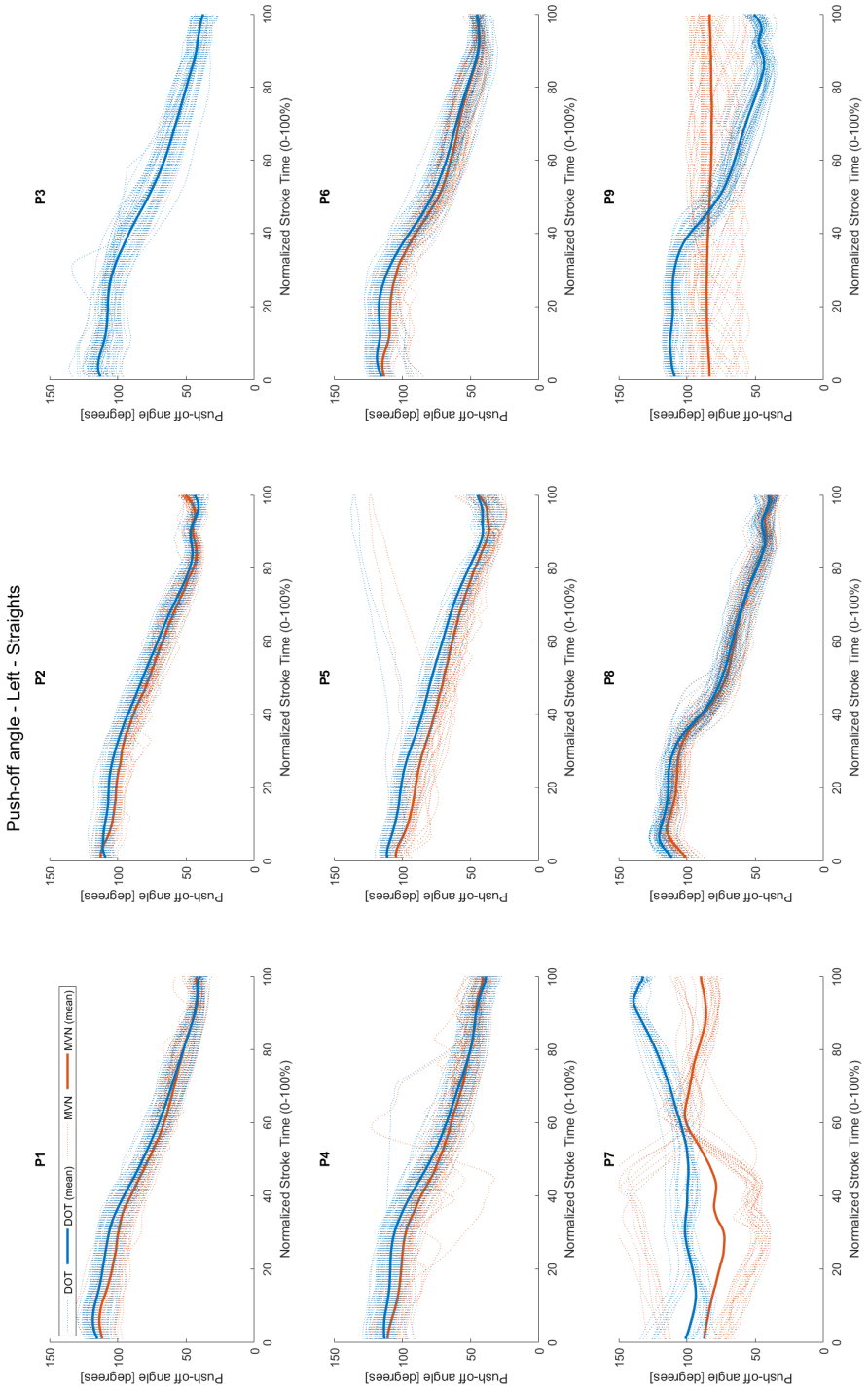

Figure 30: Push-off angle of the left skate on the straights. Blue = DOT, orange = MVN.

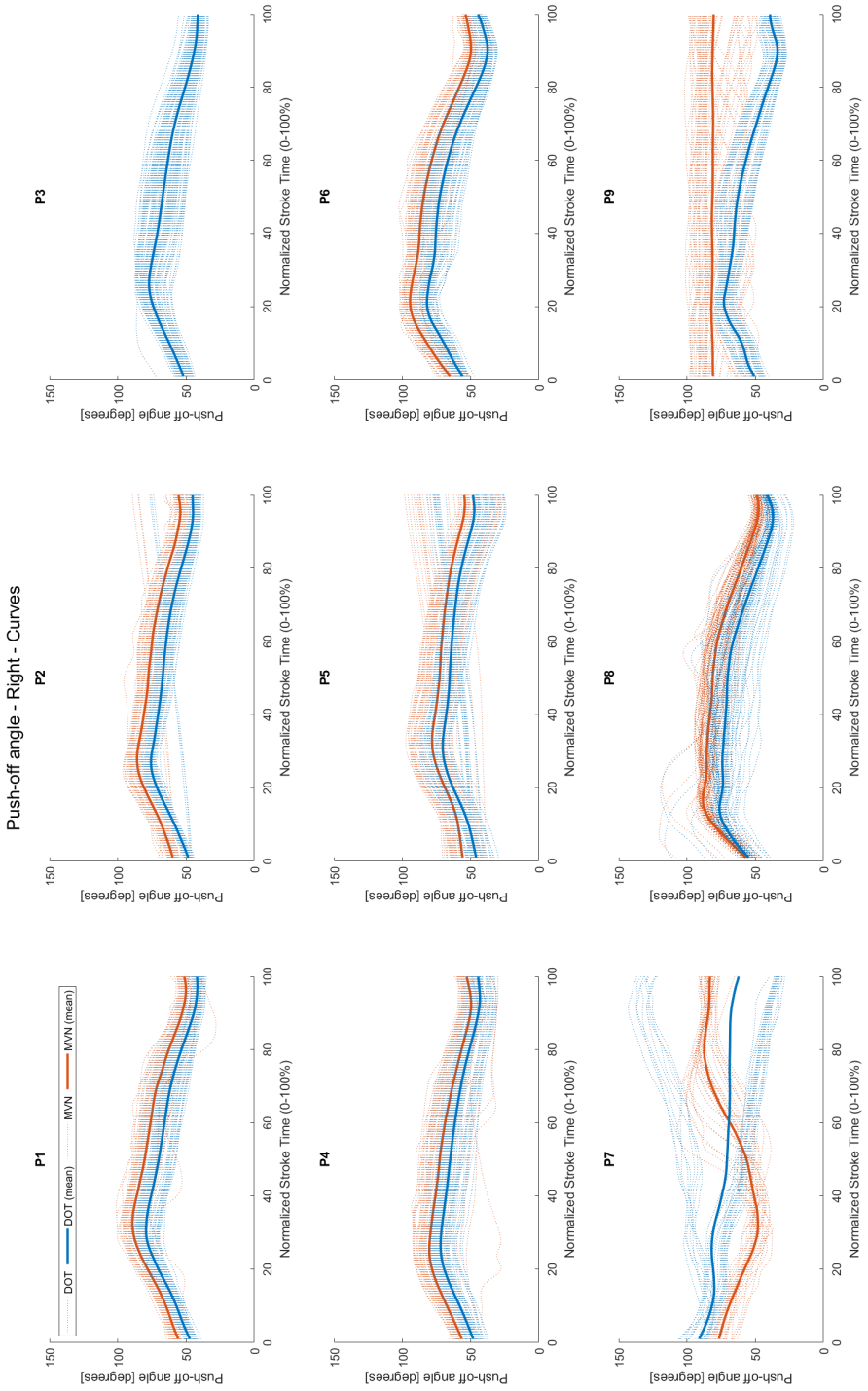

Figure 31: Push-off angle of the right skate in the curves. Blue = DOT, orange = MVN.

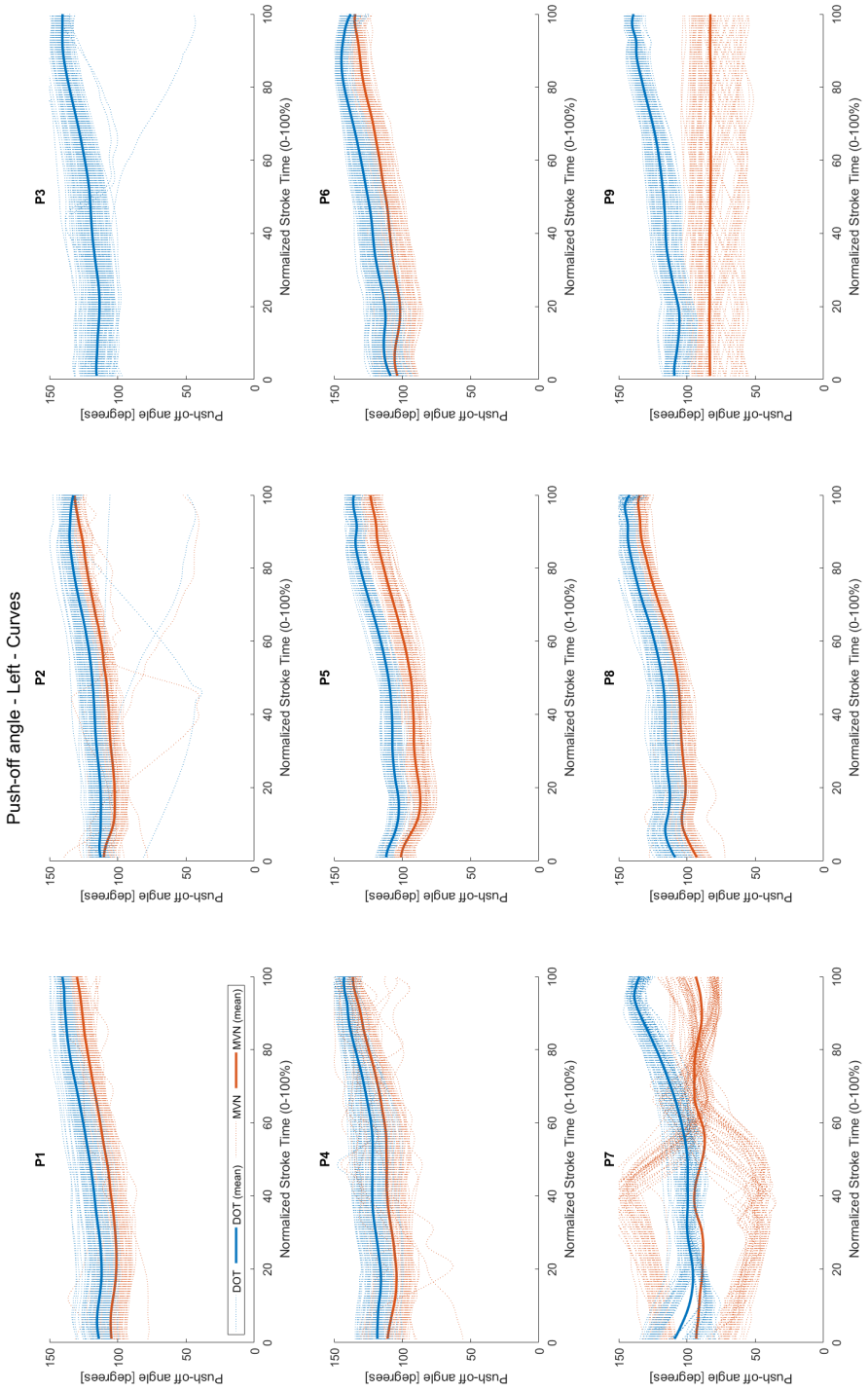

Figure 32: Push-off angle of the left skate in the curves. Blue = DOT, orange = MVN.

Appendix 7: Push-off velocity

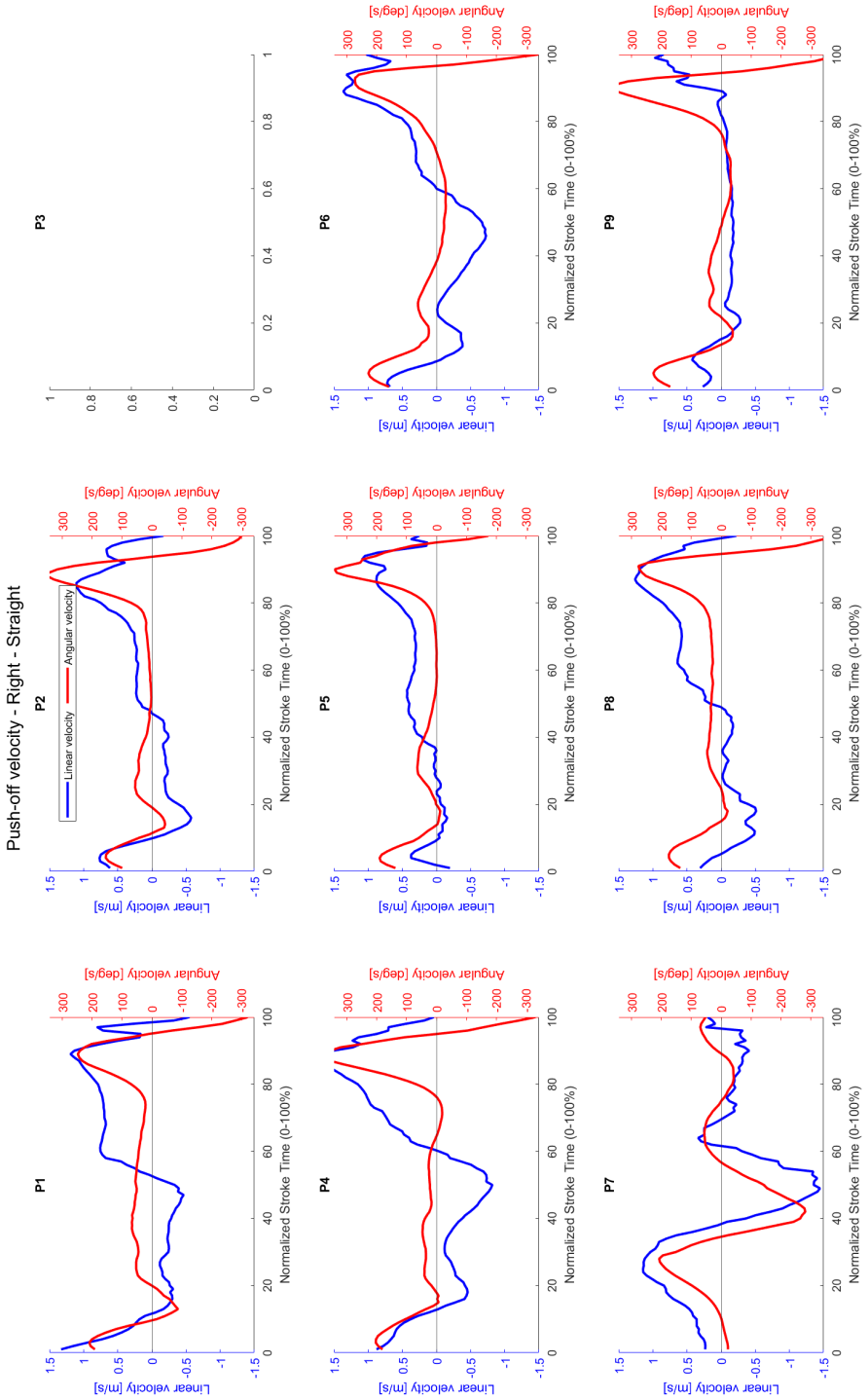

Figure 33: Push-off velocity of the right leg on the straights. Blue = linear, red = angular.

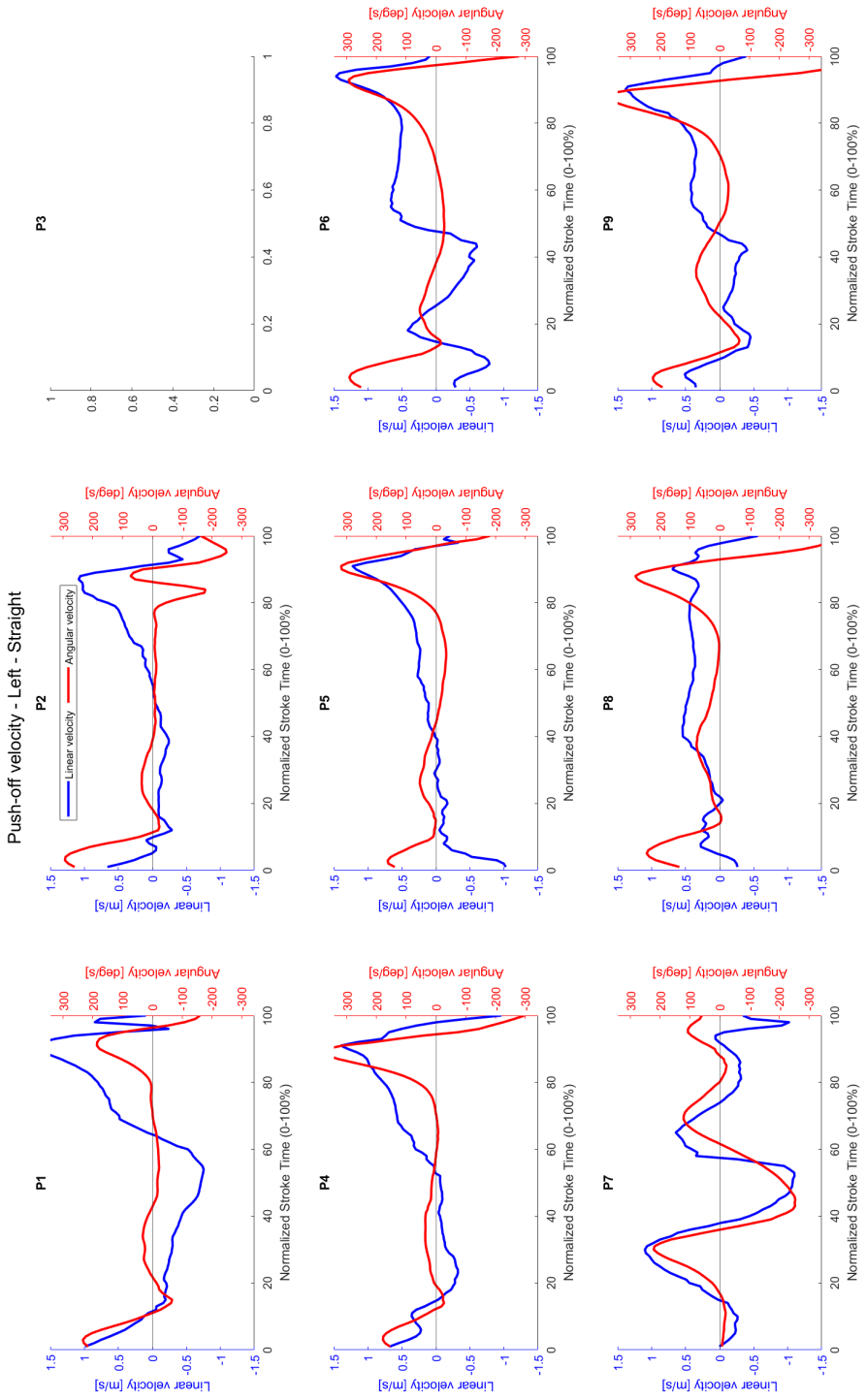

Figure 34: Push-off velocity of the left leg on the straights. Blue = linear, red = angular.

Appendix 8: Push-off acceleration

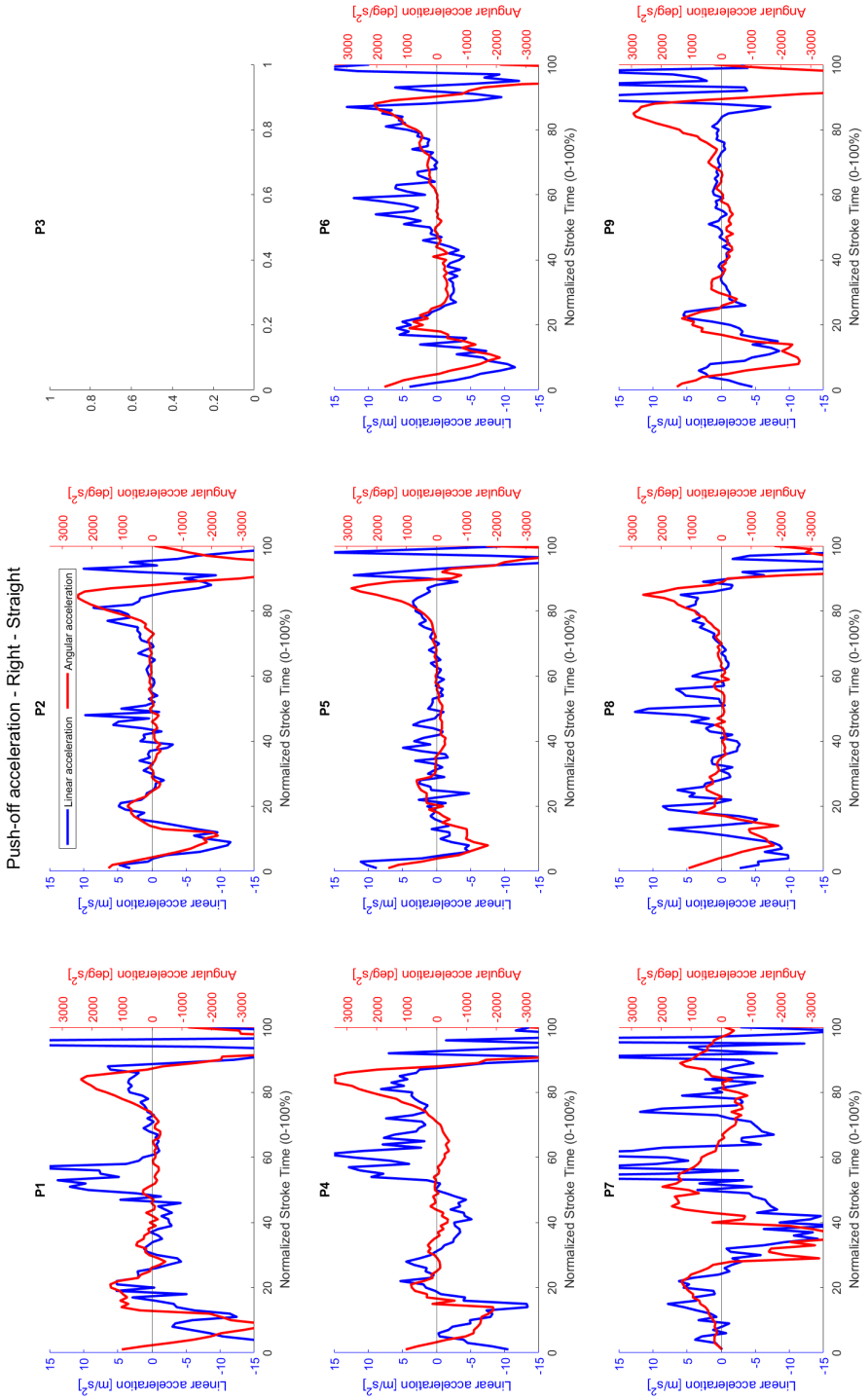

Figure 35: Push-off velocity of the right leg in the curves. Blue = linear, red = angular.

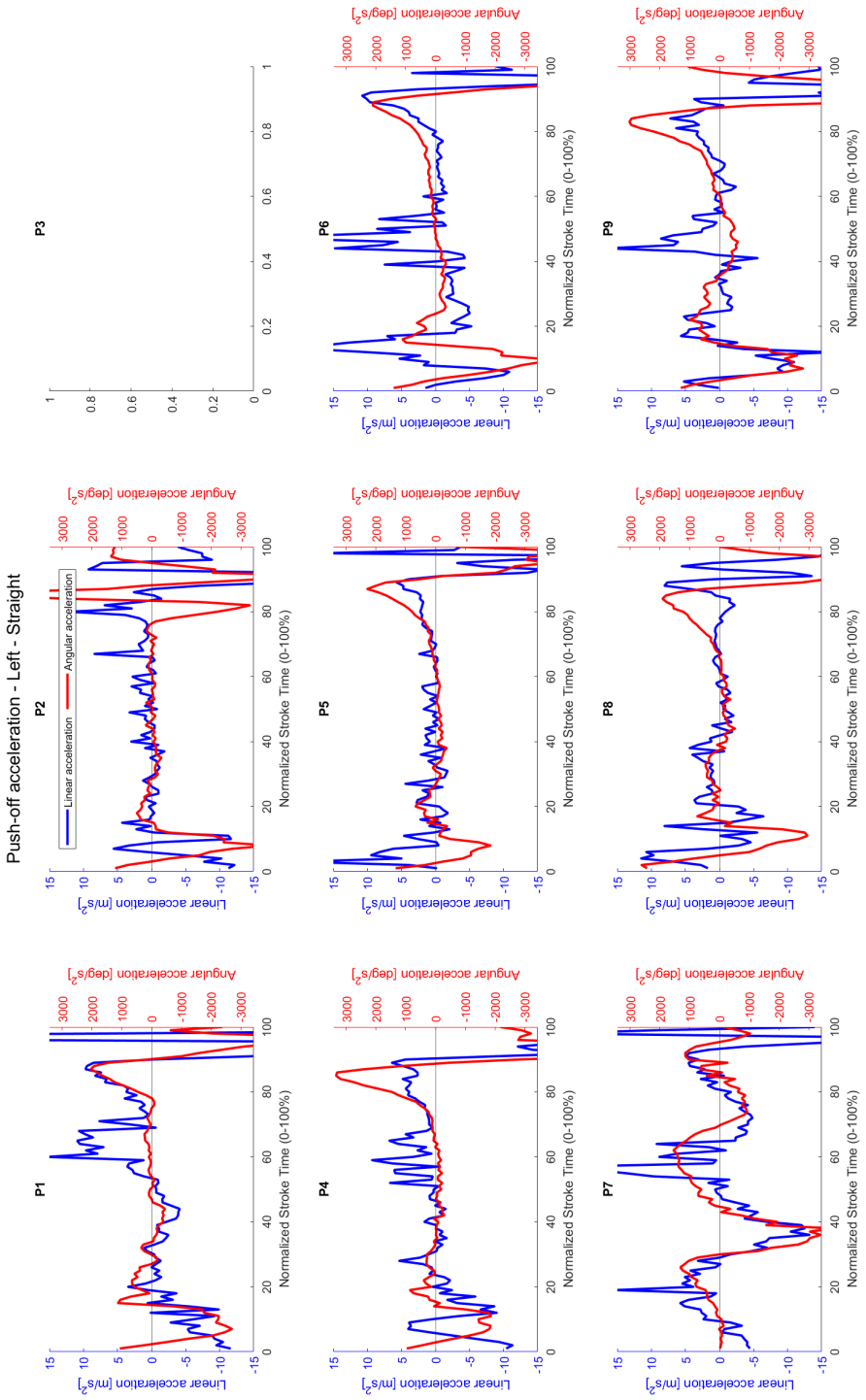

Figure 36: Push-off velocity of the left leg in the curves. Blue = linear, red = angular.